1-1-1984

The effect of thallium on the copper - zinc oxide methanol synthesis catalyst.

Paul P. Deutsch

THE EFFECT OF THALLIUM ON THE COPPER - ZINC OXIDE METHANOL SYNTHESIS CATALYST

by

Paul P. Deutsch

A Thesis

Presented to the Graduate Committee

of Lehigh University

in Candidacy for the Degree of

Master of Science

in

Chemistry

Lehigh University

December 1984

Dedicated to my parents.

CERTIFICATE OF APPROVAL

Approved and recommended for acceptance as a thesis in partial fulfillment of the requirements for the degree of Master of Science.

Nov. 27 1984
Date

Dr. Kamil Klier, Advisor

Dec. 5, 1984
Date

Robert S. Sprague
Assistant Chairman
Chemistry

ACKNOWLEDGEMENTS

The author would like to acknowledge and thank his advisor, Professor Kamil Klier, for his guidance, encouragement, assistance, and patience during the course of this research.

I would also like to express my thanks to the following people for their assistance during my career at Lehigh:

Dr. Richard G. Herman and Dr. Gary W. Simmons for their helpful comments and insights related to this work.

Paul Himelfarb, Donna Mitko, Gamini Vedage, and Chyi Woei Young for their assistance in performing this work and for their helpful discussions.

Chuck Bogdan, David Bybell, Dave Cole, John Nunan, Rangasamy Pitchai, Jose Santiesteban, and Yarw-Nan Wang for their insights, comments, and friendship.

The faculty, staff, and graduate students of the Department of Chemistry.

TABLE OF CONTENTS

CONTENTS (Cont'd)

CONTENTS (Cont'd)

LIST OF TABLES

TABLES (Cont'd)

LIST OF FIGURES

FIGURES (Cont'd)

ABSTRACT

The effect of thallium on the copper - zinc oxide methanol synthesis catalyst has been studied. This investigation was undertaken in order to determine the effect of thallium on the activity of the catalyst, to determine the nature of the observed poisoning, to gain insight into the nature of the active sites, and to gain insight into the mechanism of product formation over this catalyst. A series of thallium-doped catalysts were prepared, tested for activity, and then characterized by surface area measurements, by x-ray diffraction, and by x-ray photoelectron spectroscopy.

The major products observed during the testing of these catalysts were methanol and carbon dioxide (when water was added to the feed gas stream), with small amounts of methane, methyl formate, and ethanol also formed. The amount of methanol, methyl formate, and ethanol produced was always less than the amount of these products seen over the undoped catalyst, with the formation of these products decreasing with increasing thallium content in the catalyst. Small amounts of water in the feed gas increased formation of these products while large amounts of water inhibited their formation. The production of carbon dioxide increased with the addition of water to the synthesis gas, and was essentially the same as the production

over the undoped catalyst.

All of the thallium-doped catalysts showed a decrease in surface area upon testing, which was not observed for the undoped catalyst. This loss of surface area can be correlated with the sintering of the copper and the zinc oxide particles observed in the x-ray diffraction analysis. The x-ray photoelectron spectroscopic analysis found all of the thallium to be on the surface of the catalysts.

An attempt was made to explain the observed poisoning of the catalyst by thallium using models of the active methanol synthesis sites on the copper - zinc oxide catalyst. This analysis indicated that the models which use copper(I) dissolved in zinc oxide or the copper - zinc oxide interface as the active sites were plausible ones. The model in which the active site is the copper surface area was not plausible based on the data.

1.0 INTRODUCTION

1.1 The Role of Methanol

Methanol, a relatively simple organic molecule, is one of the most important chemicals in today's world. The production of methanol in 1983 was over three million tons. This demand ranks methanol twenty-second on the list of most produced chemicals (1).

The demand for methanol arises from a number of different areas. One of the uses for methanol is as an industrial solvent. It is used in very large quantities as a basic raw material in the production of formaldehyde, and is also used for production of acetic acid, methyl halides, methyl amines, methyl methacrylate, methyl tertiary-butyl ether, and other chemicals. The newest use for methanol is as a fuel, by itself or in blends with other fuels.

It was the potential use of methanol as a fuel which caused the great interest for research into the catalytic synthesis of methanol in the last decade. While the impact of methanol on the fuel market has not been as great as initially expected, the interest in methanol still continues (2).

1.2 Methanol Synthesis

Methanol is currently produced by hydrogenation of carbon

monoxide and carbon dioxide, equations 1 and 2. This is

$$CO + 2H_2 \rightleftharpoons CH_3OH \quad (1)$$

$$CO_2 + 3H_2 \rightleftharpoons CH_3OH + H_2O \quad (2)$$

remarkable in light of the fact that methanol is one of the least thermodynamically favorable products of this reaction (3,4). Other initial products which could be formed include methane and larger hydrocarbons by a Fischer-Tropsch reaction, equations 3 and 4, carbon dioxide via the Boudouart reaction, equation 5, and carbon dioxide or carbon monoxide from the Water-Gas Shift reaction, equation 6. Furthermore, methanol

$$CO + 3H_2 \longrightarrow CH_4 + H_2O \quad (3)$$

$$nCO + 2nH_2 \longrightarrow (CH_2)_n + nH_2O \quad (4)$$

$$2CO \longrightarrow CO_2 + C \quad (5)$$

$$CO + H_2O \rightleftharpoons CO_2 + H_2 \quad (6)$$

may not be the final product in the synthesis and may react further through a number of possible paths. Ethers, equation 7, higher alcohols, e.g. equation 8, and acids, e.g. equation 9, are

all possible products. Some of these products may react even further to produce quite a variety of final products.

$$2CH_3OH \rightleftharpoons CH_3OCH_3 + H_2O \qquad (7)$$

$$CH_3OH + CO + 2H_2 \longrightarrow C_2H_5OH + H_2O \qquad (8)$$

$$CH_3OH + CO \longrightarrow CH_3COOH \qquad (9)$$

Because of the many possible paths for the reaction of carbon monoxide and hydrogen to take, a very selective catalyst is needed for methanol synthesis. Formation of methanol by hydrogenation of carbon monoxide was commercialized in 1923 (5). This process employed a zinc oxide - chromia catalyst which operated at 20 MPa and 625 K. The inductrial manufacture of methanol began to change in the 1960's when a better catalyst based on copper was brought into use. Currently, copper - zinc oxide - alumina catalysts operating at 5 - 10 MPa and 490 - 520 K are in use. Selectivity toward methanol formation over these catalysts is near 100%. The active species here is the Cu/ZnO, with the other oxide believed functioning mainly as a stabilizing support.

The exact mechanism of the reaction of carbon monoxide and hydrogen to form methanol over these catalysts is still subject to much research and debate. Even though methanol is

being commercially produced via this route, a great deal of study is still being put into elucidation of the mechanism. The reason for the study is that when the reaction mechanism is known, one may be able to steer this reaction and other similar reactions toward any desired possible product.

1.3 The Interest in Thallium

The interest in studying the effect of thallium on the Cu/ZnO catalysts arose from the results of some recent work on this catalyst system with alkali promoters.

The effect of alkali dopants on the old high pressure methanol catalysts had been studied many years ago but the effect on the low pressure copper based catalyst was only recently investigated (6). It was found that doping a 30/70 Cu/ZnO catalyst with 0.4 atom% of lithium and sodium decreases the activity of the catalyst while potassium, rubidium, and cesium increase the rate of methanol formation over this catalyst. At 508 K and 7.6 MPa with a gas flow of 10.5 dm^3/hr of hydrogen and 4.5 dm^3/hr of carbon monoxide over 2.45 g of the catalyst, the undoped Cu/ZnO produced 240 g CH_3OH/kg catalyst/hr while the Cs/Cu/ZnO produced 455 g CH_3OH/kg catalyst/hr. The cesium also caused an increased production of ethanol and methyl formate at these conditions. Vedage (7) reported addition of small amounts of water to the feed gas increased the activity of Cu/ZnO toward methanol formation. Larger

amounts of water then decreased the activity of the catalyst. The effect of cesium doping of the Cu/ZnO catalyst on methanol formation in synthesis gas containing water has also been recently studied (8). Cesium has been shown to promote methanol formation in the water-free synthesis gas and in synthesis gas containing more than about 5 % of water.

Thallium forms a stable +1 oxidation state which has a chemistry very similar to that of the alkali ions, especially potassium and rubidium (9). The formation of this oxidation state results from the so-called inert pair effect in which the 6 s electrons in thallium form a stable subshell (10). There are many known inorganic and coordination compounds of thallium which resemble compounds of the alkali metals (11). While the chemistry of thallium (+1) is rich in this respect, there is essentially no organometallic chemistry of thallium (+1), with all of the known organometallic chemistry of thallium associated with the +3 oxidation state (12).

Because of its similarity to the alkalis, the effect of thallium on catalysts is often studied when the effect of the alkalis is studied. Thallium is seen in small amounts on dehydrogenation and oxidation catalysts where it is used as a poison to improve the catalysts' selectivity toward desired products.

The effect of thallium on the Cu/ZnO methanol synthesis catalyst has been briefly surveyed (13). It was found that

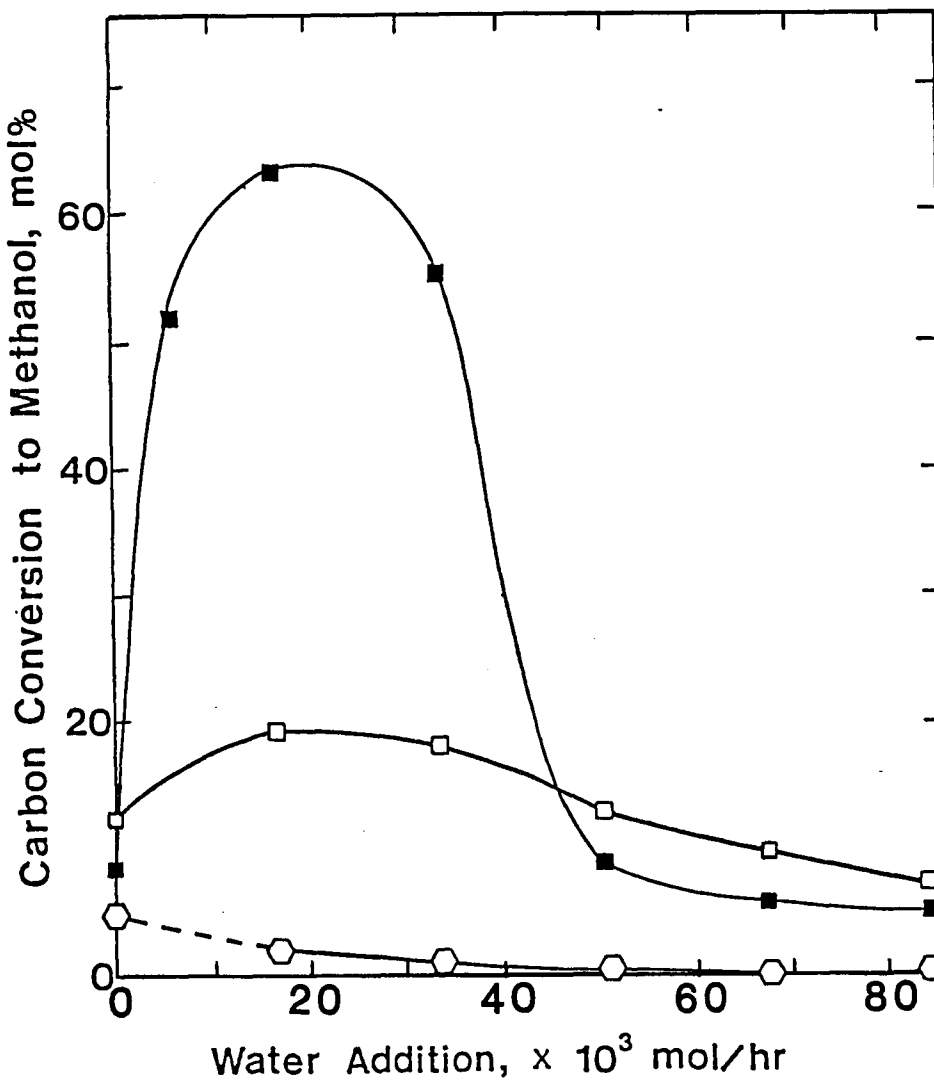

Figure 1 - Conversion of carbon monoxide to methanol versus water added to feed gas stream over Cu/ZnO based catalysts. Conversions at 508 K, 7.6 MPa, 10.5 dm^3/hr H_2, 4.5 dm^3/hr CO, 2.45 g catalyst. Catalysts - 30/70 Cu/ZnO (■), 0.4/30/70 Cs/Cu/ZnO (□), 0.4/30/70 Tl/Cu/ZnO (⬡).

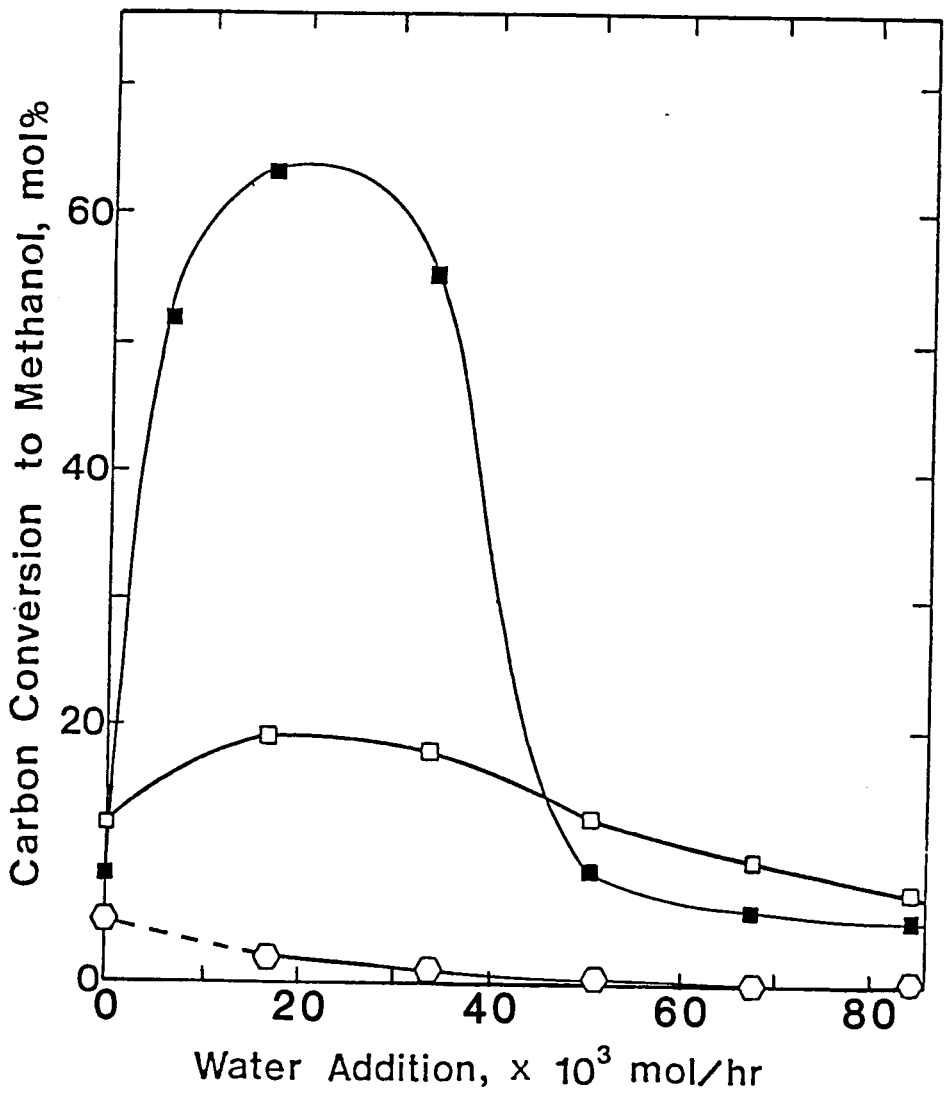

Figure 1 - Conversion of carbon monoxide to methanol versus water added to feed gas stream over Cu/ZnO based catalysts. Conversions at 508 K, 7.6 MPa, 10.5 dm^3/hr H_2, 4.5 dm^3/hr CO, 2.45 g catalyst. Catalysts - 30/70 Cu/ZnO (■), 0.4/30/70 Cs/Cu/ZnO (□), 0.4/30/70 Tl/Cu/ZnO (⬡).

small amounts of thallium poison the Cu/ZnO catalyst. This is in contrast to the effects of potassium, rubidium, and cesium which increase catalytic activity. It is this poisoning effect which, when studied further, could prove useful in helping to explain the way in which the Cu/ZnO catalyst converts carbon monoxide and hydrogen into methanol and other products and to identify the location as well as the concentration of the active centers.

1.4 Scope of the Research

The present investigation deals with the effect of thallium doping on the catalytic activity of the Cu/ZnO methanol synthesis catalyst. A number of catalysts containing thallium in varying concentrations were prepared and tested for activity toward the synthesis of methanol and other products. Furthermore, these catalysts were characterized by surface area measurements, by x-ray diffraction, and by x-ray photoelectron spectroscopy in order to determine their physical characteristics.

This study was undertaken in order to determine the effect of thallium on the activity of the catalyst, to determine the nature of the poisoning effect, to gain insight into the nature of the active catalyst sites, and to gain insight into the mechanism of product formation over this catalyst.

1.4.1 Catalyst Testing

The main objective of catalyst testing was to determine the carbon monoxide conversion activity and product distribution of the thallium containing catalysts in both water-free and water containing synthesis gas consisting of 30 parts of carbon monoxide and 70 parts of hydrogen.

The water-free synthesis gas was used in the standard testing of these catalysts, in which methanol was selectively produced. Addition of water to the feed gas stream changed the distribution of products and led to the formation of carbon dioxide.

1.4.2 Surface Area Measurements

The surface area of all catalysts was measured using the BET method. In this method, the amount of inert gas adsorbed on a weighed solid sample as a function of pressure at a constant temperature was accurately measured. The experimental adsorption isotherm data were then treated using equations which describe the adsorption process based upon the intermolecular forces (mainly van der Waals attraction) present between the gas and the solid (14).

The surface area of a catalyst is an important parameter because the number of active sites exposed to the reactants influences the rate of the reaction, and the number of sites exposed is a function of the surface area.

1.4.3 X-Ray Diffraction

X-ray powder diffraction is an important method for bulk characterization of materials. It can be used to identify the material phases present in the bulk substance, to calculate the sizes of the particles making up the component phases of the material, and to determine the deviations in the lattice structure of the components from that of standard materials.

Since x-rays have wavelengths comparable to the spacing between atoms in solid lattices, they can be diffracted by the lattices, Figure 2. The lattice planes give rise to constructive and destructive interference in these diffracted beams based upon the difference in path length of x-rays through the solid. Reflections due to constructive interference can be detected when the Bragg condition is satisfied. In the Bragg equation, equation 10, n is an integer, λ is the x-ray wave-

$$n\lambda = 2d\sin\theta \qquad (10)$$

length, d is the spacing between planes, and θ is the angle between the incident rays and the crystal plane. Powdered samples are used so that some crystallites of every orientation necessary to produce all possible reflections are present. The resulting diffraction pattern, with the location and intensity of the reflections, is characteristic of the compound making up the particle. Deviations in the lattice spacings can be

calculated using the Bragg equation and comparing experimental values with the standard values.

As particles become smaller and smaller, the ability of the particle to give rise to total destructive interference of diffracted beams decreases. The result is a broadening of the diffraction peaks. An exact treatment of this problem leads to the Scherrer formula, which can be used to calculate the thickness of particles. The Scherrer formula is (15):

$$t = \frac{0.9 \ \lambda}{(B_o^2 - B^2)^{\frac{1}{2}} \cos \theta} \qquad (11)$$

where t is particle thickness, λ is the x-ray wavelength, B_o is the instrumental broadening, B is the width of the peak at one half of its height (in radians), and θ is the Bragg angle.

1.4.4 X-Ray Photoelectron Spectroscopy

X-ray photoelectron spectroscopy (XPS) is a powerful tool used in the surface analysis of materials. It can be used to identify the elements present in a material and to determine their relative amounts and chemical oxidation state.

In XPS, monoenergetic x-rays are used to irradiate a sample. These x-rays can interact with atoms up to a few micrometers deep in the sample and can cause an electron to be emitted from the atom via the photoelectric effect, Figure 3. These photoelectrons have characteristic kinetic energy, KE, given by:

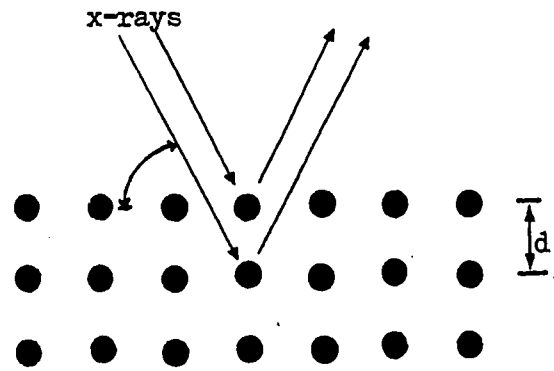

Figure 2 - Diffraction of x-rays from a crystal lattice.

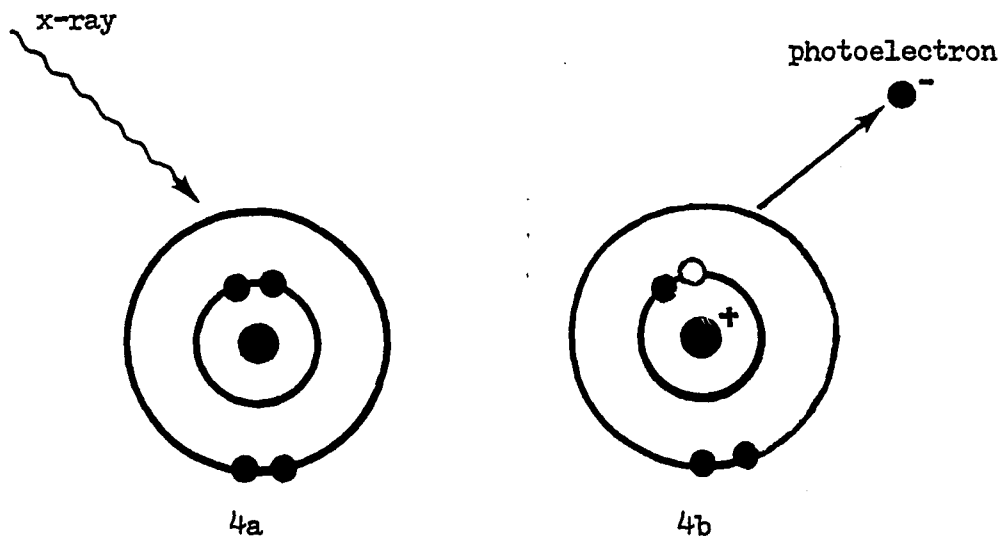

Figure 3 - The photoelectric effect: a - incoming x-rays, b - emitted photoelectron

$$KE = h\nu - BE \qquad (12)$$

where $h\nu$ is the incident x-ray energy and BE is the binding energy for the atomic level from which the photoelectron originates. Since the binding energy is close to the ionization energy of a given level, it depends upon the element it is associated with and upon the orbital that the electron comes from. Only those electrons which arise from atoms in the top few nanometers near the sample surface can leave the solid without undergoing some other interaction with the sample. It is these escaping electrons which are analyzed for kinetic energy, and therefore give an analysis of the elements present on the surface of the sample.

One must go into a more in-depth treatment in order to obtain quantitative information from the above qualitative analysis. Electrons of different energies have different probabilities of escaping from the solid, characterized by a parameter termed the escape depth. Also, electrons in different atomic orbitals have different probabilities of interacting with the incoming x-rays, called the photoionization cross sections. The amounts of surface species can be calculated based upon escape depths, photoionization cross sections, and other experimental parameters. The equation which best fits our particular purpose is the one given by Dreiling (16):

$$I_i = \frac{k\, g\, \lambda_i\, \sigma_i\, x_i}{E_i} \left[1 - \exp\left(\frac{-z}{g\, \lambda_i}\right)\right] \qquad (13)$$

where: I_i is the intensity of the detected photoelectron signal from a particular orbital of the element i; k is a constant which includes instrumental factors such as the analyzer acceptance angle and x-ray flux; g is a specimen-spectrometer geometrical factor which takes into account the angle of escape of the electron with respect to the surface normal; x_i is the atomic volume concentration of element i; σ_i is the photoionization cross section for the photoelectron observed from element i; λ_i is the escape depth for the photoelectron from element i; E_i is the kinetic energy of the photoelectron; and z is the thickness of the layer from which the signal arises. Intensities of signals from all elements present can be normalized to give the relative distribution of elements in a surface layer of the sample.

Information about the chemical state of the elements can sometimes be obtained. Since the energy of atomic levels is influenced by the bonding of the atom in the surrounding lattice, the binding energies of the levels are also slightly changed. Therefore, information about the chemical state of elements can be obtained from an analysis of the changes in the binding energy of the electrons.

X-ray photoelectron spectroscopy was used in this study

to determine the elements present on the surface of the catalyst, to determine their relative surface concentrations, and to determine the chemical state of these species if possible.

1.4.5 Scientific Information Gained

The relation between the extent of poisoning under various reaction conditions, surface area measurements, x-ray diffraction analysis, and x-ray photoelectron spectroscopic analysis allows qualitative conclusions to be drawn as to the location of active surface sites in the two phase catalyst and quantitative estimates of the surface concentration of active sites to be made.

2.0 EXPERIMENTAL

2.1 Catalyst Preparation

The thallium doped catalysts were all prepared in the same manner. The 30/70 Cu/ZnO catalyst was prepared by coprecipitation of the catalyst precursor from a solution of the nitrates by addition of sodium carbonate solution. The precursor was then calcined and reduced, giving the Cu/ZnO. Portions of this material were doped by addition to an aqueous solution of thallium formate, followed by evaporation of the water.

The CuO/ZnO base catalyst was made in 50 g batches as described previously (17). To 2000 cm^3 of distilled water in a large beaker were added 41.5 g (0.187 mol) of $Cu(NO_3)_2 \cdot 3H_2O$ (Fisher Scientific Co., Certified ACS grade) and 129.0 g (0.433 mol) of $Zn(NO_3)_2 \cdot 6H_2O$ (Fisher Scientific Co., Certified grade). The resulting solution was stirred vigorously and heated to 353 - 363 K. While maintaining the temperature, a solution of 1.0 M Na_2CO_3 (Fisher Scientific Co., Certified ACS grade) was slowly added to the nitrate solution, until the pH rose to 6.8 to 7.0. Over a period of 2 hrs, approximately 600 cm^3 of sodium carbonate solution were added. The resulting precipitate was collected, washed thoroughly with distilled water, and air dried, affording the catalyst precursor - $(Cu,Zn)_5(CO_3)_2(OH)_6$. This material was calcined in air by

heating initially to 373 K and then increasing the temperature 50 K every 30 min until a final temperature of 623 K was reached. This material was left at 623 K for 3 hrs, and then cooled, giving the desired CuO/ZnO.

The oxide powder was pelletized by addition of enough distilled water to make a thick slurry. The slurry was placed into a Teflon mold and dried overnight in an oven at 373 K, giving cylindrical pellets (3mm dia by 10 mm long). These cylindrical pellets were cut and sieved to 10/20 mesh (U.S. standard sieve size).

Approximately 4.5 g (7.5 cm^3 volume) of the 10/20 mesh CuO/ZnO pellets were diluted to 15 cm^3 volume with 3 mm glass beads and centered into the catalyst testing reactor. After attaching the reactor to the testing apparatus, a 60 cm^3/min flow of 2% H_2/N_2 (Air Products and Chemicals Inc., Zero grade gas mixture) was started over the catalyst and the temperature was raised to 523 K. The effluent gas was monitored by gas chromatography for the water produced in the reduction. When the effluent gas water concentration decreased, the reduction was stopped by cooling the reactor. Working in a glovebag (Instruments for Research and Industry) filled with nitrogen (MG Scientific Gases, 99.998%), the reduced Cu/ZnO was removed from the reactor and collected.

Two solutions of different concentrations of thallium formate were prepared and used in the doping process. Enough

Tl(OOCH) (Alfa Products, 97%) was added to 10 cm^3 of deoxygenated distilled water to make a 0.4 M solution. One cm^3 of this solution was diluted to give a 0.04 M solution.

The doping procedure, described below, was all done in a large glovebag filled with nitrogen. Based upon the weight of the Cu/ZnO and the desired concentration of thallium in the final catalyst, the necessary amount of thallium formate solution was added to 25 - 30 cm^3 of deoxygenated distilled water in a medium beaker. The reduced Cu/ZnO was added to and immersed in the thallium containing solution. A hotplate set on low heat and a slow stream of nitrogen directed into the beaker were used to evaporate off the water. After 4 - 6 hrs, the dry catalyst was collected and bottled for testing and characterization.

For characterization purposes, a portion of one of the doped catalysts was re-reduced. Working in a glovebag under nitrogen, about 0.3 g of the 0.08% Tl/Cu/ZnO was loaded into the testing reactor. The sample was reduced using the same procedure used for the Cu/ZnO. After reduction was completed, the catalyst was recovered under nitrogen and saved for characterization.

2.2 Catalyst Testing

2.2.1 Catalyst Testing Unit

The apparatus used for catalyst reduction and testing is shown schematically in Figure 4. This unit is capable of routinely operating at a pressure of 7.6 MPa and temperatures up to 573 K and higher.

The feed gases, hydrogen and carbon monoxide (MG Scientific Gases, hydrogen - 99.999%, carbon monoxide - 99.5%) were removed from the cylinders using high pressure regulators (Air Products and Chemicals Inc.) and passed through activated charcoal traps. The individual gas flows were adjusted using mass flow controllers capable of operating at high pressures (Union Carbide Corp.), and then allowed to mix together.

Water and water/isopropanol mixtures were introduced into the feed stream through the use of a high pressure liquid pump (Gilson Medical Electronics, Inc.). Initially, the pump was capable of adding liquid in multiples of 5 mm^3/min, and was later modified to allow lower pumping rates, in multiples of 0.5 mm^3/min.

The reactor was constructed from a stainless steel tube (18 mm ID x 25 mm OD x 640 mm long). A thermocouple well was incorporated into the reactor and was centered lengthwise through it to allow accurate temperature measurement of the catalyst bed. The exit end of the reactor contained a large

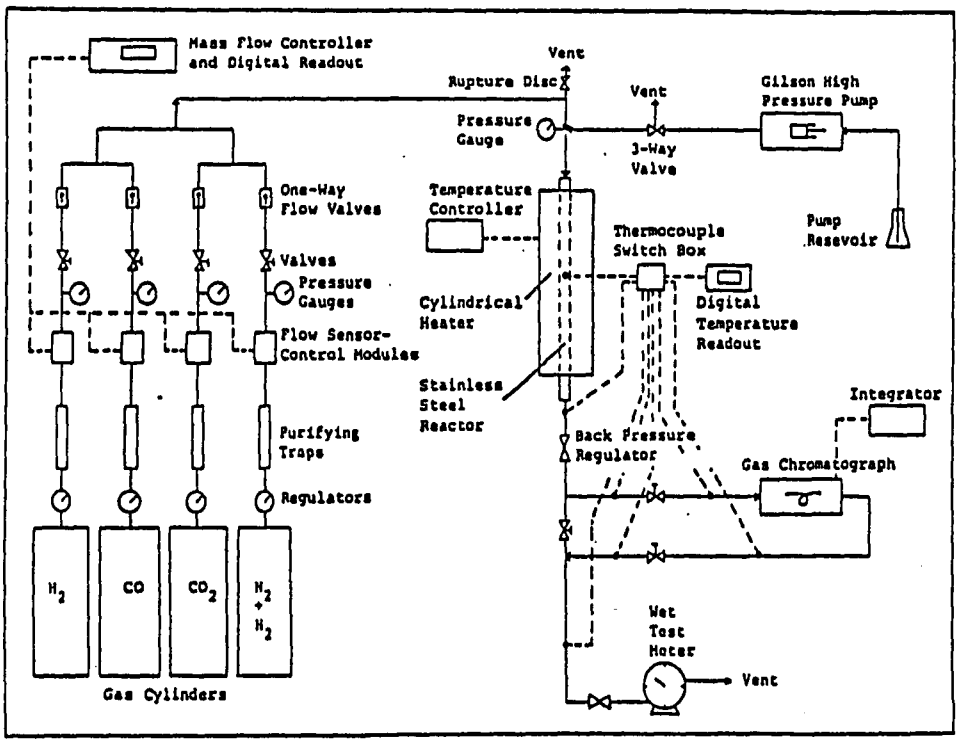

Figure 4 - Catalyst Testing Apparatus

metal "O" ring coupling which facilitated catalyst loading and unloading. The reactor was heated using a split tube furnace (S B Lindberg Co.) and was regulated by a temperature controller (Theall Engineering Co.).

Effluent gas leaving the reactor passed through stainless steel lines which were maintained at 463 K using heating tapes. A back pressure regulator (Tescom Corp.) was used to reduce the pressure to atmospheric while maintaining the upstream pressure at the desired level. The gas was then split into two streams, one of which passed through an automatic gas sampling valve attached to a gas chromatograph, after which the two streams were reunited. The gas lines downstream from the back-pressure regulator were heated to 423 K using heating tapes. Finally, the exit gas passed through a wet test meter (Precision Scientific Co.) before being directed into the exhaust system.

The temperatures of the reactor and the gas lines were monitored using thermocouples and a multichannel digital temperature readout unit (Omega Engineering).

2.2.2 Catalyst Testing Procedure

The initial testing of all of the catalysts studied here was the same. Working in a nitrogen filled glovebag, 2.45 g of doped catalyst (3 - 4 cm^3 vol) was diluted with enough 3 mm glass beads to bring the total catalyst bed volume to 10 cm^3. This mixture was then centered in the reactor through use of

more glass beads. The reactor was sealed, removed from the glovebag, and attached to the testing unit.

First, a 10.5 dm^3(STP)/hr flow of hydrogen was established over the catalyst, followed by addition of 4.5 dm^3/hr of carbon monoxide to this feed stream. After allowing the feed gas to flow through the system for about 1 hr, the pressure inside the apparatus was increased to 7.6 MPa by adjusting the back-pressure regulator, which allowed the feed gas flow to buildup the pressure. Following pressure buildup, the reactor temperature was increased at a rate of 2 - 3 K/min to 523 K. This was the initial testing condition for the thallium-doped catalysts.

This initial condition was maintained for 12 - 16 hrs before decreasing the temperature to 508 K. For the next 6 hrs, the testing conditions were 508 K, 7.6 MPa, 10.5 dm^3/hr H_2, and 4.5 dm^3/hr CO.

It was at this point that water addition to the feed stream was started. Tap water was distilled and then deoxygenated prior to use by boiling and cooling with nitrogen gas bubbling through it. Throughout the water addition, the temperature was kept at 508 K, with the gas flows and pressure as before, Initially, a water flow rate of 5 mm^3/min was started and maintained for 12 hrs using the liquid pump. The water addition was then changed to 10 mm^3/min for 6 hrs, 15 mm^3/min for 6 hrs, 20 mm^3/min for 12 hrs, and 25 mm^3/min for 6 hrs. After this point, the testing of the catalysts varied slightly from sample

to sample, and is described next.

The catalyst testing for the 0.23% Tl/Cu/ZnO was completed by stopping the water addition and allowing the system to reach a water-free steady state. Testing of this catalyst was then stopped by cooling the reactor and depressurizing the system.

The 0.08% Tl/Cu/ZnO catalyst was also allowed to reach a water-free steady state, as with the 0.23% Tl/Cu/ZnO above, before the testing was stopped.

Testing of the 0.02% Tl/Cu/ZnO catalyst was varied somewhat since it was realized that catalyst deactivation and catalyst activity in the water addition range between 0 and 5 mm^3/min had to be studied further. After the initial testing period of this catalyst, the water addition rate was reduced from 25 to 5 mm^3/min for 18 hrs. The water addition was then stopped totally for 12 hrs while the system returned to a water-free state. Then, water was again introduced at 5 mm^3/min for 12 hrs, and at 25 mm^3/min for 6 hrs, after which time the water pumping was again stopped for about 24 hrs. Since at this time the liquid pump was only capable of pumping in multiples of 5 mm^3/min, solutions containing varying amounts of water had to be used to obtain low effective water addition rates. Vedage (6) has shown that water/isopropanol solutions could be used in these systems. Isopropanol (Fisher Scientific Co., Certified grade) was deoxygenated by bubbling nitrogen through it for 2 - 4 hrs, and solutions with water were made in a nitrogen filled glovebag.

Various water/isopropanol solutions were introduced into the system at a rate of 5 mm^3/min to give effective water addition rates of 3, 2, 4, and 1 mm^3/min for about 6 hrs each. Following this, pure water was added at 5 mm^3/min for 12 hrs, and then stopped for 18 hrs while the system returned to a water-free state. The testing was stopped by cooling and depressurizing the reactor.

The last catalyst tested was a 0.17% Tl/Cu/ZnO sample. Following the initial testing in water-free synthesis gas and synthesis gas containing 5 - 25 mm^3/min of water, the water addition was reduced to 5 mm^3/min for 6 hrs and then stopped totally for 12 hrs. The liquid pump had been modified with a new pump head so that it was now capable of pumping liquid in multiples of 0.5 mm^3/min. Therefore, pure water continued to be used instead of water/isopropanol mixtures. Water was added at a rate of 1.0 mm^3/min for 6 hrs, 2.0 mm^3/min for 6 hrs, and then stopped for 12 hrs. This was followed by 3.0 mm^3/min for 6 hrs, and 4.0 mm^3/min for 6 hrs, after which the water addition was again stopped for 12 hrs. Lastly, water was added at a rate of 0.5 mm^3/min and 1.5 mm^3/min for 6 hrs each, followed by no water addition for 15 hrs. The reaction was stopped by cooling and depressurizing the system.

In order to gain more insight into the physical aspects of the catalyst deactivation, some short-term testing was done. Part of the extra doped but untested 0.08% Tl/Cu/ZnO, about

0.46 g, was loaded into the reactor and attached to the testing unit. A hydrogen flow of 10.5 dm^3/hr and a carbon monoxide flow of 4.5 dm^3/hr were introduced and the pressure was raised to 7.6 MPa. The temperature was increased 2 - 3 K/min to 523 K where it was kept for 14 hrs. The temperature was reduced to 508 K for 6 hrs, following which, the reactor was cooled and the system depressurized. Working in a nitrogen filled glovebag, the catalyst was removed from the reactor. About 40% of the catalyst was bottled and reserved for characterization, with the rest being reloaded into the reactor. The reactor was then reattached to the testing unit, placed under the same feed gas flow, pressurized, and heated to 508 K. Water was added at a rate of 5 mm^3/min for 12 hrs, after which time, the reactor was cooled and depressurized.

After testing, all catalysts were recovered. This was done by removing the reactor from the testing unit while it contained the feed gas atmosphere, and transferring it to a large glovebag filled with nitrogen. Inside the glovebag, the reactor contents were removed and the catalyst separated from the glass beads using a 10 mesh sieve.

2.2.3 Product Analysis

Analysis of reaction products was accomplished using gas chromatography. After the testing unit's back-pressure regulator reduced the effluent gas pressure to near atmospheric, part

of the effluent gas was passed through a heated automatic gas sampling valve attached to a Hewlett-Packard 5730A gas chromatograph. The gas sampling valve was heated to 423 K, and the injection port was kept at 473 K. A 2 m by 3 mm nickel column packed with 80/100 mesh Poropak Q (Foxboro/Analabs) run at various temperatures was used for all separations. Products were detected using a thermal conductivity detector, operated at 473 K with a 130 mA current. The detector signal was sent to a Hewlett-Packard 3388 integrator for quantitative analysis. The carrier gas used was helium (MG Scientific Gases, 99.997%) at a flow rate of 25 - 30 cm^3/min.

All of the products and remaining reactants in the effluent gas could not be separated and analyzed using one set of column conditions. When run isothermally at 273 K, a good analysis for carbon dioxide, water, and methanol was obtained. Carbon monoxide and methane could not be resolved under these conditions, and a combined carbon monoxide plus methane signal was obtained. Higher products did not elute from the column at this temperature. In order to prevent isopropanol from building up on the column when water/isopropanol solutions were added to the feed, the column was run isothermally for 4 min and then temperature programmed at 16 K/min to 473 K to remove the isopropanol.

For the carbon monoxide and methane separation, the column was run isothermally at 298 K, at which temperature the two

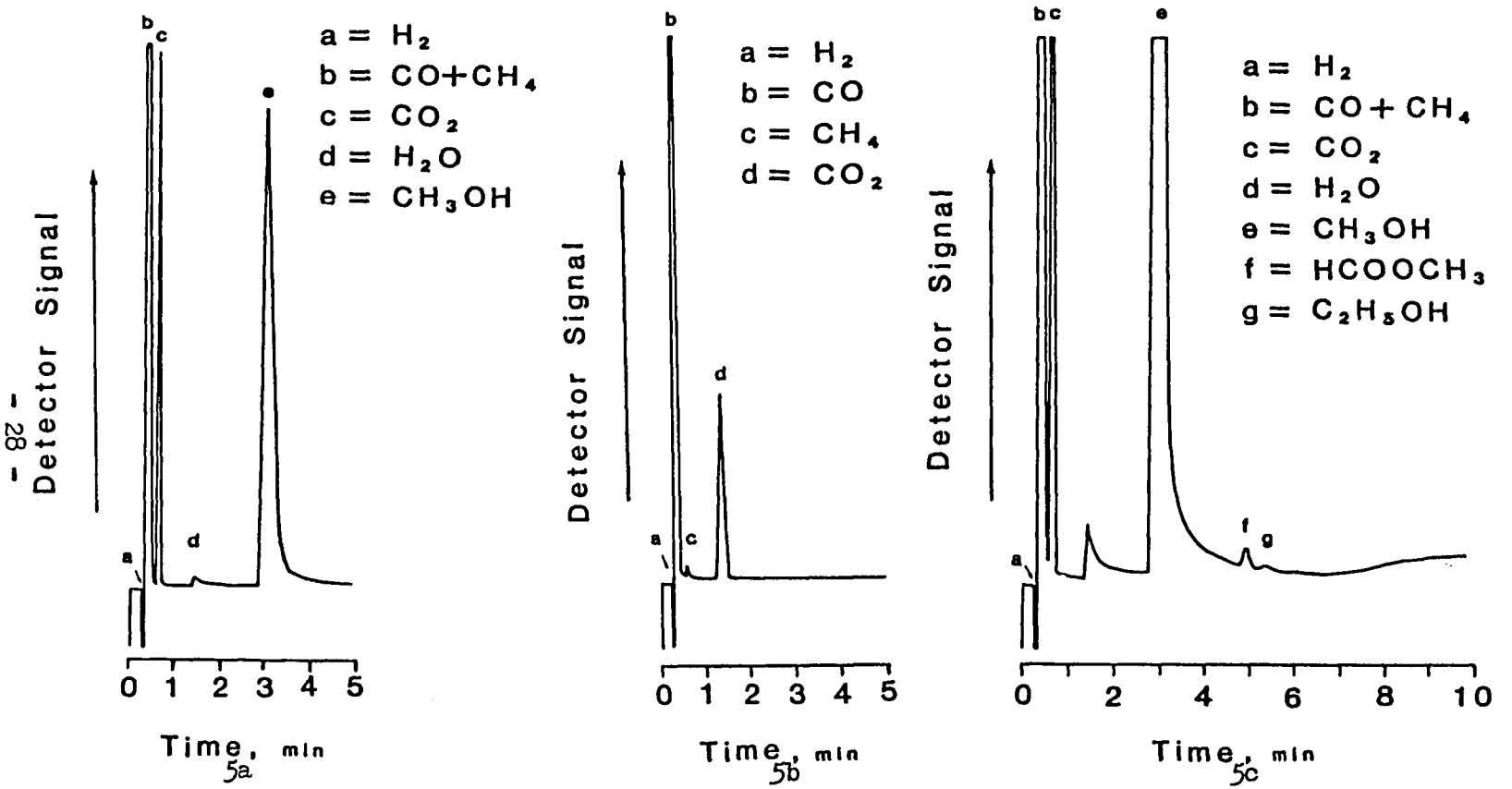

Figure 5 - Sample Gas Chromatograms, showing products and product separation at column temperatures of a) 373 K, b)298 K, c) 373 K for 2 min and 16°/min to 473 K and at 473 K for 2 min. Chromatograms from testing of 0.02% Tl/Cu/ZnO at 508 K, 7.6 MPa, 5 mm^3/min H_2O, 4.5 dm^3/hr CO, 10.5 dm^3/hr H_2. Column - Poropak Q, carrier gas - He, Detector - thermal conductivity.

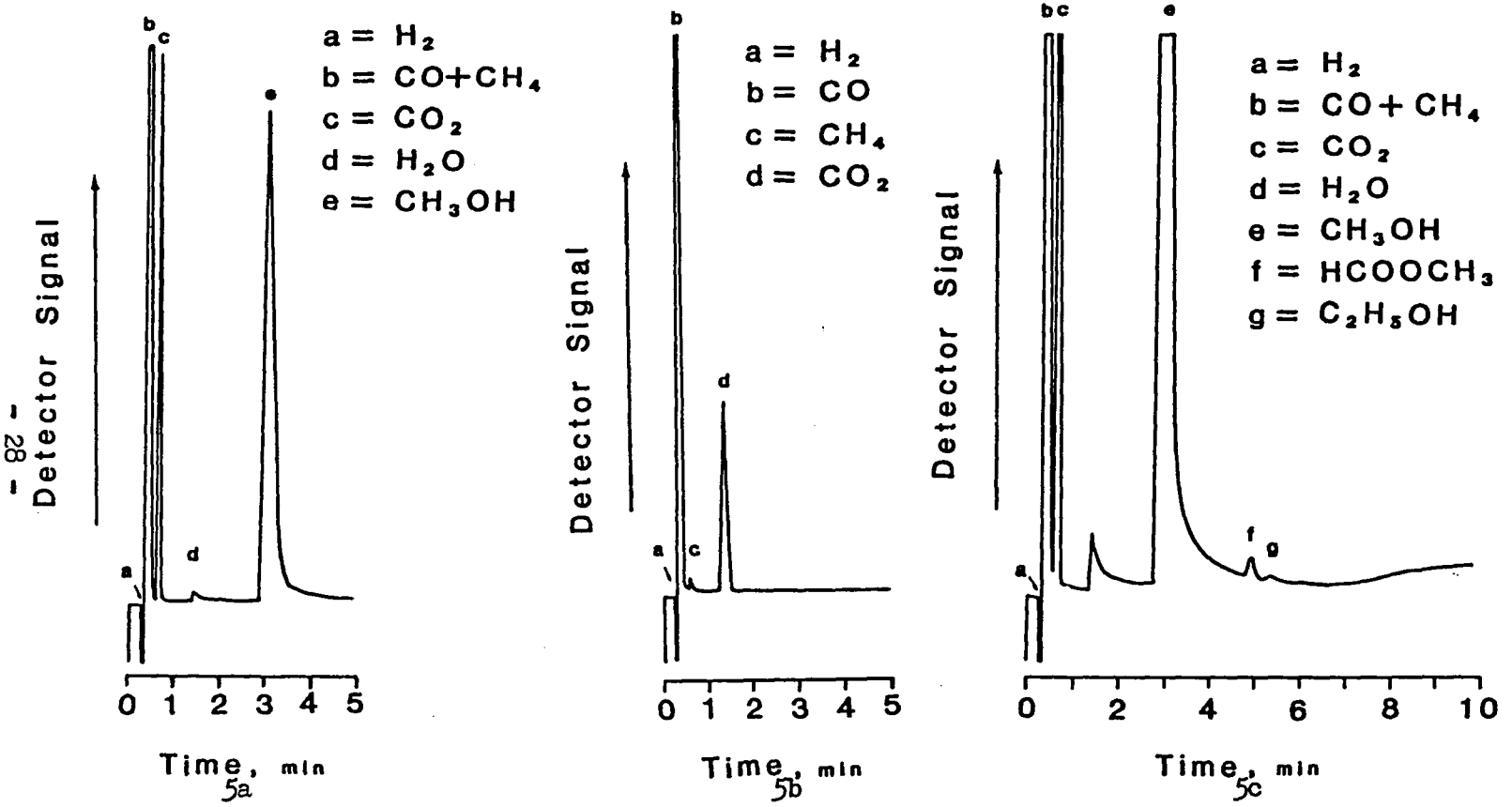

Figure 5 - Sample Gas Chromatograms, showing products and product separation at column temperatures of a) 373 K, b)298 K, c) 373 K for 2 min and 16°/min to 473 K and at 473 K for 2 min. Chromatograms from testing of 0.02% Tl/Cu/ZnO at 508 K, 7.6 MPa, 5 mm^3/min H_2O, 4.5 dm^3/hr CO, 10.5 dm^3/hr H_2. Column - Poropak Q, carrier gas - He, Detector - thermal conductivity.

signals were sufficiently resolved to obtain their relative amounts. The oven temperature was increased to 373 K (or higher if isopropanol was present) after the carbon monoxide, methane, and carbon dioxide had eluted from the column in order to drive the remaining material off of the column.

Products higher than methanol were analyzed for by temperature programming the column. The initial temperature of 373 K was maintained for 2 min, followed by a temperature increase of 16 K/min until the oven reached a final temperature of 473 K, where it was kept for 2 min. When isopropanol was present, products which might form from reaction with the isopropanol were checked for by remaining at the final temperature for 4 min.

The integrator gave relative amounts of all species except hydrogen using a combination of these three types of analysis. Hydrogen was the first compound through the column in all cases, but because of it's thermal conductivity, it produced a negative signal which could not be integrated. Direct conversion of relative amounts of products to molar concentrations based upon the effluent gas flow rate could not be done since the amount of hydrogen in the effluent gas was unknown.

The chromatographic peak areas were typically averaged over a period of 2 - 4 hrs in which the catalyst activity seemed fairly constant. The relative area percents of components were converted into relative molar concentrations (less hydrogen concentration) by dividing each component signal by a tabulated

thermal response factor (18), Table 1, followed by normalization of corrected signals to 100%. Conversion of relative molar concentrations of species to moles per unit time was done based upon balancing the amount of oxygen and carbon entering the reactor with the amount leaving the reactor in the effluent. Concentration of species in the effluent is based upon conservation of oxygen, and this concentration is checked based upon conservation of carbon. A sample calculation is shown in Table 2.

2.3 BET Surface Area Measurements

2.3.1 BET Apparatus

The apparatus used was a volumetric system designed for gas adsorption work (19). The all glass unit incorporated the following features: 1) a vacuum system consisting of a mechanical rough pump, an oil diffusion pump, and a liquid nitrogen trap, capable of giving background pressures in the range of 1×10^{-4} Pa; 2) an electric manometer attached to a 133 kPa pressure sensor (MKS Electronics), and a null offset adaptor (Datametrics Corp.) capable of giving a sensitivity of 1 Pa over the whole sensing range; 3) a glass manifold containing 5 dm^3 reservoirs of helium and argon (prepurified grade gases, further purified by passage through copper turnings at 700 K and 3A molecular sieve at 77 K); 4) a dosing volume section

Table 1 - G. C. Thermal Response Factors*

Compound	TRF
CO	42
CO_2	48
CH_4	36
H_2O	33
CH_3OH	45**
C_2H_5OH	72
$HCOOCH_3$	72

* taken from ref. 18
** this value from ref. 6

Table 2 - Example of Determination of Product Distribution from Gas Chromatographic Data

Testing Parameters: 2.45 g of 0.02% Tl/Cu/ZnO
523 K, 7.6 MPa
10.5 dm^3/hr H_2, 4.5 dm^3/hr CO
No H_2O

	CO	CO_2	H_2O	CH_3OH	CH_4
GC Peak Areas	87.580[a]	0.228	0	12.277	0.432[b]
Normalized Areas	87.202	0.228	0	12.277	0.378
TRF	42	48	33	45	36
Area/TRF	2.0762	0.0048	0	0.2728	0.0120
Molar Concentration	87.813	0.201	0	11.539	0.448
Yield[c] mol/hr	0.1623	0.0004	0	0.0213	0.0008
Molecular Weight	28.01	44.01	18.01	32.04	16.04
Yield g/hr	4.5460	0.0176	0	0.6820	0.0128
kg/kg cat/hr	1.8555	0.0072	0	0.2780	0.0052

a - area of CO and CH_4 signals
b - signal relative to CO of 100%
c - based upon conservation of incoming oxygen from
CO - 0.1844 mol/hr
O in products: CO 87.813
CO_2 2x 0.201
H_2O 0
CH_3OH 11.539
99.754 mol% - 0.1844 mol/hr

consisting of four accurately calibrated bulbs connected to give progressively larger dosing volumes; 5) and a sample vessel made of glass tubing, about 200 mm long fitted with a glass joint at one end (for attaching to the unit) and a small bulb for samples blown out at the other end.

Every time a new sample was tested, the volume of the sample vessel had to be redetermined, and helium was used for this purpose. Argon gas was used as the adsorbate for surface area determinations. Both the volume and the surface area measurements were done with the sample vessel immersed in liquid nitrogen to a mark specified on the vessel. Since the temperature of the liquid nitrogen varied from one measurement to another, the vapor pressure of the argon at the liquid nitrogen temperature had to be calculated. This was done by determining the vapor pressure of nitrogen at the temperature of the liquid using a differential mercury manometer filled with nitrogen gas in one leg as a gas thermometer. The vapor pressure of the nitrogen was converted to a vapor pressure of argon using a calibration plot.

2.3.3 Isotherm Measurement

The first step in the experimental method was to accurately weigh the sample vessel fitted with a cork in the ground joint. Working in a glovebag filled with nitrogen, the weighed vessel was then loaded with approximately 0.1 g of catalyst pellets,

sealed using the cork, removed from the glovebag, and reweighed. The sample vessel was then attached to the adsorption unit and evacuated for a minimum of 6 - 8 hrs, followed by one hour of heating to 373 K under vacuum. The sample vessel was cooled using liquid nitrogen, and the larger dosing volumes were filled with helium for the volume measurement. The smallest dosing volume was filled with a certain dosing pressure of helium, P_d. The stopcock connecting this volume to the sample vessel was then opened, allowing the helium to expand and the pressure to come to an equilibrium value, P_e. After measuring this pressure, the stopcock was closed, and the process was repeated, starting with repressurization. Six helium dosing pressures, ranging from 0.2 - 1.6 kPa, were used for the volume determinations for each sample. The sample was warmed to room temperature and evacuated for at least one hour after the volume measurement. The sample was then again cooled in liquid nitrogen and the dosing volumes were filled with argon gas. Using a procedure similar to the volume measurement with helium, the sample was exposed to 11 dosing pressures of argon in order to obtain 11 equilibrium pressures ranging from 0.6 - 11 kPa.

2.3.3 Surface Area Calculation

The volume of the sample vessel, V_s, was determined using:

$$V_s = \frac{(P_d - P_e)}{(P_e - P'_e)} V_d \qquad (14)$$

where: P_d is the dosing pressure of helium, P_e is the equilibrium pressure of helium for the P_d, P'_e is the equilibrium pressure for the previous point, and V_d is the dosing volume. This gave six values for V_s, which were then averaged for further calculations.

The surface area was determined using the BET equation (14):

$$\frac{P}{V(P_o - P)} = \frac{1}{V_m C} + \frac{C - 1}{V_m C} \frac{P}{P_o} \qquad (15)$$

where: P is P_e, V is the amount of gas adsorbed at the equilibrium pressure P/P_o, V_m is the monolayer capacity, and C is the BET constant related to the first layer heat of adsorption. A linear regression analysis of the relationship between $P/V(P_o-P)$ and P/P_o between P/P_o of 0.05 and 0.30 gives V_m. Multiplication of V_m by the cross sectional area of argon, 0.168 nm^2 (19), gave the surface area of the sample.

2.4 X-Ray Diffraction

2.4.1 Instrumentation

The instrument used for all x-ray diffraction work was a Phillips Electronics APD-3600 automatic x-ray powder diffracto-

meter, connected to a Phillips Electronics XRG-3100 x-ray generator. The diffractometer was interfaced with a Tektronix 4010 terminal and a Tektronix 4631 hard copy unit. The x-rays were produced using a copper anode x-ray tube operated at 45 kV and 30 mA. The counter was of the scintillation type, and scanned the range of 2θ in a stepwise manner. The counter measured the diffracted beam intensity in 0.01° increments of 2θ for a time of 0.6 sec at each increment. This gave an effective scanning rate of 1.0°/min. The raw data were stored on floppy discs for workup using the software associated with the APD-3600 system. A software program (APDPEAK) was used to find peaks and to determine the position and intensity of each peak. Since this program was not infallible, all data plots were checked manually as well. A second software program (APDPLOT) was used to plot the total scans as well as to enlarge portions of the scans for further analysis.

The instrument typically uses a sample holder having an open sample cavity in it. This holder is convenient for some x-ray work since it fits into the instrument's automatic sample changer, but it exposes the samples to the atmosphere. To permit analysis without exposure to the air, a special holder was previously fabricated. This holder consists of a beryllium window mounted above a hole cut into a piece of aluminum, forming a sample cavity. A second piece of metal was then attached to the first, and gave an airtight seal through use of a rubber

"O" ring. The design was such that the top of the sample against the beryllium window was in the correct geometrical position for analysis when placed in the diffractometer.

2.4.2 X-Ray Analysis of Samples

The x-ray diffraction pattern of tested and untested samples of the 0.23, 0.08, and 0.02% Tl/Cu/ZnO catalysts and copper and zinc oxide standards were measured using the special sample holder. Working in a nitrogen-filled glovebag, the samples were ground to a fine powder and then loaded into the holder. The holder was then removed from the glovebag and placed into the diffractometer for analysis. The copper standard, zinc oxide standard, tested 0.23% Tl/Cu/ZnO, and untested 0.23% Tl/Cu/ZnO were scanned from 5 to 95° (in 2θ) at 1°/min. The other samples were scanned from 25 to 45° at 1°/min, since this range included the three most intense zinc oxide reflections, (100), (002), and (101), and the most intense copper reflection, (111).

All other samples were analyzed using the ordinary sample holders. In order to minimize air exposure, the samples were ground in the glovebag and placed into sample vials. The sealed vials were then taken to the diffractometer, and the samples quickly loaded into the holder and immediately analyzed. These samples were all analyzed from 25 to 45° at a rate of 1°/min.

2.4.3 Calculations

X-ray diffraction scans of the copper and zinc oxide standards indicated that one peak due to the sample holder window occured at 41.34^{o}. This was used as an internal standard, and values for this reflection were adjusted to 41.34^{o} in all subsequent measurements. Other peak values were also adjusted based upon this beryllium reflection. Values for lattice spacings of the samples were calculated using the Bragg equation, equation 10, with the Cu K_{α} wavelength 0.15418 nm (15).

The reflections of interest were enlarged and the widths of the peaks at one half of their heights were determined. Values for particle sizes were then determined using the Scherrer equation, equation 11, with the same value for the x-ray wavelength as above. The values for instrumental line broadening were those determined from the analysis of the copper and zinc oxide standards: ZnO (100) - 0.00312 radians, ZnO (002) - 0.00342 radians, ZnO (101) - 0.00347 radians, and Cu (111) - 0.00546 radians.

2.5 X-Ray Photoelectron Spectroscopy

2.5.1 Instrumentation

The x-ray photoelectron spectroscopy was carried out using a Physical Electronics Model 548 electron spectrometer. The

x-rays were produced using a magnesium x-ray anode operated at 10 kV and 38 - 40 mA. The energy of the photoelectrons was analyzed using a double-pass cylindrical mirror analyzer which detected the electrons as discrete events. The analyzer was run as an energy window accepting electrons within the span of the window. Increasing the energy of the window, known as the pass energy, increased the signal but decreased the resolution. A variable retarding field placed before the analyzer was used in the system to scan the energy spectrum. The vacuum chamber used an ion pump to reduce the pressure to 1×10^{-7} Pa. The chamber also incorporated a 12 place sample carousel, a microscope for sample positioning, and equipment to do Auger electron spectroscopy. The system contained a multichannel analyzer (Nicolet), for signal averaging work. This analyzer was attached to a tape deck to store data on magnetic tape.

2.5.2 Sample Preparation

Samples were prepared and mounted on the carousel for analysis in two different ways, depending upon the type of analysis desired.

The first method was used for the tested 0.02, 0.08, and 0.23% Tl/Cu/ZnO catalysts and for the untested 0.23% Tl/Cu/ZnO catalyst in order to analyze for thallium, zinc, copper, and oxygen. The method used double stick tape to hold the sample in place for analysis. One side of a piece of gold plated

copper, about 15 x 10 mm, was covered with double stick adhesive tape. A layer of powdered sample was placed on top of the tape and pressed onto it. This metal piece was then mounted on the carousel. Carbon analysis could not be accurately done on these samples since the adhesive tape contained carbon.

The second method was used for analysis of surface carbon and made use of aluminum holders. The holders were approximately 18 mm long x 10 mm wide x 2 mm thick, and had a 6 mm dia x 1 mm deep cavity in the center. The holders were washed in distilled water, trichloroethylene, and absolute ethanol before being used. Powdered samples were pressed into the cavity. The aluminum holder was then mounted onto the carousel. This method was used for three samples, reduced undoped Cu/ZnO, untested 0.23% Tl/Cu/ZnO, and tested 0.23% Tl/Cu/ZnO.

Sample preparation was done in air for both analysis methods. Air exposure time was from 30 to 60 min in the first method, and from 15 to 30 min in the second method.

2.5.3 Data Acquisition

Initially, a survey scan covering the full range of binding energies was performed on each sample. This scan ran from 1100 to 0 eV binding energy, and was done with a pass energy of 100 eV, a time constant (response time) of 0.1 sec, a scan rate of 2 eV/sec, and a sensitivity of 30 - 300 k (k = 1000 events). This survey scan was used to determine the elements present.

High resolution scans were then performed on the most intense signal or signals for all of the elements present. The signals used were Zn $2p_{\frac{3}{2}}$ and $2p_{\frac{1}{2}}$, Cu $2p_{\frac{3}{2}}$ and $2p_{\frac{1}{2}}$, and O 1s. These high resolution single scans were done using a 50 eV scanning range centered on the peak or peaks, a pass energy of 100 eV, a time constant of 0.1 sec, a scan rate of 0.2 eV/sec, and a sensitivity of 30 - 300 k. The thallium signal was too weak to be analyzed using a single pass scan. The Tl $4f_{\frac{7}{2}}$ and $4f_{\frac{5}{2}}$ signals were scanned along with the Zn 3p signal using signal averaging on the multichannel analyzer. The three peaks were analyzed within a 50 eV scan range and scanned 32 times with a 50 eV pass energy, 0.1 sec time constant, a 0.5 eV/sec scan rate, and a 1 k sensitivity. An analysis of a catalyst containing no thallium showed a small Cu 3s peak located where the Tl $4f_{\frac{5}{2}}$ peak would appear in doped catalysts. Because of the signal averaging, the thallium signal could not be directly compared to the zinc, copper, and oxygen peaks, and a comparison had to be done in a stepwise manner. One more scan was done on each sample, using a 500 eV range which included the O 1s and Zn 3p peaks. Eight scans were signal averaged using a 100 eV pass energy, 5 eV/sec scanning rate, 0.1 sec time constant, and a 30 k sensitivity. This gave the ratio of the O 1s to Zn 3p signals, and since the Tl $4f_{\frac{7}{2}}$ to Zn 3p ratio could be determined from the thallium analysis, the thallium signal could be determined relative to the O 1s signal.

The analysis for surface carbon was done on samples mounted on the aluminum holders. Again, the first scan done was a survey scan from 1100 to 0 eV, using a 100 eV pass energy, 0.1 sec time constant, a 2 eV/sec scanning rate, and a 100 - 300 k sensitivity. A high resolution scan was performed on the Zn 2p doublet using a 50 eV scanning range, with a 100 eV pass energy, 0.1 sec time constant, 0.2 eV/sec scanning rate, and a 100 - 300 k sensitivity. The carbon signals were signal averaged due to the low intensity. This was done using a 50 eV scanning range which included the C 1s and Zn LMM signals. For this signal averaging, 16 scans were averaged using a 100 eV pass energy, 0.1 sec time constant, 0.5 eV/sec scanning rate, and a 10 - 30 k sensitivity. The averaged data was then stored on magnetic tape for analysis.

2.5.4 Data Treatment

Identification of elements present was done by identifying the signals on the survey scan and high resolution scans and comparing the experimental binding energies with tabulated values (20). Determination of true binding energies for the above analysis and for possible determination of chemical state of species required some data treatment. The raw data values for binding energy may be higher than the true binding energies because when electrons are lost from these catalyst samples, the samples may become charges which results in an apparant

increase in binding energy. It is known that zinc is present as zinc oxide, and the Zn $2p_{\frac{3}{2}}$ signal was therefore set equal to a known value of 1021.7 eV for zinc oxide (20). All other peaks were shifted by the same amount to give corrected binding energies, which could then be compared to tabulated values.

Determination of the surface concentration of thallium required a number of calculations, some of which were based on assumptions and on the experimental results themselves. Dreiling's equation, equation 13, related the intensity of an observed signal to the atomic volume concentration of that element. The catalyst samples analyzed are not homogeneous with respect to the distribution of elements and Dreiling's equation needed to be further modified. The thallium doped onto the already prepared Cu/ZnO was assumed to be present only on the surface of the sample, as depicted in Figure 6. In this model, the value for z in Dreiling's equation, the thickness of the particle from which the signal originates, becomes equal to the diameter of thallium when one considers the intensity of the thallium signal, and equal to the thickness of the ZnO particle when one considers the intensity of the zinc signal. For the thallium, z_{Tl} is small compared to $g\lambda_{Tl}$ and the intensity equation is simplified to equation 16. The value of z_{Zn} is large when compared to $g\lambda_{Zn}$, and the intensity equation can also be simplified. The intensity of the zinc signal is attenuated by the thallium on the surface by a factor of

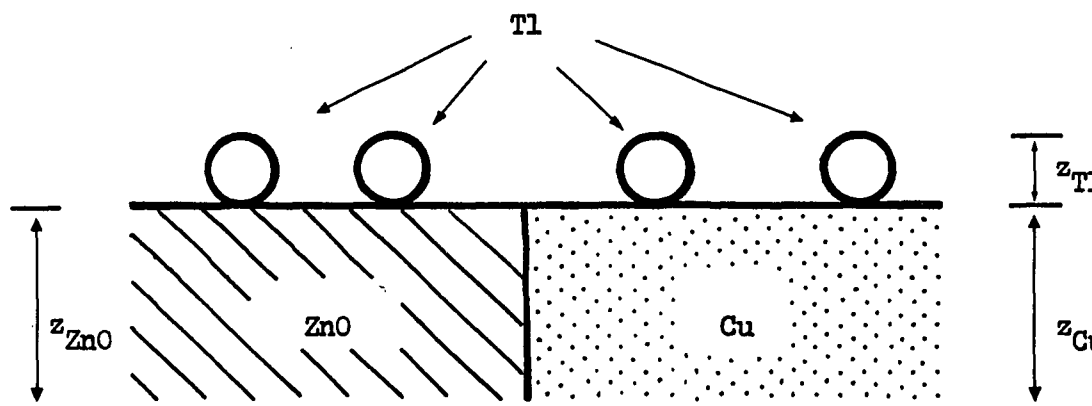

Figure 6 - Model of Tl/Cu/ZnO catalyst surface used in XPS calculations. Thallium is present only on the surface of copper and/or zinc oxide particles.

exp ($-z_{Tl}/g\,\lambda_{Zn}$), which is approximated as ($1 - z_{Tl}/g\,\lambda_{Zn}$) for the thin thallium layer. The factor z_{Tl} here is the effective thickness, which is an approximation for $z_{Tl}(x^s_{Tl}/x^s_{Zn})$ where x^s_i is the surface concentration of species i. These approximations lead to the equation for the intensity of the zinc signal, equation 17. One can rearrange these equations to

$$I_{Tl} = \frac{k\,\sigma_{Tl}\,x_{Tl}\,z_{Tl}}{E_{Tl}} \qquad (16)$$

$$I_{Zn} = \frac{k\,\sigma_{Zn}\,x_{Zn}\,g\,\lambda_{Zn}}{E_{Zn}} \left\{ 1 - \frac{z_{Tl}}{g\,\lambda_{Zn}} \right\} \qquad (17)$$

solve for the atomic volume concentrations, x_i. To get surface concentrations, each side of the equation is then multiplied by the thickness of a monolayer, t^o_{Tl} or t^o_{Zn}. The ratio of the surface concentrations of thallium and zinc can then be determined by division of the two equations. In equation 18, X^s_i represents the surface concentration of each of the species,

$$\frac{X^s_{Tl}}{X^s_{Zn}} = \frac{I_{Tl}\,g\,\lambda_{Tl}}{I_{Zn}\,t^o_{Zn}} \Bigg/ \left\{ \frac{\sigma_{Tl}\,E_{Zn}}{\sigma_{Zn}\,E_{Tl}} + \frac{t^o_{Tl}\,I_{Tl}}{t^o_{Zn}\,I_{Zn}} \right\} \qquad (18)$$

thallium or zinc. The intensities, I_i, are the measured peak areas; g is an instrumental factor, equal to 0.75 (16); λ_{Zn} is the escape depth for zinc, equal to 0.86 nm (23); σ_i are the photoionization cross sections; relative cross sections 11.77 for Tl and 18.01 for Zn (24); E_i are the kinetic energies of the

electrons determined from equation 12; t^{o}_{Tl} is the thickness of a monolayer of thallium, 0.28 nm (9); and t^{o}_{Zn} is the thickness of a monolayer of zinc in the sample, set equal to the spacing between the (100) planes of zinc oxide 0.2824 nm (25).

The amount of zinc on the surface had to be independently determined in order to determine the concentration of thallium on the surface using equation 18. This was because equations similar to equation 17 for copper and oxygen could not be used due to the unknown amount of oxidation of the catalyst. Data from the BET surface area analysis and x-ray diffraction analysis were used to determine the zinc oxide surface area. The value for the thickness of the copper particles from the Cu (111) reflection was used as the diameter of spherical copper particles assumed to be in the catalyst. This diameter value was used to calculate the volume of the spheres, the number of spheres in each gram of catalyst, the surface area of each of the spheres, and finally, the copper surface area. The contribution of copper to the surface area was then subtracted from the total BET surface area, leaving a value for the zinc oxide surface area. The value of 1.1744×10^{19} zinc atoms per square meter of zinc oxide (100) was used to determine the number of zinc surface atoms (25). From this value and the ratio of zinc to thallium atoms, one could determine the concentration of thallium on the surface of the Tl/Cu/ZnO catalysts. A sample calculation is given in Table 3. Values

for all parameters are listed in Table 4.

The surface carbon analysis was not straight forward. Carbonaceous species in the air caused sample contamination upon exposure of the sample to the air (20). In order to see if the carbon signal consisted of peaks other than this contamination peak, the carbon signals were analyzed using a computer peak fitting program. The raw data, on magnetic tape, were fed into a computer and analyzed using the fitting program. The Zn LMM auger signal was used to determine the baseline under the carbon signal. The minimum number of peaks necessary to make up the carbon signal were used.

Table 3 - Sample Calculation of Surface Thallium Concentration

Parameter	Value
Sample	Tested 0.08% Tl/Cu/ZnO
I_{Tl}/I_{Zn}	0.003534
x^s_{Tl}/x^s_{Zn}	0.05887
Cu particle thickness	16.01 nm
Cu sphere volume	1.248×10^{-18} mL
Cu spheres/g catalyst	2.235×10^{16} / g
Cu sphere surface	$5.607 \times 10^{-16} m^2$/sphere
Cu surface area/g catalyst	12.53 m^2/g catalyst
Total surface area	21.2 m^2/g catalyst
ZnO surface area/g catalyst	8.7 m^2/g catalyst
Surface zinc atoms	1.022×10^{20}/g catalyst
Surface thallium atoms	6.016×10^{18}/g catalyst
	$2.837 \times 10^{17}/m^2$ catalyst

Table 4 - XPS Parameter Values

Parameter	Zinc[a]	Thallium[b]
E_i, eV	232.3	1136.4
σ_i	18.01	11.77
λ_i, nm	0.86	---
t_i^o, nm	0.2824	0.28

a - for Zn $2p_{3/2}$
b - for Tl $4f_{7/2}$

3.0 RESULTS

3.1 Observations About the Catalysts

3.1.1 Untested Catalysts

Four thallium-doped catalysts were prepared using the procedure described previously. Three of the catalysts were prepared from one batch of Cu/ZnO (30/70 mol%) and had thallium concentrations of 0.02, 0.08, and 0.23% (mol% on a metals basis)(21). A catalyst containing 0.17% thallium was prepared using a second batch of Cu/ZnO (21). The observations made during the catalyst preparations were the same in all cases.

The calcined material, CuO/ZnO, was a brown powder which became hard and brittle upon pelletization. The reduced Cu/ZnO pellets were an intense black color. When the reduced Cu/ZnO was added to the thallium containing solutions, there was an immediate gas evolution, an effervescence. This gas evolution slowed after a few seconds and then eventually stopped in less than a minute. After the water was evaporated off, the doped catalyst pellets were a dark grey color, but had a definite green to yellow-green tint. Based upon the weight of the recovered catalyst, the doped pellets typically contained an estimated 2 - 4% by weight of water.

Re-reduction of the 0.08% Tl/Cu/ZnO produced a black catalyst without the green color. Not much water was detected from the gas chromatographic analysis of the effluent gas.

3.1.2 Tested Catalysts

The recovered tested catalysts were all red-brown in color. The weight of the recovered catalysts and a visual inspection of them indicated no large amount of carbon buildup on the surface. There was also no visual indication of any material buildup on the glass beads, in the reactor, or in any of the gas lines.

The red-brown color was also seen on the short-term tested 0.08% Tl/Cu/ZnO catalysts although the intensity of the color may have been less than in the fully tested catalysts.

3.2 Catalyst Testing

The results of the testing of the thallium doped catalysts are shown in Figures 7 - 9 and in Tables 5 - 10. In all cases, the major products were methanol and carbon dioxide (when water was contained in the feed gas), with small amounts of methane, methyl formate, and ethanol produced. The catalysts showed decreasing activity toward methanol, methyl formate, and ethanol with increasing concentration of thallium. Methane did not appear to vary with thallium concentration. Unreacted hydrogen, carbon monoxide, and water (if added to the feed) were also present in the effluent gas. The detailed results are separated

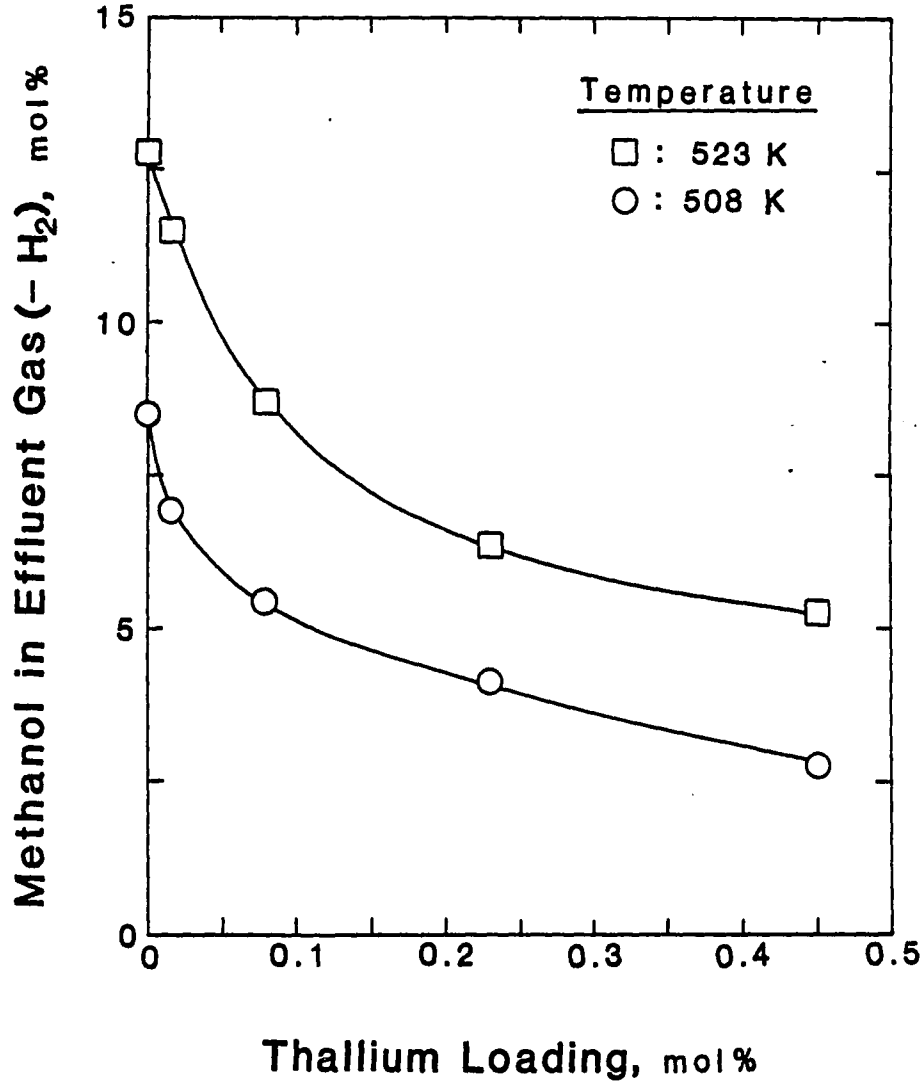

Figure 7 - Methanol in effuent gas (less H_2) versus the thallium loading on the catalyst. Conditions: 523 K (□) or 508 K (○), 7.6 MPa, 10.5 dm^3/hr H_2, 4.5 dm^3/hr CO, 2.45 g of x/30/70 Tl/Cu/ZnO catalyst.

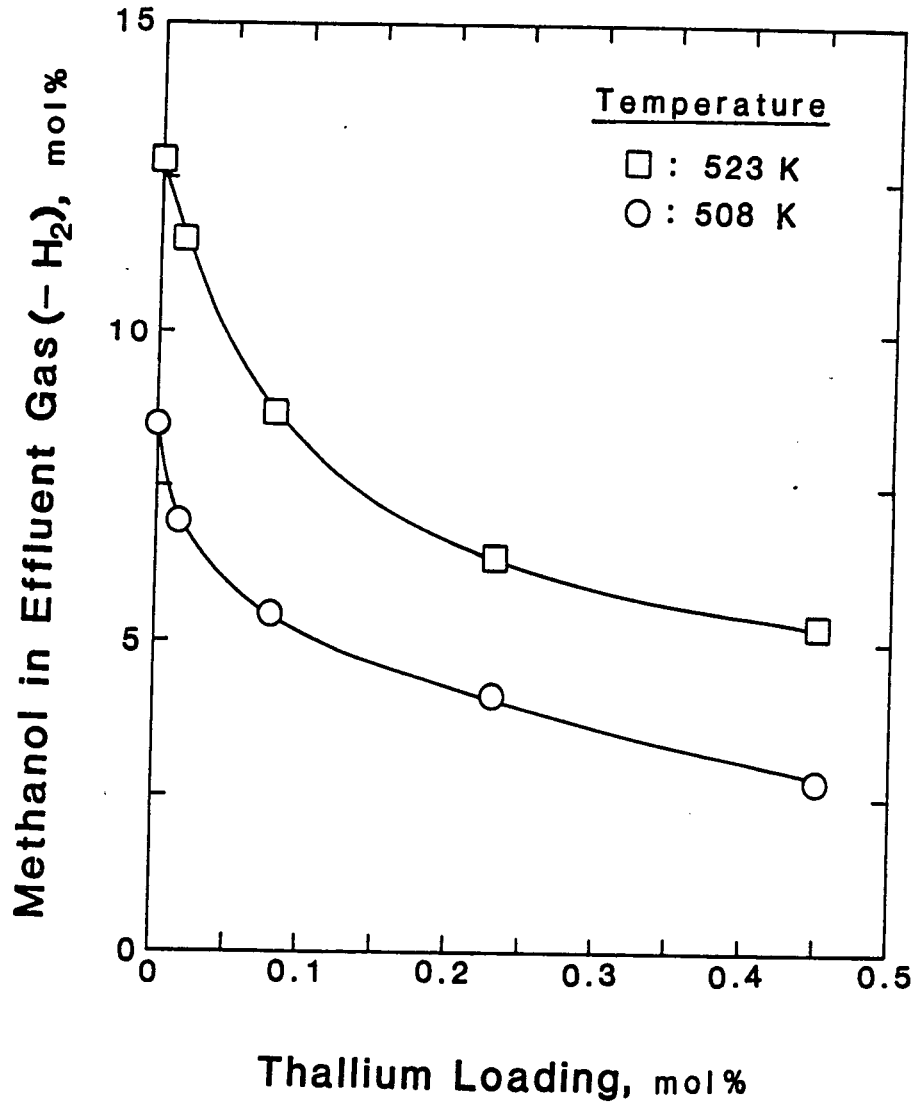

Figure 7 - Methanol in effuent gas (less H_2) versus the thallium loading on the catalyst. Conditions: 523 K (□) or 508 K (○), 7.6 MPa, 10.5 dm^3/hr H_2, 4.5 dm^3/hr CO, 2.45 g of x/30/70 Tl/Cu/ZnO catalyst.

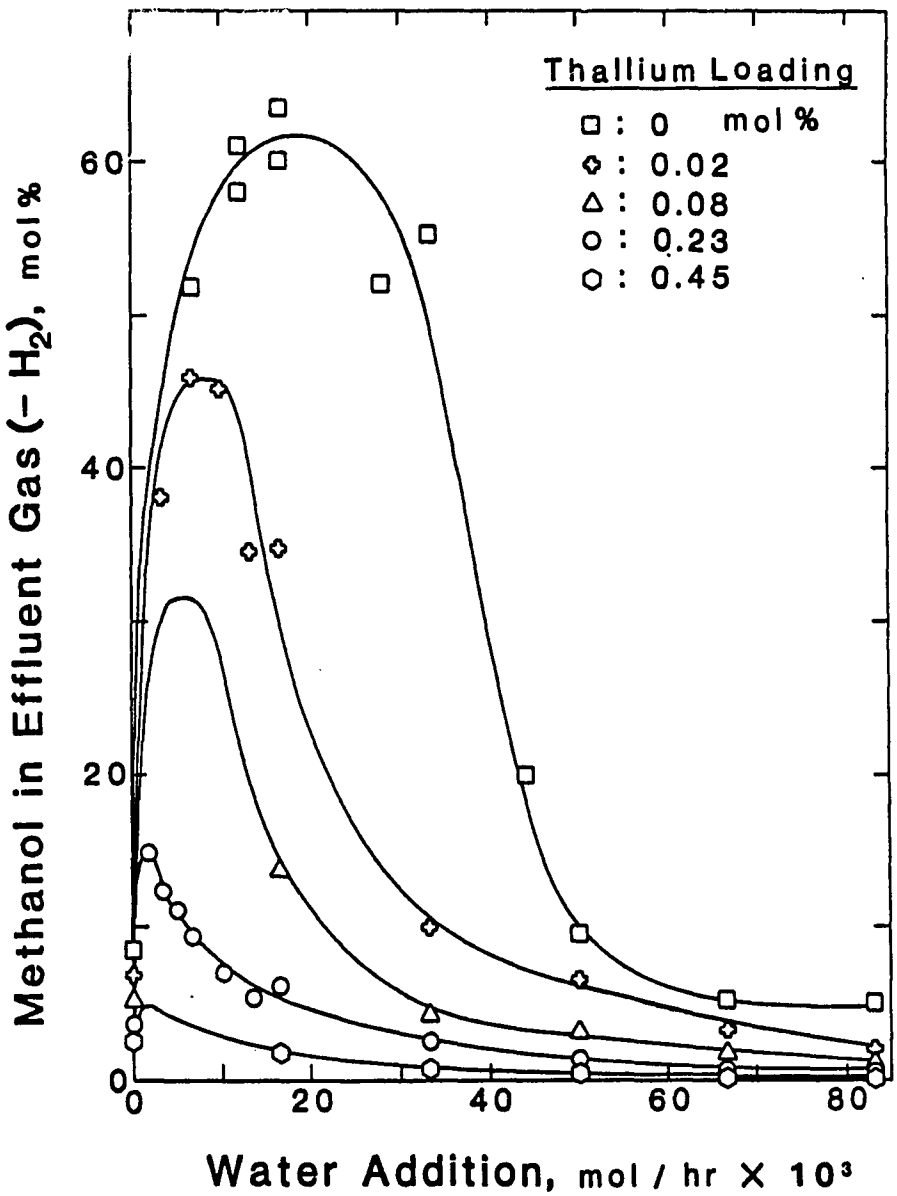

Figure 8 - Methanol in effluent gas (less H_2) versus the amount of water added to the feed gas stream. Conditions: 508 K, 7.6 MPa, 10.5 dm^3/hr H_2, 4.5 dm^3/hr CO, 2.45 g of x/30/70 Tl/Cu/ZnO catalyst, x = 0 (□), 0.02 (◇), 0.08 (△), 0.23 (○), 0.45 (⬡).

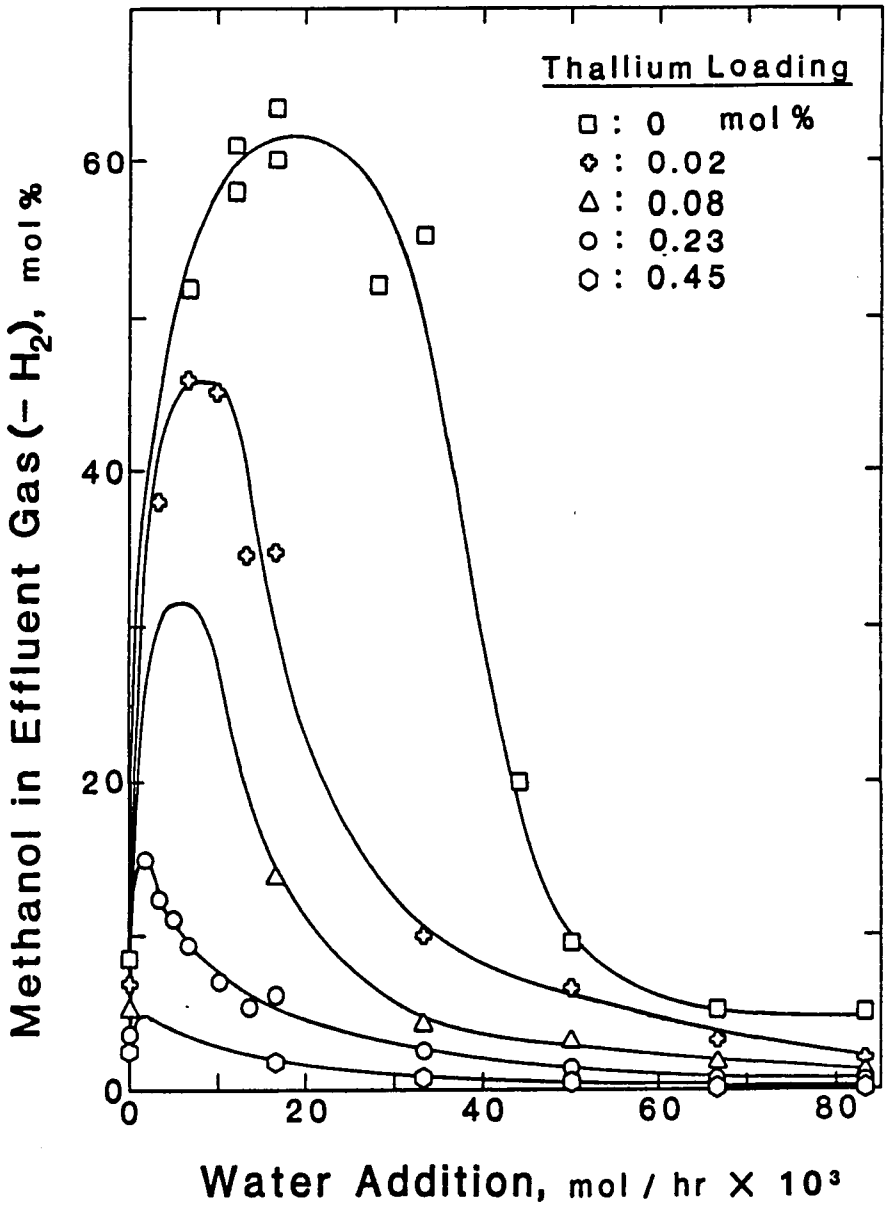

Figure 8 - Methanol in effluent gas (less H_2) versus the amount of water added to the feed gas stream. Conditions: 508 K, 7.6 MPa, 10.5 dm^3/hr H_2, 4.5 dm^3/hr CO, 2.45 g of x/30/70 Tl/Cu/ZnO catalyst, x = 0 (□), 0.02 (✣), 0.08 (△), 0.23 (○), 0.45 (⬡).

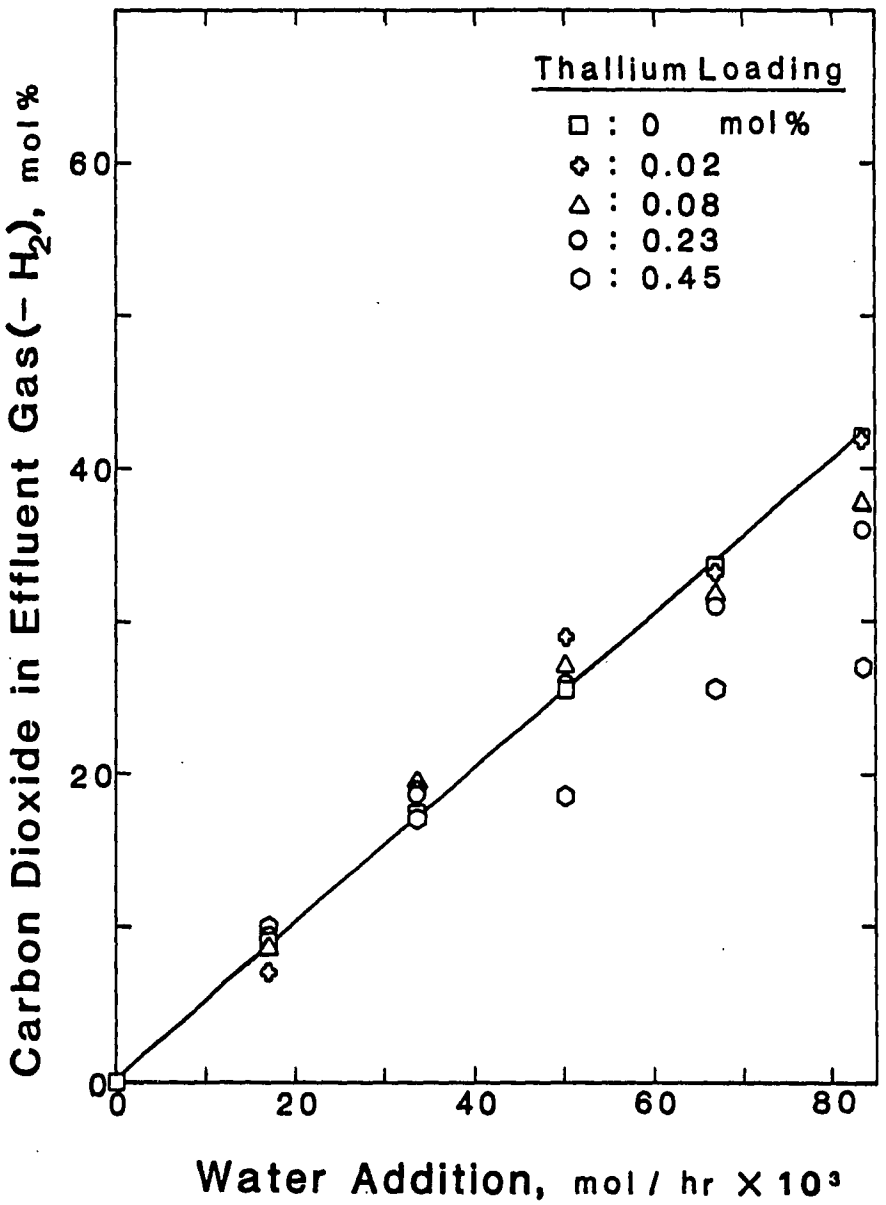

Figure 9 - Carbon dioxide in effluent gas (less H_2) versus the amount of water added to the feed gas stream. Conditions: 508 K, 7.6 MPa, 10.5 dm^3/hr H_2, 4.5 dm^3/hr CO, 2.45 g ov x/30/70 Tl/Cu/ZnO catalyst x - 0 (□), 0.02 (◇), 0.08 (△), 0.23 (○), 0.45 (⬡).

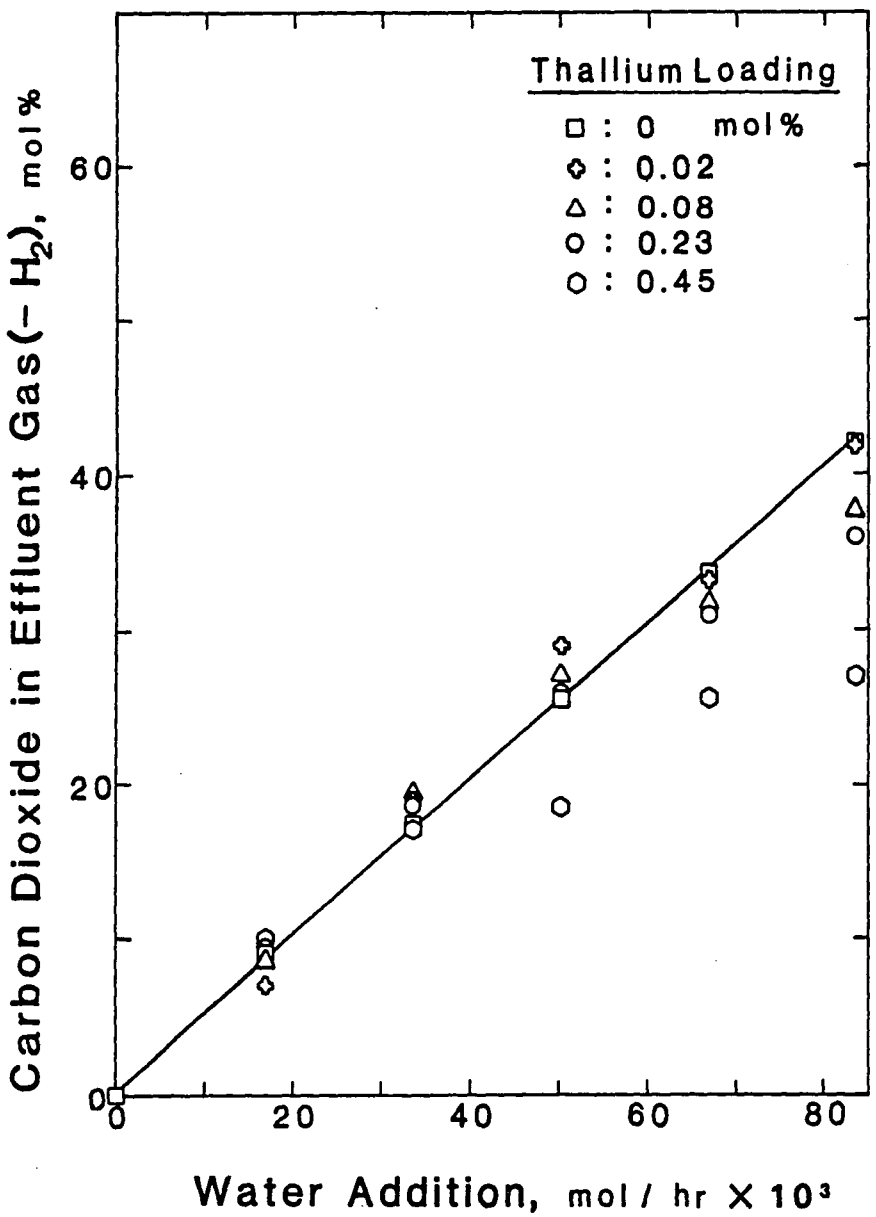

Figure 9 - Carbon dioxide in effluent gas (less H_2) versus the amount of water added to the feed gas stream. Conditions: 508 K, 7.6 MPa, 10.5 dm^3/hr H_2, 4.5 dm^3/hr CO, 2.45 g ov x/30/70 Tl/Cu/ZnO catalyst x - 0 (□), 0.02 (◇), 0.08 (△), 0.23 (○), 0.45 (⬡).

Table 5 - Product Distribution over 0.02% Tl/Cu/ZnO

Conditions		Products						
Temp. K	Water $\frac{mmol}{hr}$	CO mol %	CH_4 mol %	CO_2 mol %	H_2O mol %	CH_3OH mol %	$HCOOCH_3$ mol %	C_2H_5OH mol %
523	0	87.813	0.448	0.201	0	11.539	a	a
508	0	92.662	0.421	0.048	0	6.869	a	0
508	16.6	57.394	0.275	6.997	0.616	34.654	0.064	a
508	33.2	68.250	0.506	19.080	2.195	9.920	0.048	a
508	49.9	57.898	0.347	29.035	6.187	6.533	a	0
508	66.5	55.154	0.313	33.296	7.886	3.350	a	0
508	83.1	45.754	0.266	41.805	10.117	2.057	a	0
508	3.3	71.679	a	2.251	0.079	26.026	a	0
508	6.7	64.119	a	4.224	0.228	31.386	a	0
508	10.0	63.327	0	5.421	0.340	30.881	0.031	0
508	13.3	68.540	0	7.368	0.595	23.458	0.038	0

a - trace amount observed, less than 0.02 mol %

Table 6 - Product Distribution over 0.08% Tl/Cu/ZnO

Conditions		Products						
Temp. K	Water $\frac{mmol}{hr}$	CO mol%	CH_4 mol%	CO_2 mol%	H_2O mol%	CH_3OH mol%	$HCOOCH_3$ mol%	C_2H_5OH mol%
523	0	91.499	0.246	0.106	0	8.148	a	0
508	0	94.491	0.328	0.071	0	5.109	a	0
508	16.6	76.499	0.394	8.722	0.802	13.583	a	0
508	33.2	74.112	0.325	19.650	1.731	4.183	a	0
508	49.9	65.110	0.198	27.119	4.324	3.248	a	0
508	66.5	59.699	0.199	31.804	6.533	1.765	0	0
508	83.1	52.073	0.175	37.620	8.985	1.147	0	0

a - trace amount observed, less than 0.02 mol %

Table 7 - Product Distribution over 0.17% Tl/Cu/ZnO

Conditions		Products						
Temp. K	Water $\frac{mmol}{hr}$	CO mol %	CH_4 mol %	CO_2 mol %	H_2O mol %	CH_3OH mol %	$HCOOCH_3$ mol %	C_2H_5OH mol %
523	0	90.768	0.089	0.188	a	8.956	a	a
508	0	94.603	0.113	0.123	a	5.161	a	0
508	16.6	81.746	0.042	9.870	0.727	7.616	a	a
508	33.2	74.671	0.085	19.787	1.912	3.546	a	0
508	49.9	67.505	0.119	26.698	3.701	1.977	0	0
508	66.5	59.304	0.043	32.805	6.655	1.193	0	0
508	83.1	51.304	0.076	37.765	9.955	0.863	0	0
508	1.7	88.476	b	1.038	a	10.485	a	a
508	3.3	88.469	b	1.798	0.109	9.623	a	0
508	5.0	88.851	b	3.047	0.167	7.935	a	0
508	6.7	88.537	b	3.964	0.243	7.255	a	0
508	10.0	88.414	b	5.980	0.426	5.179	a	0
508	13.3	87.560	b	7.941	0.535	3.964	a	0

a - trace amount observed, less than 0.02 mol %; b - not measured

Table 8 - Product Distribution over 0.23% Tl/Cu/ZnO

Conditions		Products						
Temp. K	Water $\frac{mmol}{hr}$	CO mol %	CH_4 mol %	CO_2 mol %	H_2O mol %	CH_3OH mol %	$HCOOCH_3$ mol %	C_2H_5OH mol %
523	0	93.554	a	0.098	0	6.348	a	a
508	0	95.859	0.191	0.084	0	3.866	a	a
508	16.6	83.427	0.327	9.439	0.739	6.067	a	a
508	33.2	76.288	0.254	18.840	2.081	2.537	a	a
508	49.9	67.755	0.398	25.891	4.584	1.372	a	a
508	66.5	60.504	0.168	31.107	7.336	0.885	a	a
508	83.1	53.849	0.244	36.094	9.156	0.657	a	a

a - not measured

Table 9 - Methanol Yield Over Tl/Cu/ZnO Catalysts

Conditions		Methanol Yield g/hr/kg catalyst			
Temp. K	Water $\frac{mmol}{hr}$	0.0% Tl/Cu/ZnO	0.02% Tl/Cu/ZnO	0.08% Tl/Cu/ZnO	0.23% Tl/Cu/ZnO
523	0	301.4[a]	270.2	192.3	150.9
508	0	199.4[a]	161.0	120.7	92.1
508	16.6	1462.9[b]	827.3	321.7	143.8
508	33.2	1288.5[b]	230.7	97.3	59.9
508	49.9	213.3[b]	150.6	76.5	32.9
508	66.5	---	80.1	42.9	21.8
508	83.1	121.4[b]	49.3	28.4	16.6

a - data from screening of Cu/ZnO used in preparation of Tl/Cu/ZnO catalysts
b - from ref. 8.

Table 10 - Carbon Dioxide Yield Over Tl/Cu/ZnO Catalysts

Conditions		Carbon Dioxide Yield, g/hr/kg catalyst			
Temp. K	Water $\frac{mmol}{hr}$	0.0% Tl/Cu/ZnO	0.02% Tl/Cu/ZnO	0.08% Tl/Cu/ZnO	0.23% Tl/Cu/ZnO
523	0	6.3[a]	6.6	3.6	3.2
508	0	4.3[a]	1.6	2.3	2.9
508	16.6	293.6[b]	236.8	292.9	316.9
508	33.2	587.0[b]	629.0	648.2	630.4
508	49.9	869.7[b]	949.2	905.0	880.6
508	66.5	---	1128.0	1095.7	1084.7
508	83.1	1474.1[b]	1418.7	1322.6	1292.5

a - data from screening of Cu/ZnO used in preparation of Tl/Cu/ZnO catalysts
b - from ref. 8.

into sections: reaction in water-free synthesis gas, reaction in synthesis gas containing water, and catalyst deactivation.

3.2.1 The Reaction in Water-Free Synthesis Gas

The initial catalyst activities toward methanol formation in water-free synthesis gas at 523 K and 508 K are shown in Figure 7. The value for conversion to methanol on a catalyst containing no thallium was a value found during screening of the undoped Cu/ZnO catalyst that was subsequently also used in the preparation of the 0.02, 0.08, and 0.23% Tl/Cu/ZnO catalysts. The amount of methanol produced decreased with increasing thallium content in the catalyst. This decrease was not linearly dependent upon the molar thallium concentration, and the relative effect of the thallium decreased as its concentration increased. Except for the 0.45% Tl/Cu/ZnO points, the two curves appear to be converging.

When the testing of the catalysts was commenced, the system took about two hours to come to near steady state conditions after reaching 523 K. The activity of each of the catalysts continued to decrease slightly with time, and the points plotted in Figure 7 are those from the end of the 523 K testing when the catalyst was most stable. The catalyst bed temperature was then quickly changed to 508 K, and the system took from 1 to 2 hrs to reach a steady state. The carbon monoxide conversion to methanol was fairly constant during

the remaining time at 508 K in the absence of water.

After the Tl/Cu/ZnO catalysts were tested in water containing synthesis gas, the activity in water-free synthesis gas was again checked. Each of the thallium-doped catalysts showed some deactivation after the first water cycle, with the deactivation ranging from relative 12 to 30% (see section 3.2.3).

Other products seen in the effluent gas were carbon dioxide, methyl formate, ethanol, and methane. Carbon dioxide was always present, ranging from 0.1 to 0.4 mol% in the effluent gas at 523 K, and from 0.05 to 0.25 mol% at 508 K. In each case, the amount of carbon dioxide formed decreased with temperature. Methyl formate was found to be a product over all catalysts at 523 K, with the amount formed (estimated from gas chromatograms) decreasing with increasing thallium concentration. In all cases, the amount of methyl formate formed at 523 K was less than 0.01 mol% in the effluent gas. Methyl formate was also found at 508 K, but in smaller quantities than at 523 K. The formation of the methyl formate followed the same trend with respect to thallium concentration at both temperatures. Ethanol was seen in trace quantities at some testing conditions. It was detected for most catalysts at 523 K but in smaller concentrations than the methyl formate. Again, the amount formed decreased with increasing thallium concentration in the catalyst. The ethanol was not detected in the water-free synthesis gas at 508 K over any of the Tl/Cu/ZnO

catalysts. Methane was always found in the effluent gas, with the concentration ranging from about 0.1 to 0.4 mol%. The amount of methane did not seem to follow any trend with respect to temperature or thallium content.

3.2.2 The Reaction in Synthesis Gas Containing Water

The effects of water on the conversion of carbon monoxide to methanol and carbon dioxide are shown in Figures 8 and 9, respectively. Data obtained by Vedage (7) for the undoped catalyst were used in the figures for comparison. The effect of water on methanol formation for the thallium-doped catalysts was similar to the effect on the undoped catalyst. Conversion to carbon dioxide was essentially the same as for the undoped catalyst until higher water concentrations were reached. The points at water addition rates of 0, 17, 33, 50, 67, and 83 mmol/hr (per 2.45 g of catalyst) are the uncorrected (for deactivation) steady state data points from the initial testing of the catalysts. For the 0.02% Tl/Cu/ZnO catalyst, the extra points between 0 and 17 mmol/hr of added water are steady state points which were measured last in the testing cycle and are corrected for catalyst deactivation. The curve shown for the 0.23% Tl/Cu/ZnO catalyst was composed of data from two catalyst testings. The points at 0, 17, 33, 50, 67, and 83 mmol/hr were from the 0.23% Tl/Cu/ZnO catalyst. The extra points are from the 0.17% Tl/Cu/ZnO catalyst testing, with the

height of the steady state points adjusted to fit the height of the transient maximum observed during testing of the 0.23% Tl/Cu/ZnO catalyst.

The most interesting effect observed was that of water on the formation of methanol. When water was first added to the feed stream, about $1\frac{1}{2}$ hrs passed before water appeared in the gas chromatograms. As soon as a trace of water was observed, the methanol yield rose dramatically. In all of the catalyst testings, a series of chromatograms indicated that the yield rapidly went through a maximum and then decreased until a steady state was reached, which was 4 to 8 hrs after the start of the water addidion to the feed gas. Progressively more water was added to the stream after the testing at 17 mmol/hr (5 mm^3/min). The conversion to methanol decreased and the steady states were reached within 1 to 2 hrs. On the curve for the 0.02% Tl/Cu/ZnO catalyst in Figure 8, the data points for water addition rates between 0 and 17 mmol/hr were obtained by addition of water/isopropanol solutions, and are corrected for catalyst deactivation. The values for methanol formation at 6.7 and 10.0 mmol/hr of added water, corrected for catalyst deactivation, are about equal to the value for methanol formation observed in the transient maximum when water was first introduced into the feed gas stream in the initial catalyst testing. The height of the maximum on the 0.08% Tl/Cu/ZnO curve was based upon the conversion to methanol in the transient

maximum, observed when initially going from the 0 mmol/hr steady state point to the 17 mmol/hr steady state point. The location of this maximum with respect to water addition was estimated. The 0.23% Tl/Cu/ZnO catalyst was not tested with water/isopropanol solutions and the exact location of its maximum for methanol formation was not determined. This was the reason for testing the 0.17% Tl/Cu/ZnO catalyst. There was always a trace amount of water present during this testing which created a problem in determining the methanol formation in the water-free synthesis gas and in calculation of the extent of catalyst deactivation based on this "water-free" state. The data points for methanol formation over the 0.17% Tl/Cu/ZnO catalyst at water addition rates between 0 and 17 mmol/hr, when corrected for catalyst deactivation, were close to the value for the transient maximum observed over the 0.23% Tl/Cu/ZnO catalyst when water was first introduced into the feed gas stream. Therefore, the 0.17% Tl/Cu/ZnO catalyst points are plotted as the maximum in the 0.23% Tl/Cu/ZnO curve. Since the maximum formation of methanol occurred at such low concentrations of water in the feed, no great error was made by combining these points. The height of the maximum for conversion of carbon monoxide to methanol over the 0.45% Tl/Cu/ZnO catalyst was based upon a series of gas chromatograms of this transient maximum, and the location with respect to water concentration in the feed was estimated from the observed concentrations of

water and carbon dioxide in the gas chromatograms.

From the data, one observes that: the rate of methanol formation decreased with increasing thallium content in the catalyst; the maximum amount of methanol formed occurred at low concentrations of water in the feed gas stream; and the location of the maximum for methanol production shifted to lower water concentrations as the amount of thallium in the catalyst was increase.

The effect of water on formation of carbon dioxide differed markedly from the effect on methanol formation. Figure 9 shows that there was an almost linear increase in carbon dioxide production as more water was added to the synthesis gas mixture. The line in Figure 9 was drawn through the points for the undoped catalyst, the data being that of Vedage (7). When water was initially added to the system, the carbon dioxide peak in the gas chromatograms began to rise as the water began to appear. Unlike the methanol amount, the amount of carbon dioxide in the effluent gas just continued to increase until it leveled off, about 2 to 4 hrs after the water addition was started. When more water was added, steady state was again reached within 2 to 4 hrs. For water addition rates of 0, 17, 33, and 50 mmol/hr (per 2.45 g of catalyst), the correlation between the amount of carbon dioxide formed and the thallium concentration could not be established since the data points were scattered about the undoped catalyst points. However, for

higher water concentrations, the carbon dioxide formation decreased as the concentration of thallium in the catalyst increased.

Methyl formate and ethanol were also formed in trace quantities, and appeared to follow the same trends as methanol. The production of methyl formate and ethanol decreased with increasing thallium content in the catalysts, and went through a maximum at the same place as the methanol. The amount of methyl formate produced was always greater than the amount of ethanol.

Methane was always found in small amounts in the gas chromatograms. From the data, it was difficult to determine any general trend for methane production.

3.2.3 Catalyst Deactivation

The activity toward methanol formation decreased slightly with time for each of the catalysts. These decreases were detected by periodically returning to the water-free state at 508 K. The activity decreases after the initial testing procedure were typically about relative 30%, and are listed in Table 11. The results of testing of the 0.02% Tl/Cu/ZnO catalyst are shown in Figure 10. The first two water cycles show a progressive deactivation toward methanol formation. The conversion to methanol was only 88% of its original value of 11.5% upon returning to the water-free state after the first cycle. The conversion was down to 68% of the original value at

Table 11 - Deactivation of Methanol Synthesis Activity in Tl/Cu/ZnO Catalysts

Catalyst	Deactivation* relative %
Cu/ZnO	0
0.02% Tl/Cu/ZnO	12
0.08% Tl/Cu/ZnO	29
0.23% Tl/Cu/ZnO	31

* Deactivation after initial testing cycle as percentage of initial activity at 508 K in water-free synthesis gas.

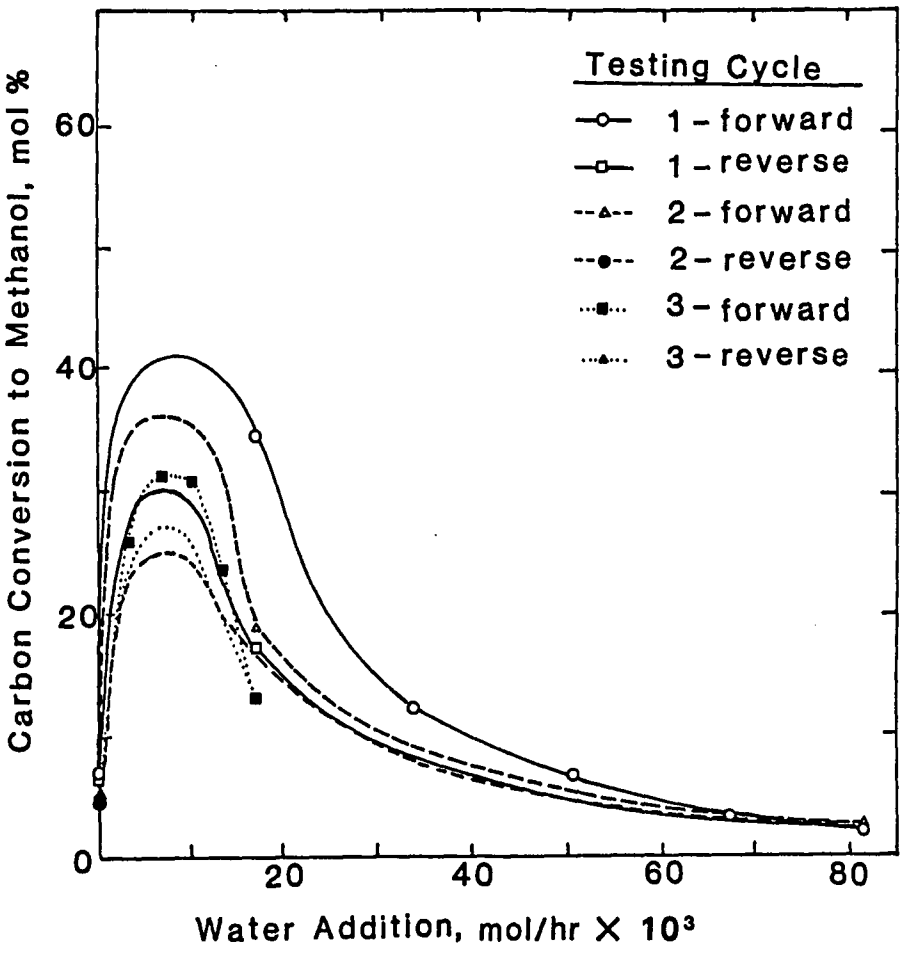

Figure 10 - Deactivation of 0.02% Tl/Cu/ZnO catalyst during testing, as carbon conversion to methanol versus water added to feed gas stream in successive testing cycles. Conditions: 508 K, 7.6 MPa, 10.5 dm^3/hr H_2, 4.5 dm^3/hr CO, 2.45 g of catalyst. Maxima heights based on transient values, locations based on third testing cycle.

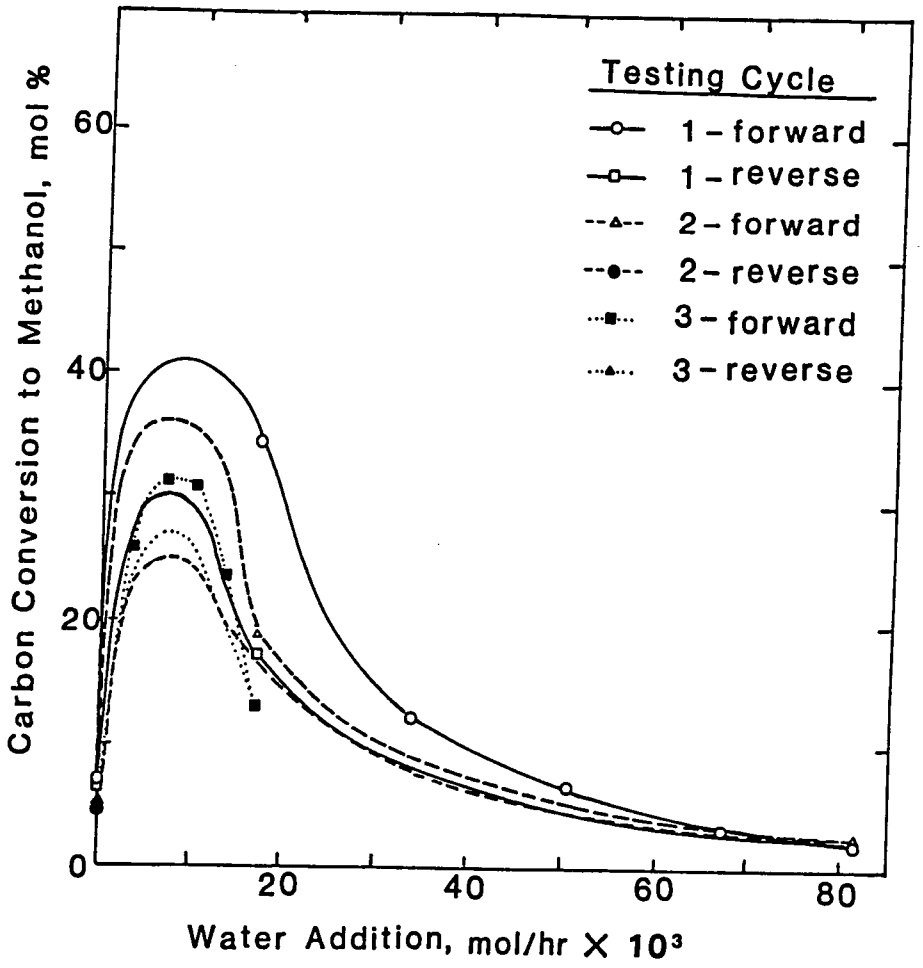

Figure 10 - Deactivation of 0.02% Tl/Cu/ZnO catalyst during testing, as carbon conversion to methanol versus water added to feed gas stream in successive testing cycles. Conditions: 508 K, 7.6 MPa, 10.5 dm^3/hr H_2, 4.5 dm^3/hr CO, 2.45 g of catalyst. Maxima heights based on transient values, locations based on third testing cycle.

the end of the second cycle. In the third cycle of testing, water/isopropanol mixtures were used to determine the position of the maximum of methanol formation. At 2 and 3 mm^3/min (per 2.45 g of catalyst), the conversions of carbon monoxide to methanol were approximately 31%, compared to the 42% conversion to methanol in the initial transient maximum, and no deactivation was observed during this cycle. When the deactivation was taken into account, the 31% conversion of carbon monoxide to methanol observed during the third water addition cycle was corrected to about 45% conversion of carbon monoxide to methanol and this value is near to the value observed for the initial transient maximum.

The catalysts did not show much deactivation toward the formation of carbon dioxide during the course of the testing. The conversion of carbon monoxide to carbon dioxide over the 0.02% Tl/Cu/ZnO catalyst with 17 mmol/hr of water added to the feed gas decreased from an initial value of 7.0 mol% to a value of 6.3 mol% at the end of the testing. When considering the activity of the catalysts toward formation of carbon dioxide, the fact that the Water-Gas Shift reaction is running at near equilibrium under these conditions must be taken into account.

3.3 BET Surface Areas

The results of the surface area measurements are shown in Table 12. The highest surface area was observed for the reduced

Table 12 - BET Surface Areas (m^2/g)

Catalyst	Untested	Tested
Cu/ZnO	37.9[a]	37.1[b]
0.02% Tl/Cu/ZnO	34.7	22.4
0.08% Tl/Cu/ZnO	36.3[c]	21.2[d]
0.23% Tl/Cu/ZnO	36.6	21.5

a - reduced, undoped Cu/ZnO used to prepare the Tl/Cu/ZnO catalysts.

b - from ref. 6.

c - rereduced catalyst had a surface area of 36.6 m^2/g.

d - when tested 16 hrs 523 K, 6 hrs 508 K - 32.6 m^2/g
when tested 12 hrs 16.6 mmol/hr water - 26.6 m^2/g.

undoped Cu/ZnO. After doping, the untested Tl/Cu/ZnO catalysts had slightly lower surface areas, 34.7 to 36.6 m^2/g. The surface area of the re-reduced 0.08% Tl/Cu/ZnO catalyst was 36.6 m^2/g, which was essentially the same as that before reduction. The surface areas decreased markedly upon testing. The tested doped samples had surface areas of 21.2 to 22.4 m^2/g. The 0.08% Tl/Cu/ZnO catalyst which was tested for 14 hrs at 523 K and for 6 hrs at 508 K in water-free synthesis gas had a surface area of 32.6 m^2/g, indicating that a loss of surface area had already occurred. Upon further testing at 508 K in synthesis gas which contained water, the surface area decreased from 32.6 to 26.6 m^2/g. This value was now closer to the 21 to 22 m^2/g average for the tested catalysts.

3.4 X-Ray Diffraction

3.4.1 Identification of Bulk Phases

The copper standard and the zinc oxide standard were analyzed first in order to locate reflections due to the beryllium window of the sample holder (see section 2.4). The experimentally found value of the reflection angle 2θ (where θ is the Bragg angle) for the Cu(111) lattice spacing was adjusted from 43.28° to 43.33° to fit the literature value (22). When all other peaks in the x-ray diffraction pattern were shifted by this 0.05°, a reflection due to the beryllium window

was observed at 41.35°. The zinc oxide standard was analyzed next in order to confirm the identification of the beryllium reflection. The reflection for the ZnO (101) lattice spacing occurred at 36.26°, in accordance with the literature value (22). In this zinc oxide diffraction pattern, the reflection due to the beryllium window occurred at 41.33°. This sample holder line was used as the reference line in all subsequent x-ray diffraction scans, with an assigned average reflection angle of 41.34°.

The tested and untested 0.23% Tl/Cu/ZnO samples were scanned from 2θ = 5 to 95° to identify the bulk phases present in the catalyst, as shown in Figures 12a and 12b. Reflections attributed to the ZnO phase were observed in both the tested and untested samples. These reflections were not interfered with to any extent by the singals from the sample holder. The nature of the copper in the untested samples differed from the copper in the tested samples. The metallic Cu (111) reflection at 2θ = 43.3° in the untested samples was very broad and weak. In the tested samples, this copper reflection was much more pronounced. The Cu (200) peak was masked by a very intense sample holder signal, as was the Cu (311) peak. The Cu (220) reflection was not interfered with, but was small compared to the Cu (111) reflection, which was consistent with the literature (22). Reflections from a Cu_2O phase, if present, would be interfered with by other signals. The Cu_2O (111) would be

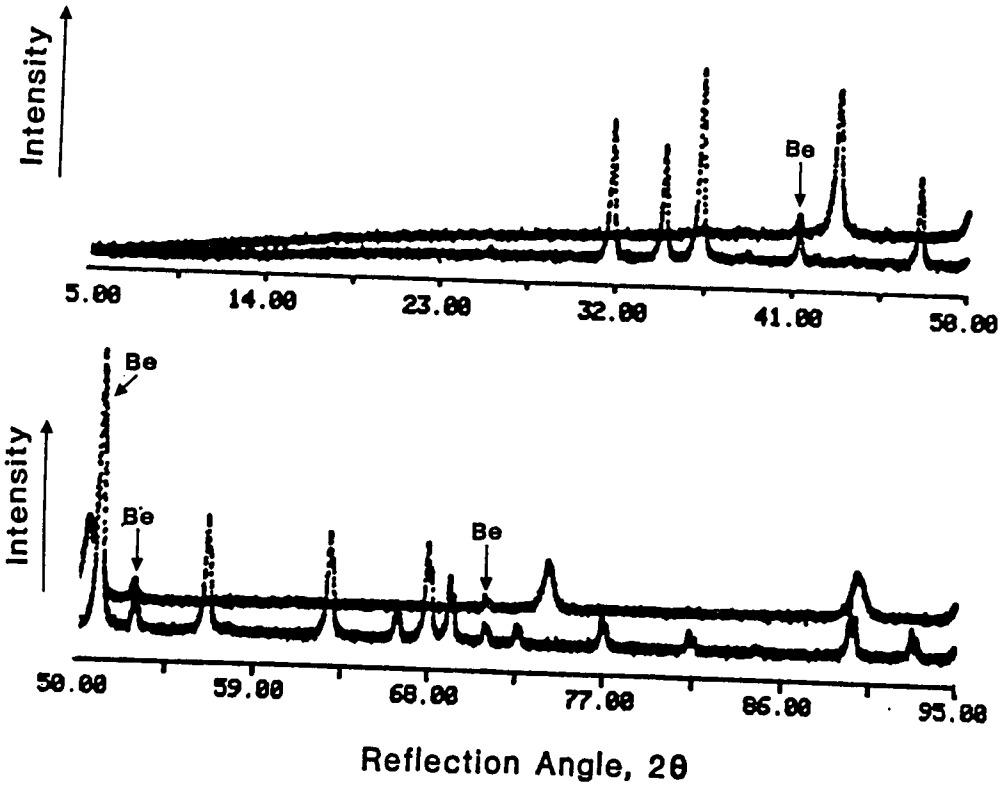

Figure 11 - X-ray diffraction patterns of copper and zinc oxide standards, indicating peaks due to beryllium window of sample holder.

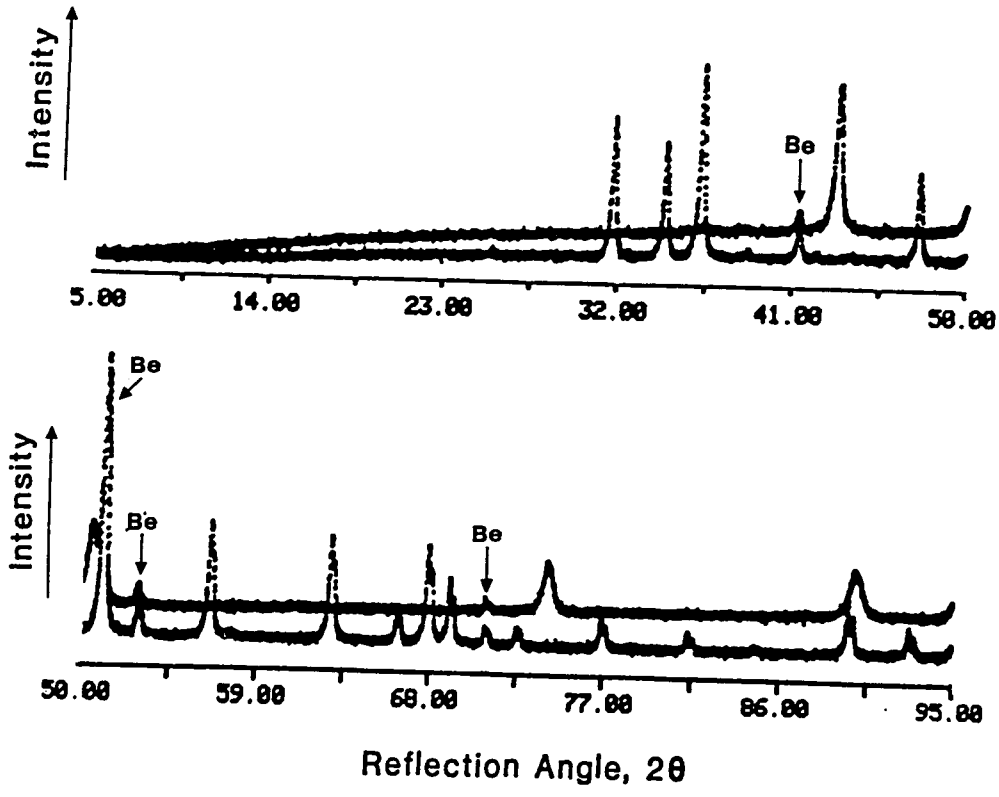

Figure 11 - X-ray diffraction patterns of copper and zinc oxide standards, indicating peaks due to beryllium window of sample holder.

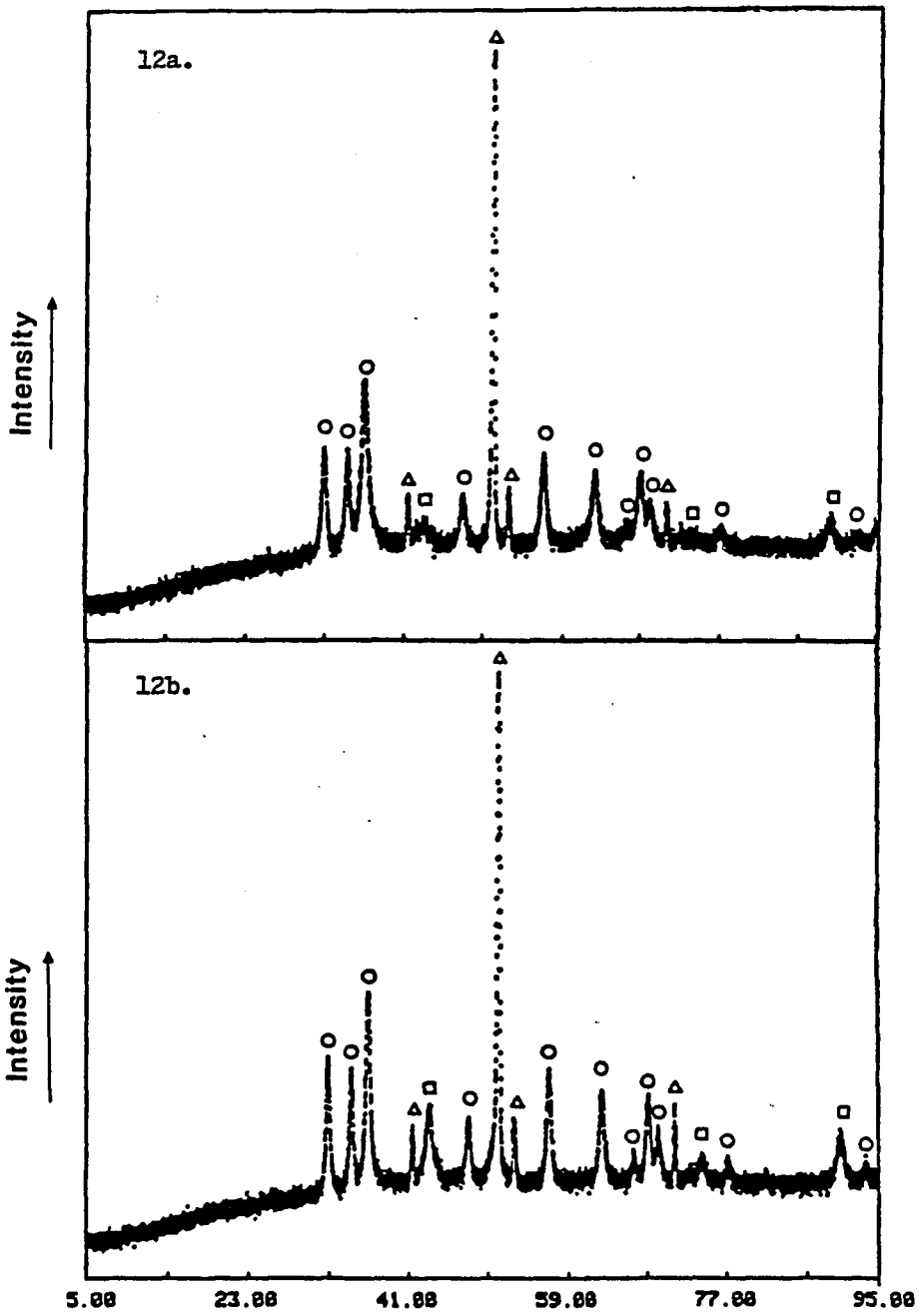

Figure 12 - XRD scans of the untested (12a) and tested (12b) 0.2% Tl/Cu/ZnO catalysts. Peaks identified as copper (□), zinc oxide (○), or beryllium (△).

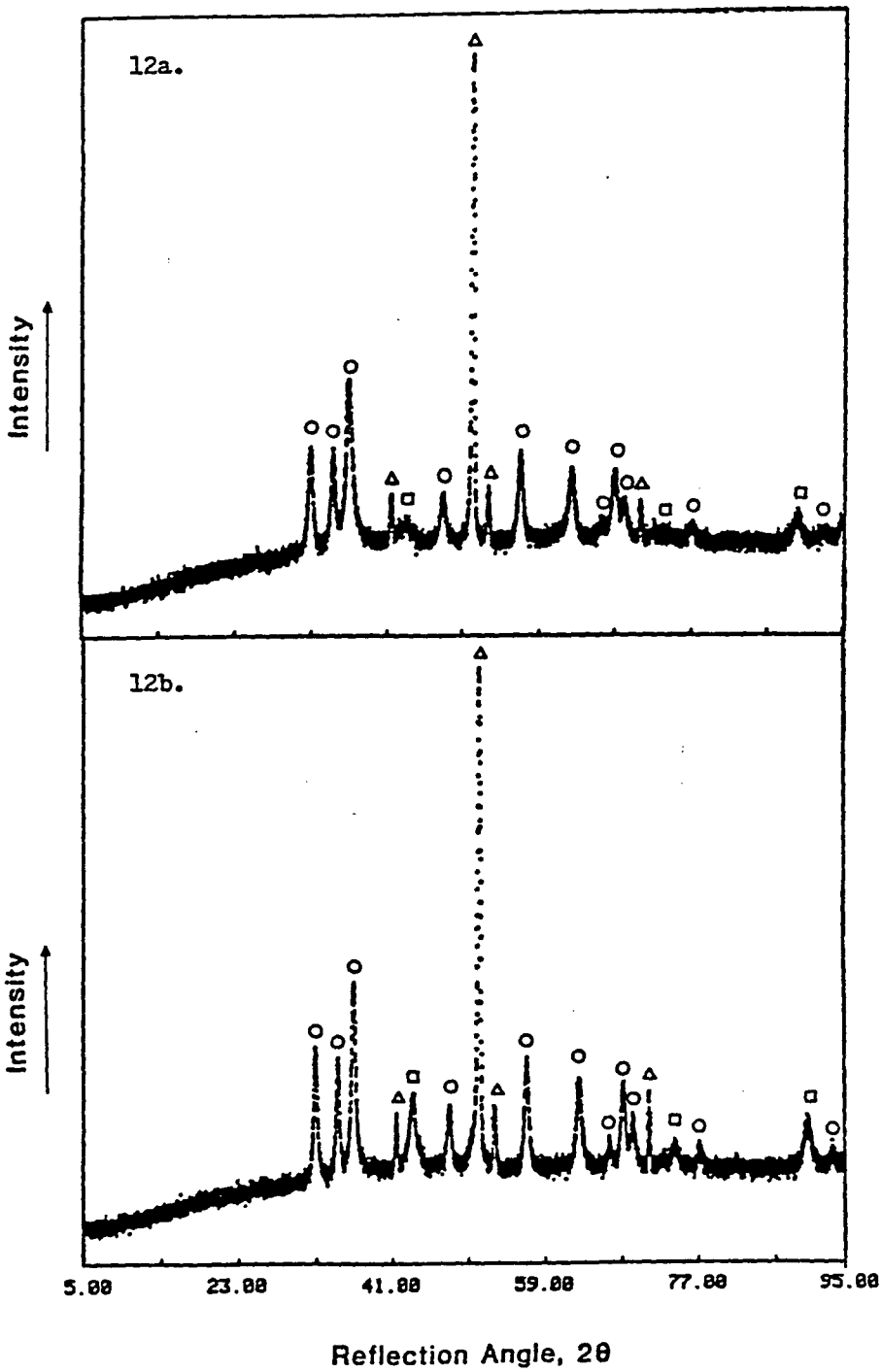

Figure 12 - XRD scans of the untested (12a) and tested (12b) 0.23% Tl/Cu/ZnO catalysts. Peaks identified as copper (□), zinc oxide (○), or beryllium (△).

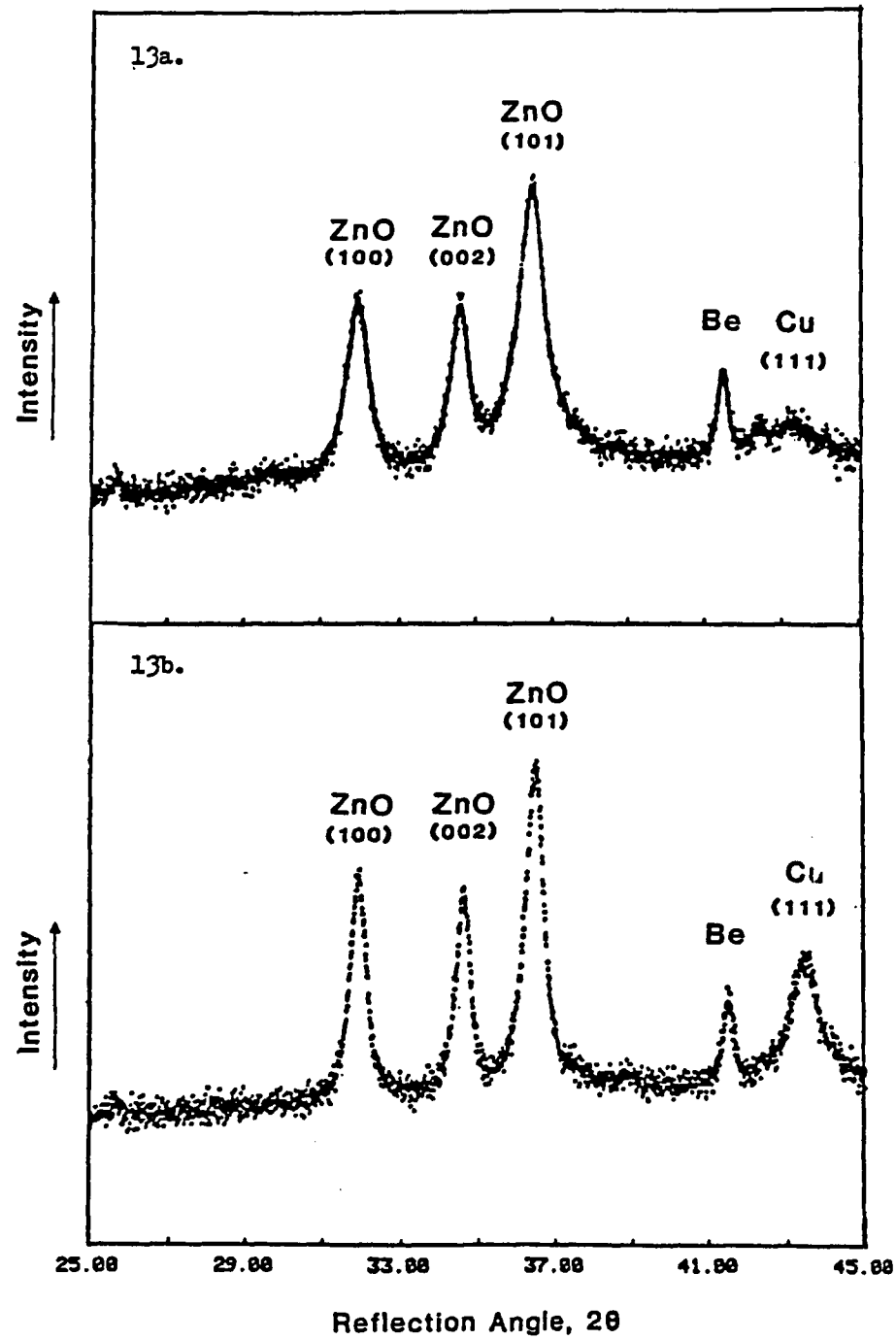

Figure 13 - XRD scans of the untested (13a) and tested (13b) 0.23% Tl/Cu/ZnO catalysts. Scans show the peaks used in the analysis of all samples.

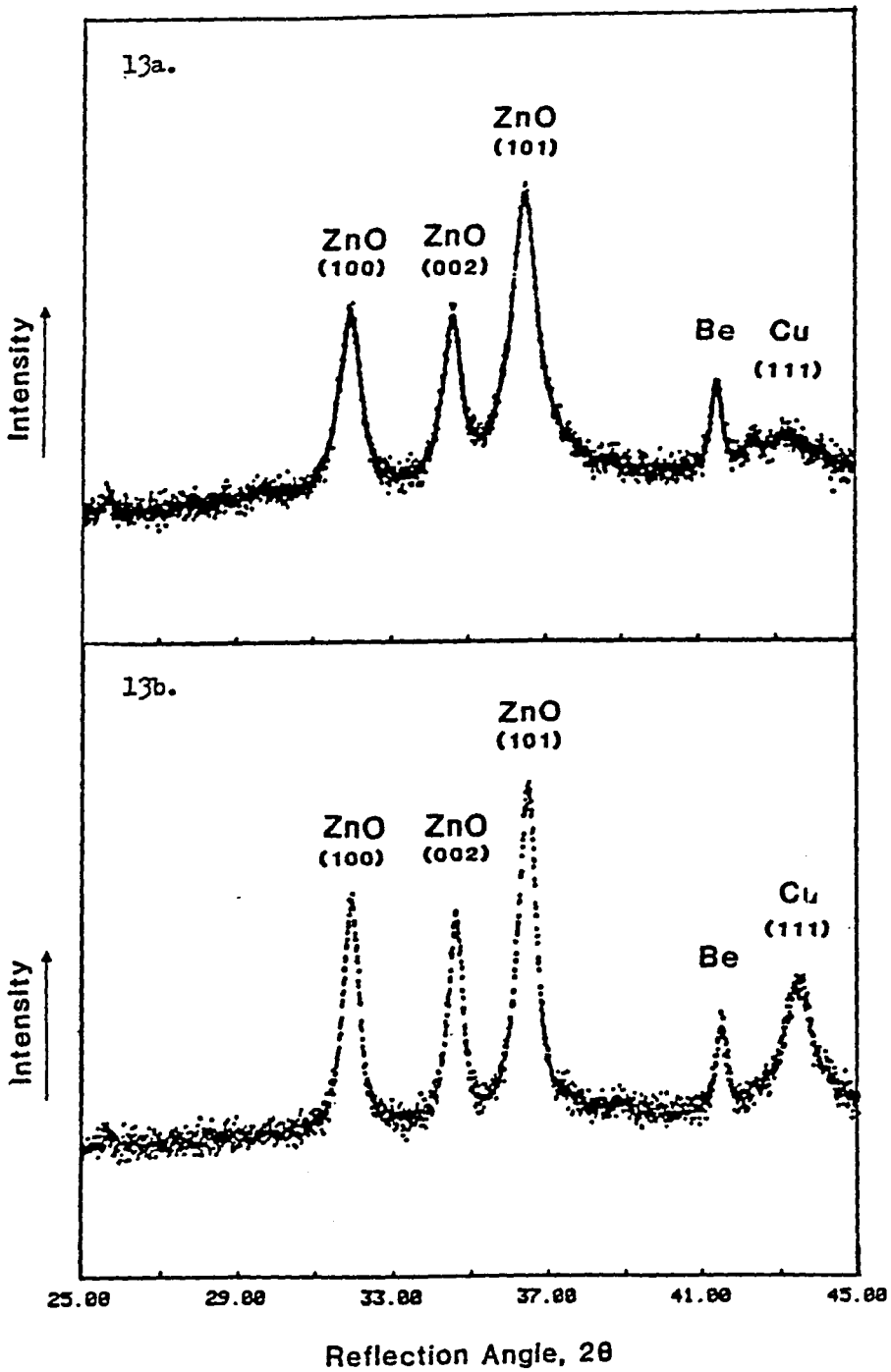

Figure 13 - XRD scans of the untested (13a) and tested (13b) 0.23% Tl/Cu/ZnO catalysts. Scans show the peaks used in the analysis of all samples.

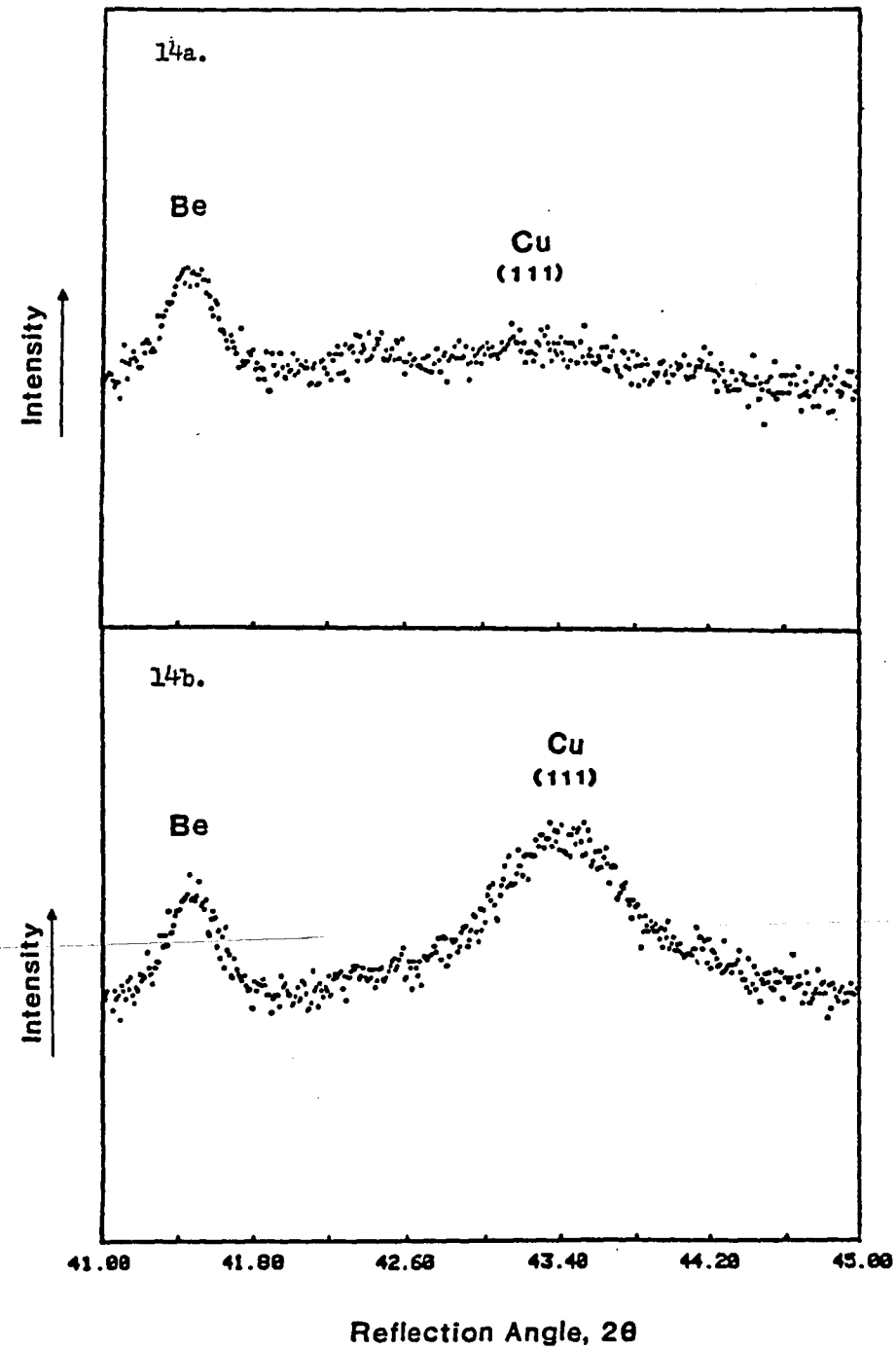

Figure 14 - XRD scans of the untested (14a) and tested (14b) 0.23% Tl/Cu/ZnO catalysts. Scans show change in Cu(111) peak upon testing.

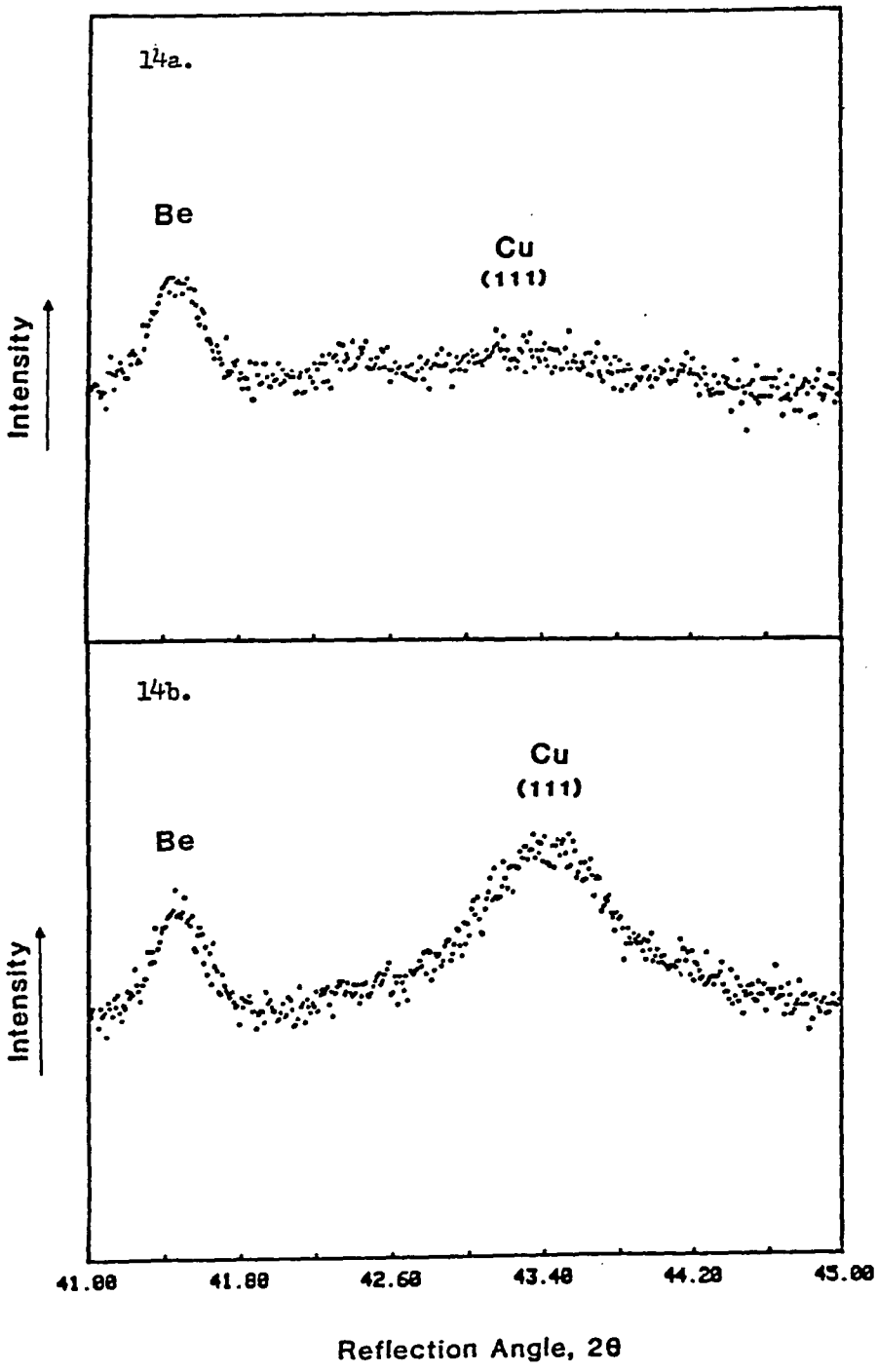

Figure 14 - XRD scans of the untested (14a) and tested (14b) 0.23% Tl/Cu/ZnO catalysts. Scans show change in Cu(111) peak upon testing.

covered up by the ZnO (101). No CuO reflections were observed in any of the analyzed samples.

No unidentified peaks were present in any of the samples except for those assigned to the sample holder. These sample holder reflections could not be identified since the beryllium window was above the rest of the holder and was therefore out of proper geometric alignment for analysis of the diffraction angles.

3.4.2 Lattice Spacings

Values for lattice spacings, d, calculated from values of 2θ (corrected) are listed in Table 13. The accuracy of the d spacings was estimated to be within 0.0002 nm.

Three reflections due to the zinc oxide phase were routinely analyzed. The values for the lattice plane spacings of the untested samples were slightly higher than for the ZnO standard. While this change was only 0.0002 nm, which is within the experimental error, the values for the d spacings were always on the high side. The d spacings were reduced slightly and were more nearly equal to the standard values after testing. The undoped Cu/ZnO catalyst showed similar behavior.

Untested catalyst samples had very low and broad peaks due to the metallic Cu (111) reflection. This peak was too low and broad to be used to calculate the d spacing. Tested samples showed the Cu (111) spacing to be greater than in the copper

Table 13 - Lattice Spacings (d) and Particle Sizes (t) Determined by XRD

Sample		Reflection							
		ZnO (100)		ZnO (002)		ZnO (110)		Cu (111)	
		d*	t*	d	t	d	t	d	t
Cu, ZnO Standards		0.2816		0.2605		0.2477		0.2088	
Cu/ZnO	R	0.2819	13.0	0.2608	15.0	0.2481	11.7	0.2094	9.4
Cu/ZnO	T	0.2817	15.1	0.2606	17.9	0.2478	14.6	0.2102	10.7
0.02% Tl/Cu/ZnO	U	0.2819	16.93	0.2610	16.86	0.2479	12.76	---	7.9
0.02% Tl/Cu/ZnO	T	0.2817	25.34	0.2605	28.58	0.2478	22.75	0.2092	16.01
0.08% Tl/Cu/ZnO	U	0.2817	15.21	0.2607	18.67	0.2478	13.80	---	8.7
0.08% Tl/Cu/ZnO	T	0.2816	23.63	0.2605	25.29	0.2477	20.28	0.2090	13.36
0.23% Tl/Cu/ZnO	U	0.2817	16.32	0.2606	18.90	0.2477	13.20	---	8.9
0.23% Tl/Cu/ZnO	T	0.2816	22.61	0.2605	26.62	0.2477	20.17	0.2090	14.72
0.08% Tl/Cu/ZnO	S1	---	14.33	---	15.43	---	12.95	---	8.3
0.08% Tl/Cu/ZnO	S2	0.2817	15.67	0.2604	18.35	0.2471	14.87	0.2090	13.78

R - reduced; U - untested; T - tested; S1 - short test, no H_2O; S2 - short test H_2O.
* d and t values in nm.

standard. This trend was also observed in the tested undoped Cu/ZnO. A reduced but untested sample of Cu/ZnO showed a slightly increased Cu (111) lattice spacing. The Cu_2O reflections could not be detected.

It should be noted that the tested samples of undoped Cu/ZnO had undergone more severe testing than the other samples.

3.4.3 Particle Sizes

Listed in Table 13 along with the values for lattice spacings, d, are the particle sizes, t, determined from the line broadening using the Scherrer equation. The values for the instrumental broadening were determined using the copper and zinc oxide standards, which had particle sizes in the micron range.

The size of zinc oxide particles was observed to increase upon testing. This was observed for all samples although it was noticed that the doped samples increased more in size than the undoped samples.

Values for the particle size for copper were estimated for the untested samples based on the small Cu (111) reflection. Particle sizes for the tested samples were easier to determine since the intensity of the reflection at maximum was greater than for the untested samples. As with zinc oxide, the particle size of the copper increased upon testing. The particle size increases of zinc oxide and copper were not proportional, with

the copper particles increasing to a greater extent. The observed increases were greater for the doped samples than for the undoped sample. Particle sizes for copper species other than metallic copper could not be determined even if they were present.

3.5 X-Ray Photoelectron Spectroscopy

3.5.1 Surface Concentrations of Thallium

XPS was performed on the tested 0.02, 0.08, and 0.23% Tl/Cu/ZnO samples and on an untested 0.23% Tl/Cu/ZnO sample in order to determine the surface concentration of thallium. Samples of typical XPS scans are shown in Figures 15 and 16. The survey scan shown in Figure 15 indicates the peaks which were used for anslysis, and Table 14 accounts for all peaks in the scan.

The values for the surface concentrations of thallium in the samples are listed in Table 15. These values were calculated based on the discussion given in Section 2.5.4, which is taken from Himelfarb et al. (26). The value for λ_{Zn} used in these calculations, 0.86 nm (23), was chosen over another reported value, 1.46 nm (27). The value of 0.86 nm gave surface thallium concentrations which were realistic, while the other value gave impossibly high surface thallium concentrations, greater than theoretically possible. Also listed in Table 15

are these theoretical values for thallium concentration which were calculated using the elemental analysis for the bulk thallium content assuming all the thallium to be on the surface. These data are presented in Figure 17.

The values for the surface concentration of thallium on the tested 0.08 and 0.23% Tl/Cu/ZnO catalysts were near to the theoretical values, but were slightly low. No value for the 0.02% Tl/Cu/ZnO catalyst was calculated because the Tl $4f_{\frac{7}{2}}$ signal could not be separated from the other Tl signal and the Cu 3s signal for accurate integration. The value for thallium concentration on the untested sample was less than on its tested counterpart and was again less than the theoretical amount.

3.5.2 Chemical State Identification

Values for the binding energies of the observed photoelectron signals are given in Table 16. These values were calculated by correcting the experimental binding energies for charging of the samples. This was done by setting the Zn $2p_{\frac{3}{2}}$ signal equal to 1021.7 eV and adjusting the other values accordingly.

The average position of the Cu $2p_{\frac{3}{2}}$ signal was 932.0 eV in the tested and untested samples. The O 1s signal was at about 530.0 eV in the tested samples but occurred at a slightly lower value in the untested sample. The Tl $4f_{\frac{7}{2}}$ signal occurred at an average value of 117.5 eV. The center of the signal on the 0.02% Tl/Cu/ZnO sample could not be determined.

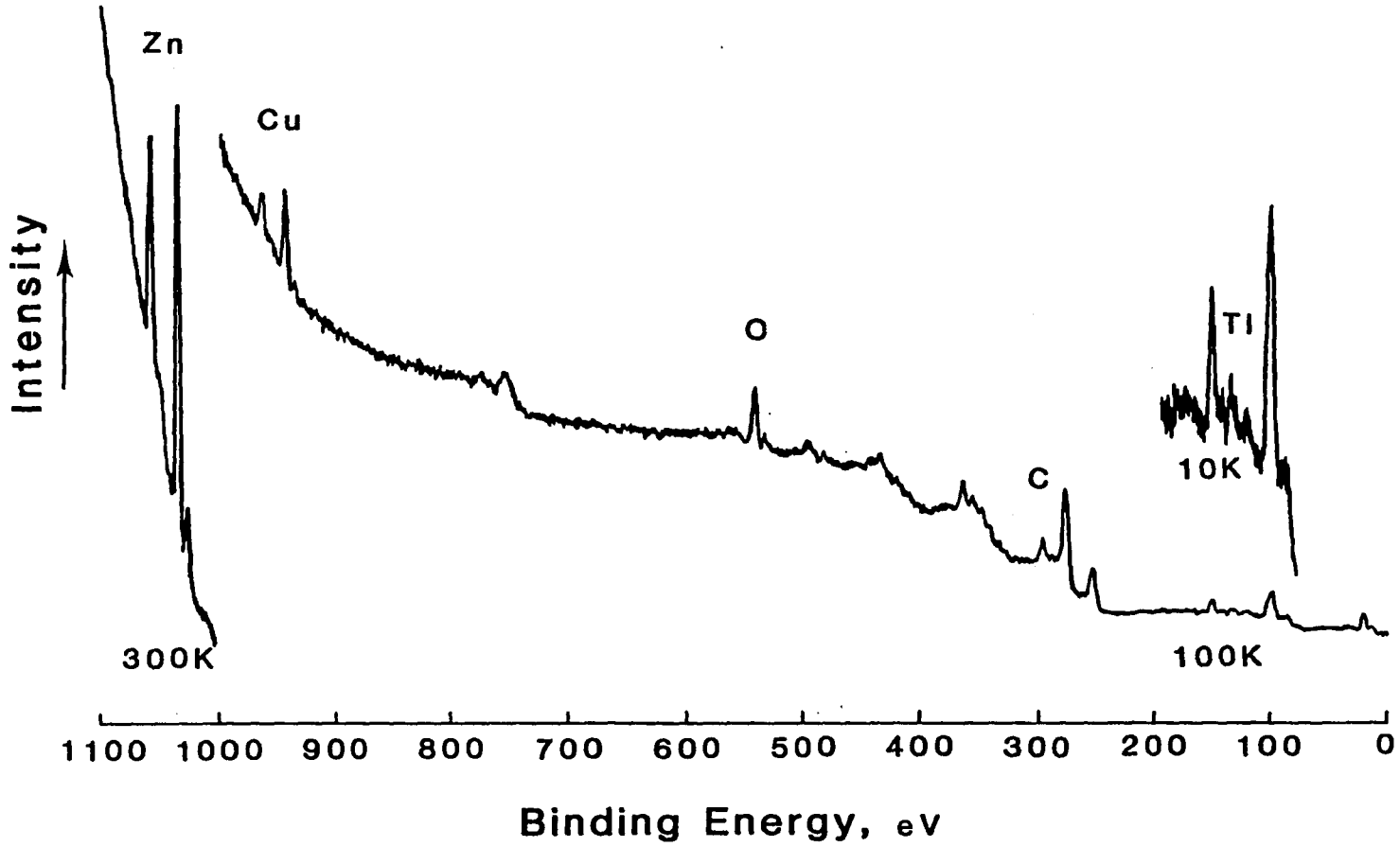

Figure 15 - X-ray photoelectron spectrum of the tested 0.08% Tl/Cu/ZnO catalyst. Scan indicates the peaks used in subsequent analyses.

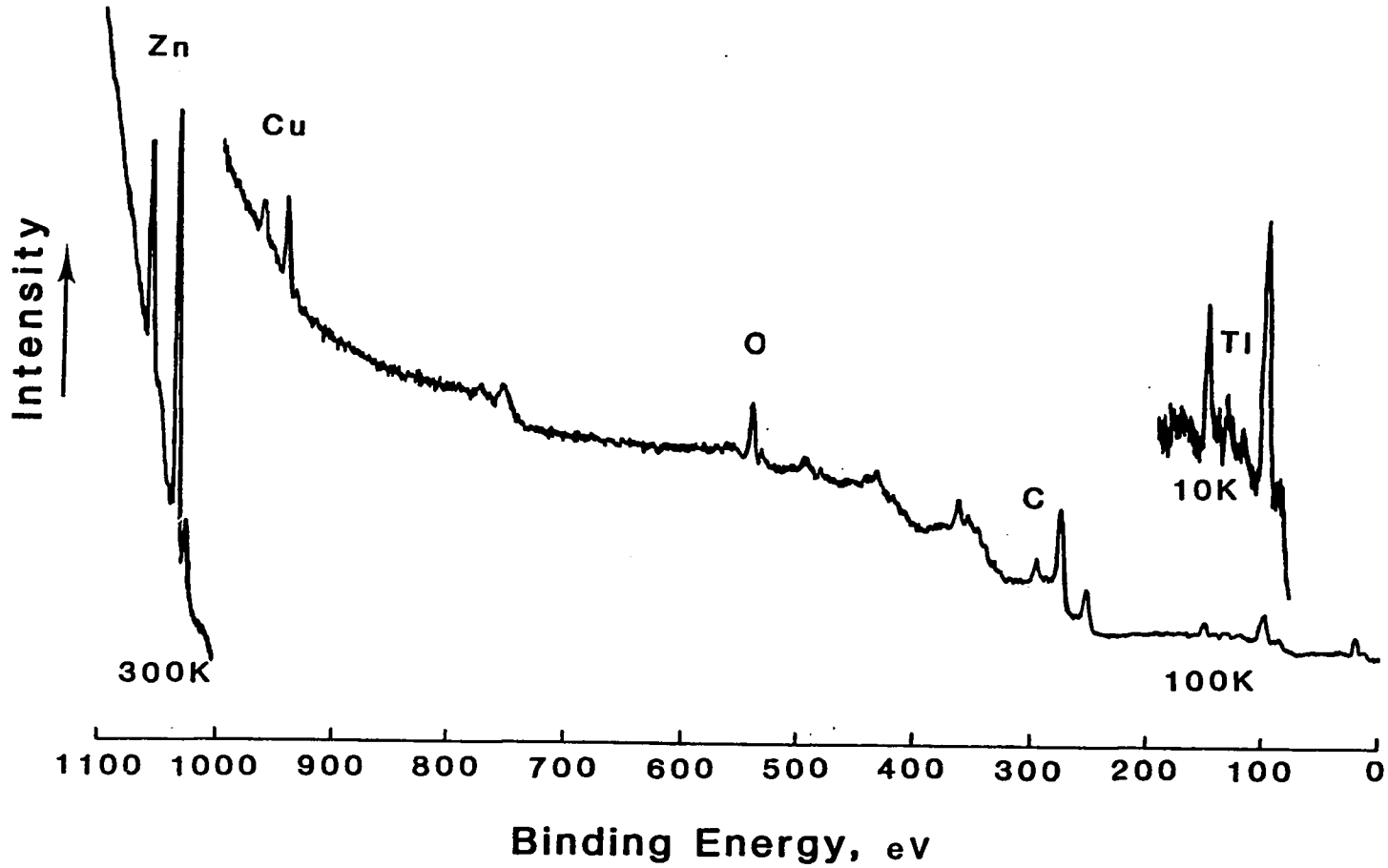

Figure 15 - X-ray photoelectron spectrum of the tested 0.08% Tl/Cu/ZnO catalyst. Scan indicates the peaks used in subsequent analyses.

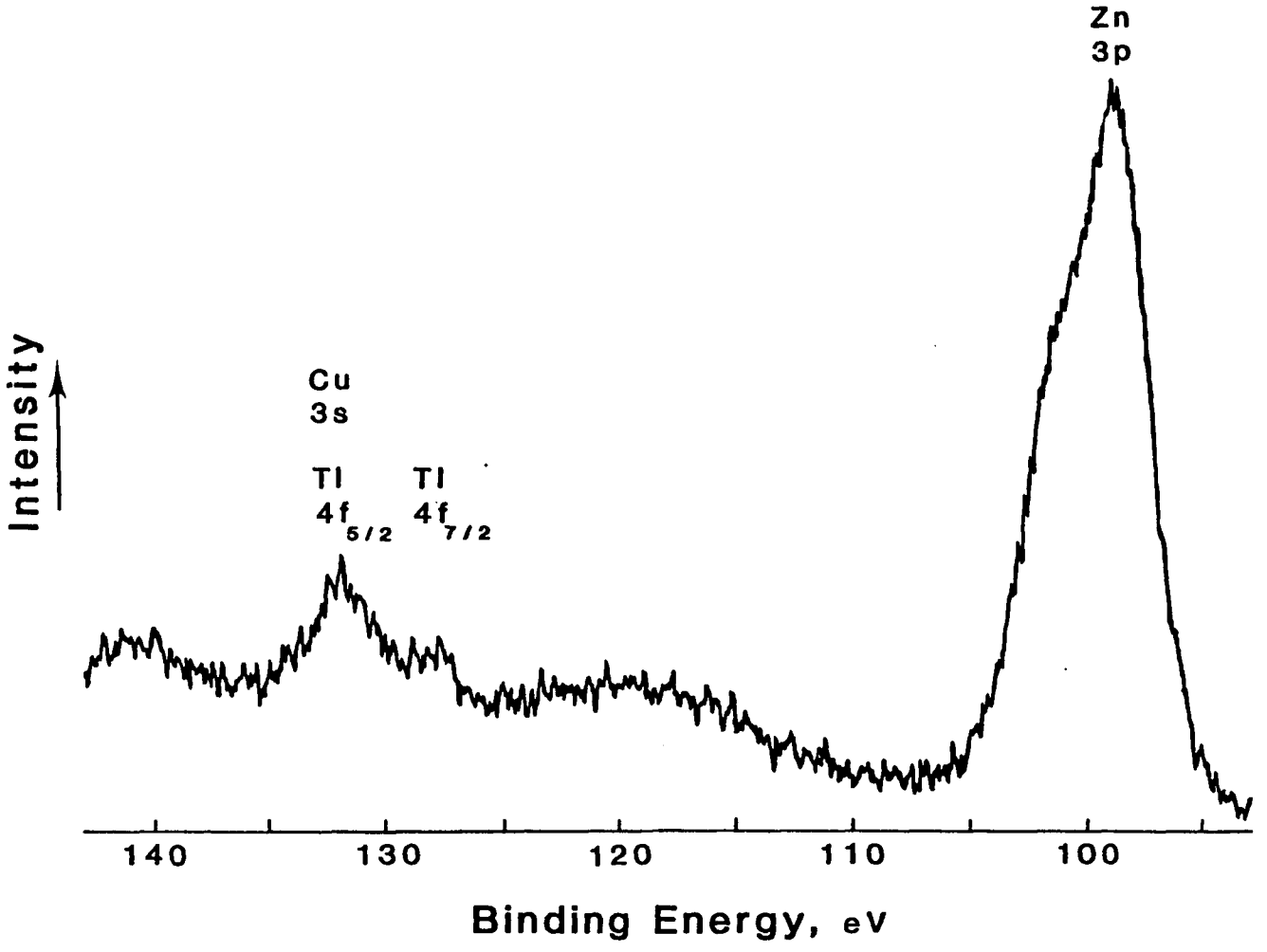

Figure 16a

Figure 16 - X-ray photoelectron spectra of: Tl 4f doublet and Zn 3p signal (16a); Zn 2p doublet (16b); O 1s signal (16c); and Cu 2p doublet (16d).

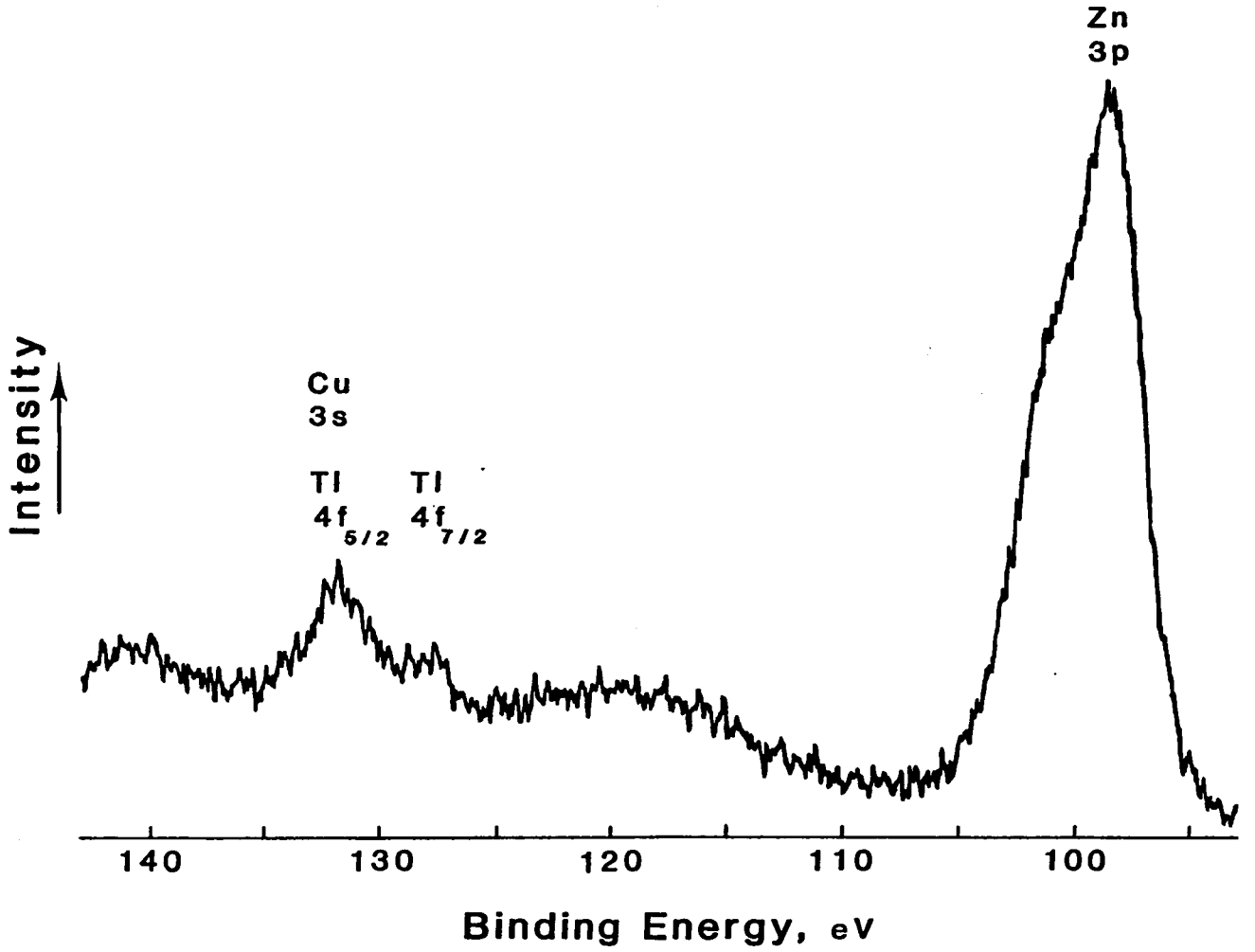

Figure 16a

Figure 16 - X-ray photoelectron spectra of: Tl 4f doublet and Zn 3p signal (16a); Zn 2p doublet (16b); O 1s signal (16c); and Cu 2p doublet (16d).

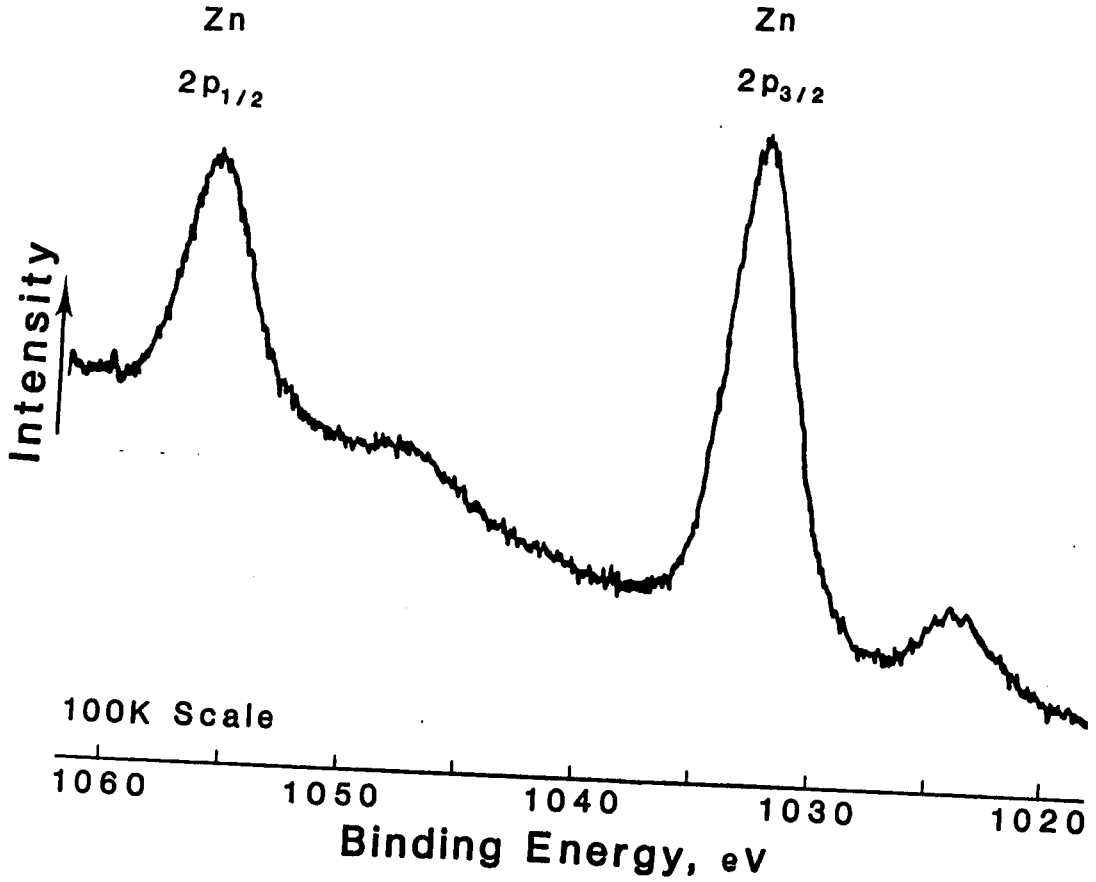
Zn
2p1/2
Zn
2p3/2
Intensity
100K Scale
1060
1050
1040
1030
1020
Binding Energy, eV

Figure 16b

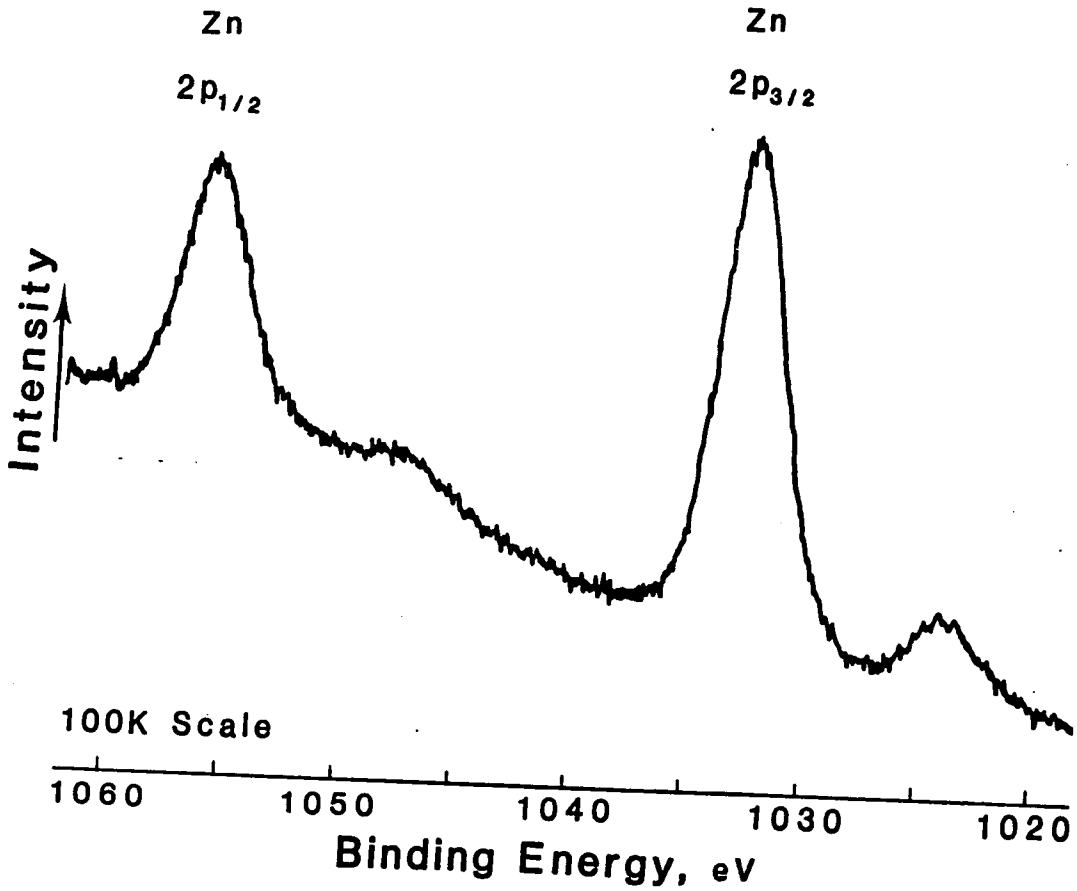
Zn
2p1/2
Zn
2p3/2
Intensity
100K Scale
1060
1050
1040
1030
1020
Binding Energy, eV

Figure 16b

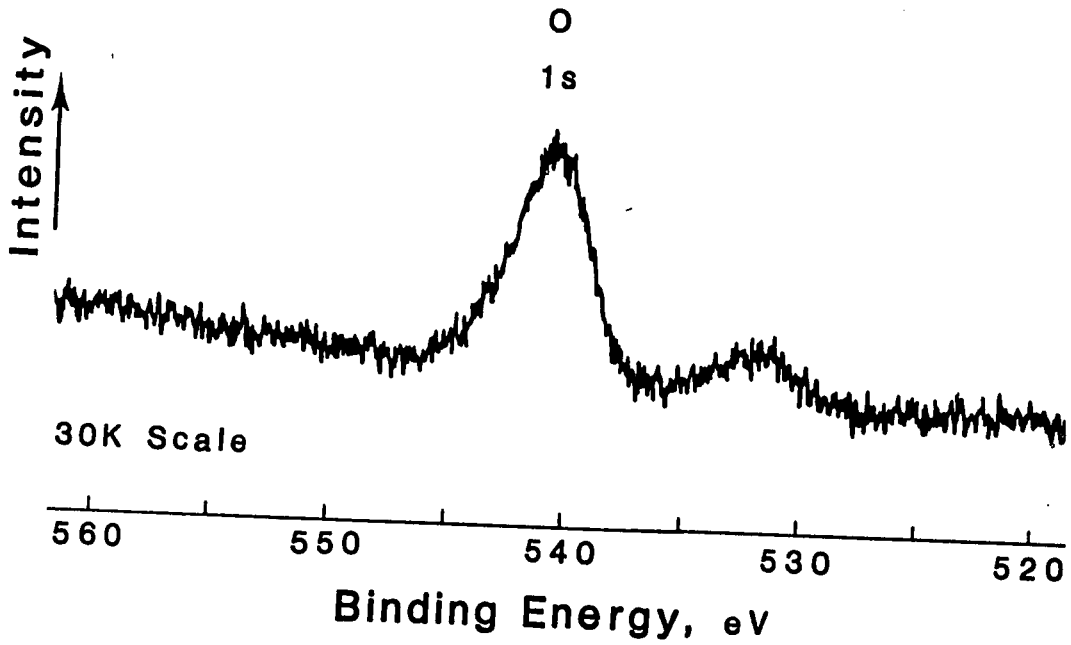
O
1s
Intensity
30K Scale
560
550
540
530
520
Binding Energy, eV

Figure 16c

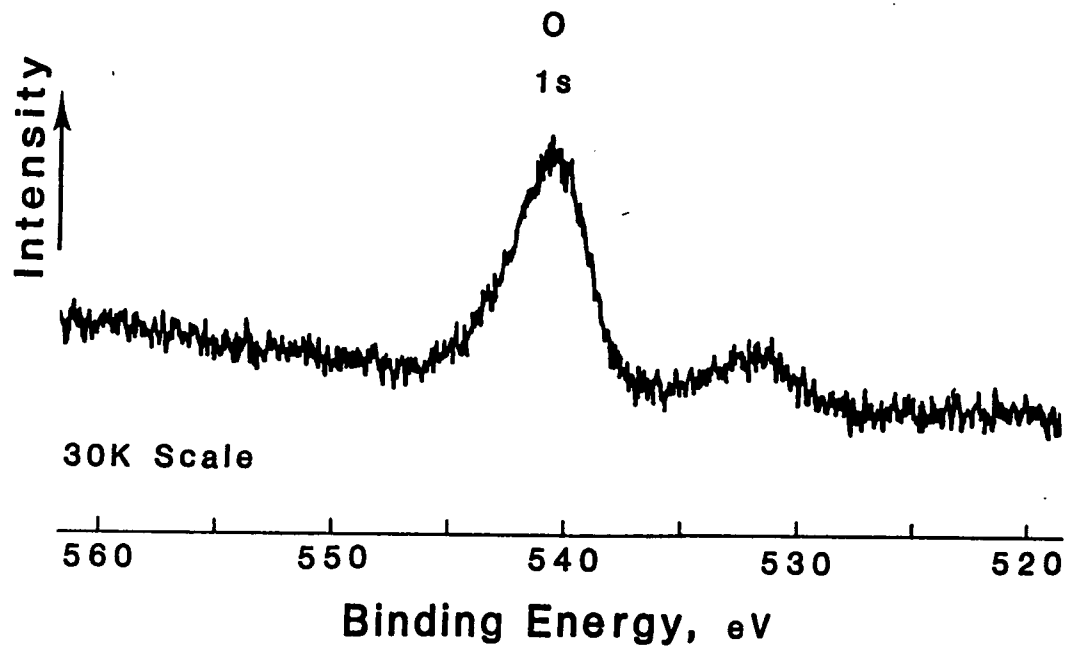
O
1s
Intensity
30K Scale
560
550
540
530
520
Binding Energy, eV

Figure 16c

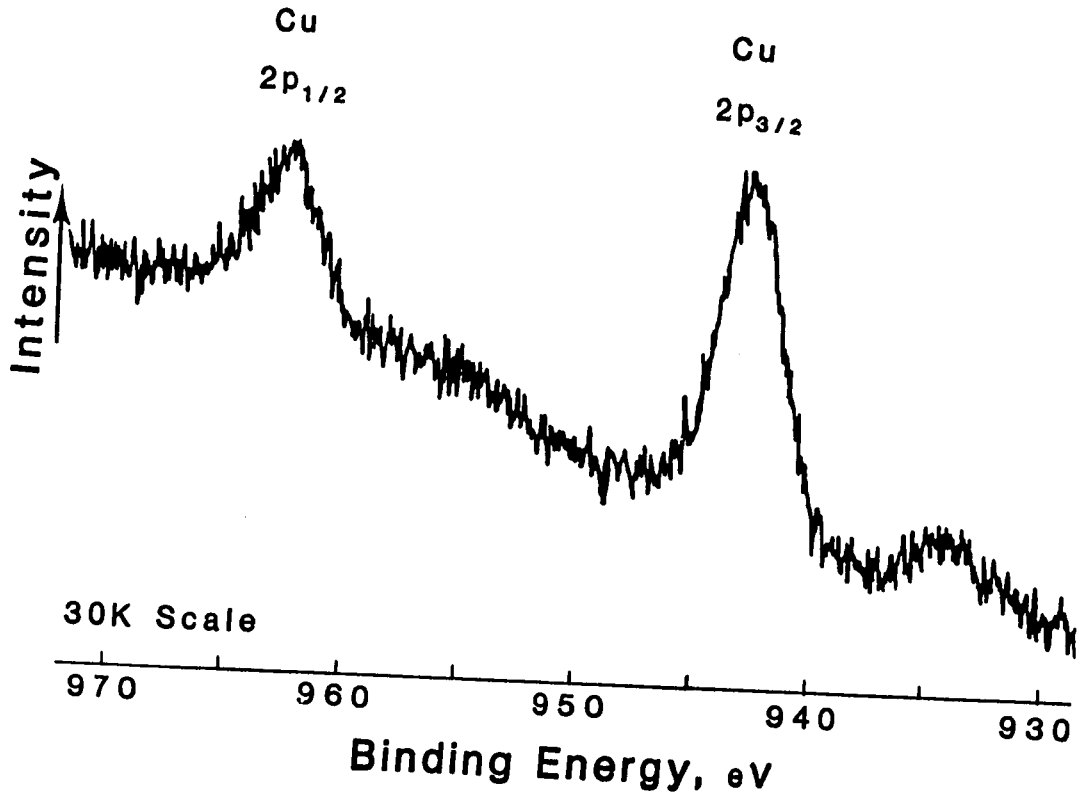
Cu
2p1/2
Cu
2p3/2
Intensity
30K Scale
970
960
950
940
930
Binding Energy, eV

Figure 16d

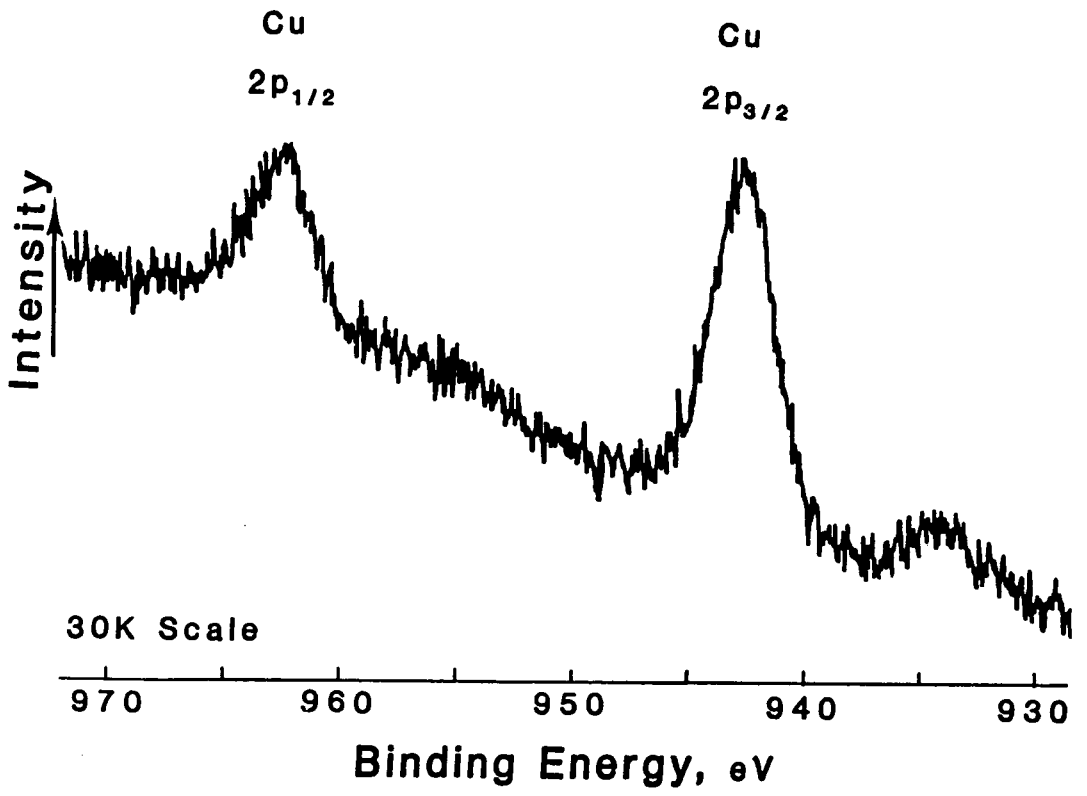
Cu
2p1/2
Cu
2p3/2
Intensity
30K Scale
970
960
950
940
930
Binding Energy, eV

Figure 16d

Table 14 - XPS Peak Assignments

B.E*, eV	Source
1044	Zn 2p
1021	Zn 2p
953	Cu 2p
933	Cu 2p
765 - 745	O KVV A**
531	O 1s
490	Cu LMM A
425	Cu LMV A
"	Zn LMM A
350 - 335	Zn LMM A
"	Cu LVV A
285	C 1s
265 - 240	Zn LMM A
140	Zn 3s
130	Tl 4f
"	Cu 3s
"	Tl 4f
90	Zn 3p
75	Cu 3p
10	Zn 3d

* adjusted for 10 eV charging
** A - Auger signal

Table 15 - Surface Thallium Concentrations

Catalyst	Thallium Concentration		
	Experimental		Theoretical[b]
	atoms/g	atoms/m^2	atoms/m^2
Cu/ZnO	0	0	0
Tested 0.02% Tl/Cu/ZnO	---[a]	---	0.57×10^{17}
Tested 0.08% Tl/Cu/ZnO	6.02×10^{18}	2.84×10^{17}	2.94×10^{17}
Tested 0.23% Tl/Cu/ZnO	1.74×10^{19}	8.09×10^{17}	8.47×10^{17}
Untested 0.23% Tl/Cu/ZnO	1.27×10^{19}	3.44×10^{17}	4.97×10^{17}

a - none detected

b - calculated as molar Tl concentration (atoms/g) divided by catalyst surface area (m^2/g).

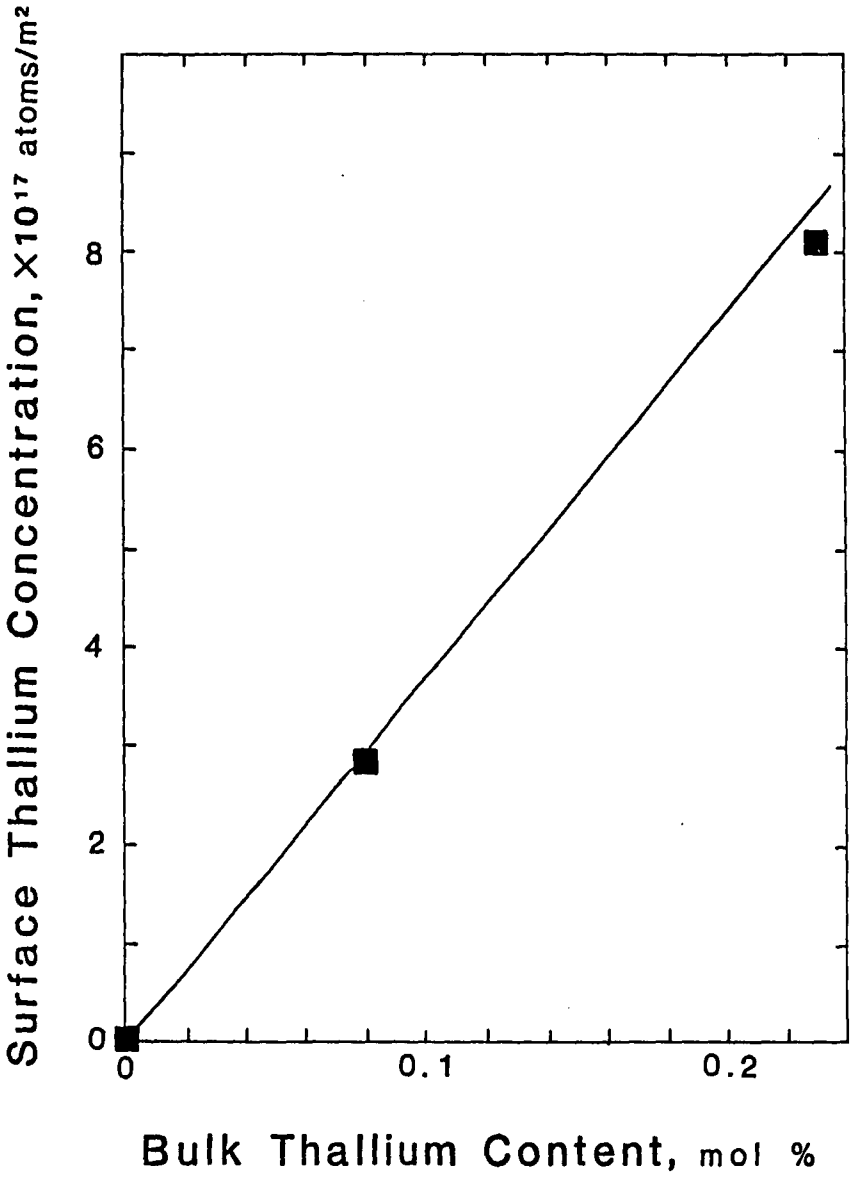

Figure 17 - Surface thallium concentration versus bulk thallium content in Tl/Cu/ZnO catalysts. Line depicted is theoretical surface concentration for given bulk content.

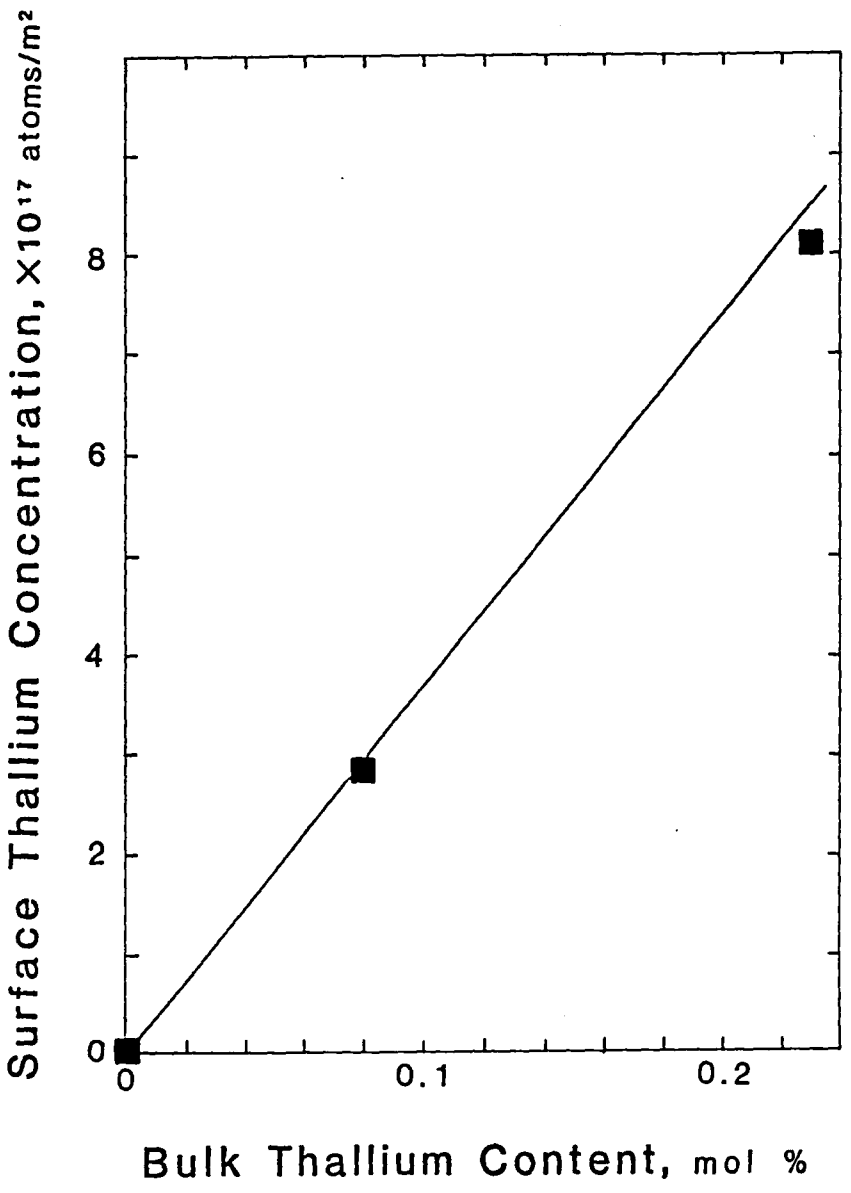

Figure 17 - Surface thallium concentration versus bulk thallium content in Tl/Cu/ZnO catalysts. Line depicted is theoretical surface concentration for given bulk content.

Table 16 - XPS Peak Binding Energies (eV)

Sample	Zn 2p	Cu 2p	O 1s	Tl 4f
0.02% Tl/Cu/ZnO T	1021.7*	932.0	530.1	---
0.08% Tl/Cu/ZnO T	1021.7	932.0	529.9	117.3
0.23% Tl/Cu/ZnO T	1021.7	932.1	530.2	117.6
0.23% Tl/Cu/ZnO U	1021.7	932.2	529.5	117.6

* Zn 2p doublet peaks set equal to literature values for ZnO (20)

T - tested; U - untested

3.5.3 Carbon Analysis

Carbon signals were seen on all samples, including the reduced undoped Cu/ZnO. Since carbon was observed on this reduced undoped Cu/ZnO, where none was expected, the carbon must be attributed to exposure of the samples to air. Carbon signals at about 284 eV are sometimes observed in XPS analyses on samples which were exposed to air (20). The small signal seen for the samples analyzed actually correspond to a large amount of material on the catalyst surfaces, probably about 70%. Because of this large amount, an accurate analysis for residual carbon on the surface due to formate groups in the untested sample or carbon fouling in the tested sample was impossible.

The raw carbon XPS analysis data was analyzed by a peak fitting program. This was done to determine if there was more than one signal contributing to each observed peak. Spectra from the reduced undoped Cu/ZnO, untested 0.23% Tl/Cu/ZnO, and tested 0.23% Tl/Cu/ZnO samples are shown in Figure 18. Computer fits of the Zn LMM auger signals were used to set the baselines under the carbon signals. The computer program was able to fit the experimental data in each case by using only one carbon signal in each of the scans. The program did not need to use two peaks to accurately fit any of the experimental signals. The one peak on each of the scans, between 290 and 300 eV binding energy (uncorrected for sample charging), was due to

the air contamination. When corrected for sample charging, these peaks shift to about 284 eV, which is the value found for hydrocarbons. Binding energies expected for other types of carbon would be: 290 eV for oxygenated carbon, 282 eV for surface carbon; or 285 eV for graphitic carbon (20).

It may not have been possible to see small amounts of other types of carbon on the surface due to the large amount of this contamination signal. It is estimated that there should have been about 5% carbon on the surface of the untested Tl/Cu/Z Tl/Cu/ZnO due to the formate groups. This signal would have to have been very small because of the small photoionization cross section of carbon. Likewise, if the amount of carbon buildup on a sample was small it may not be seen for the same reason.

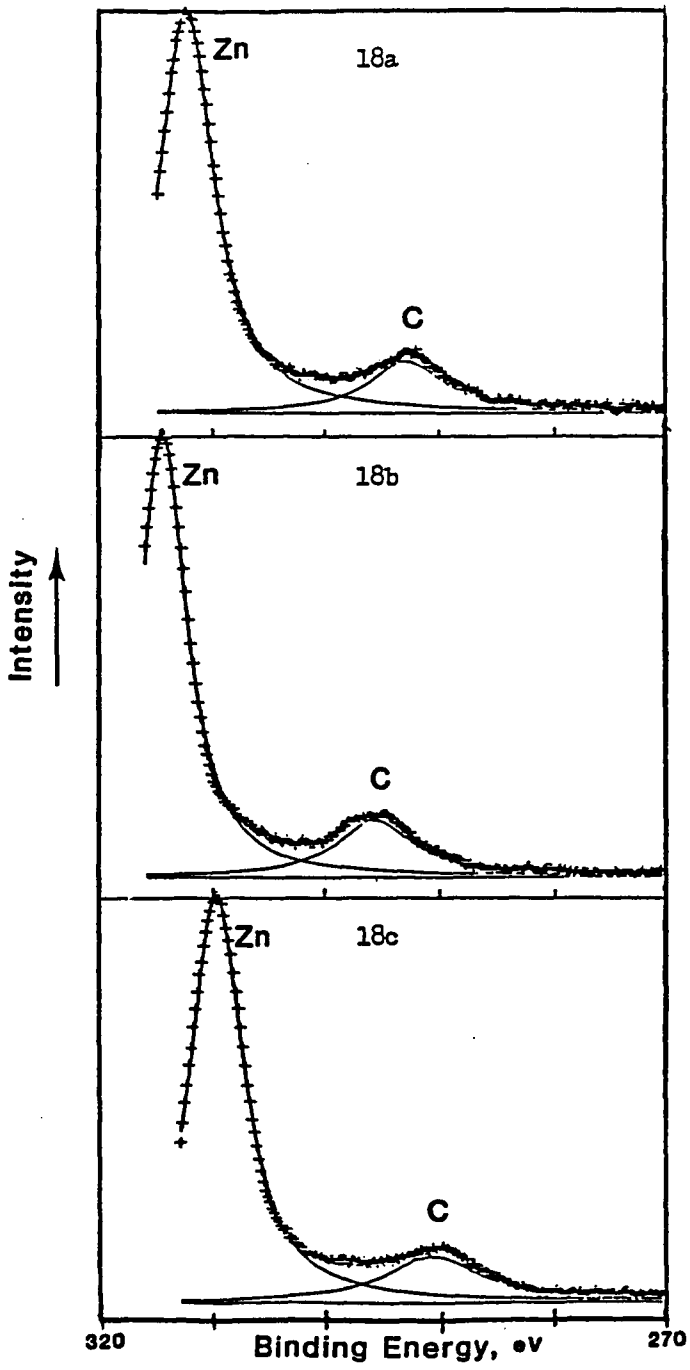

Figure 18 - Computer peak fits of carbon 1s XPS signal. Cu/ZnO (18a), 0.23% Tl/Cu/ZnO untested (18b) and tested (18c).

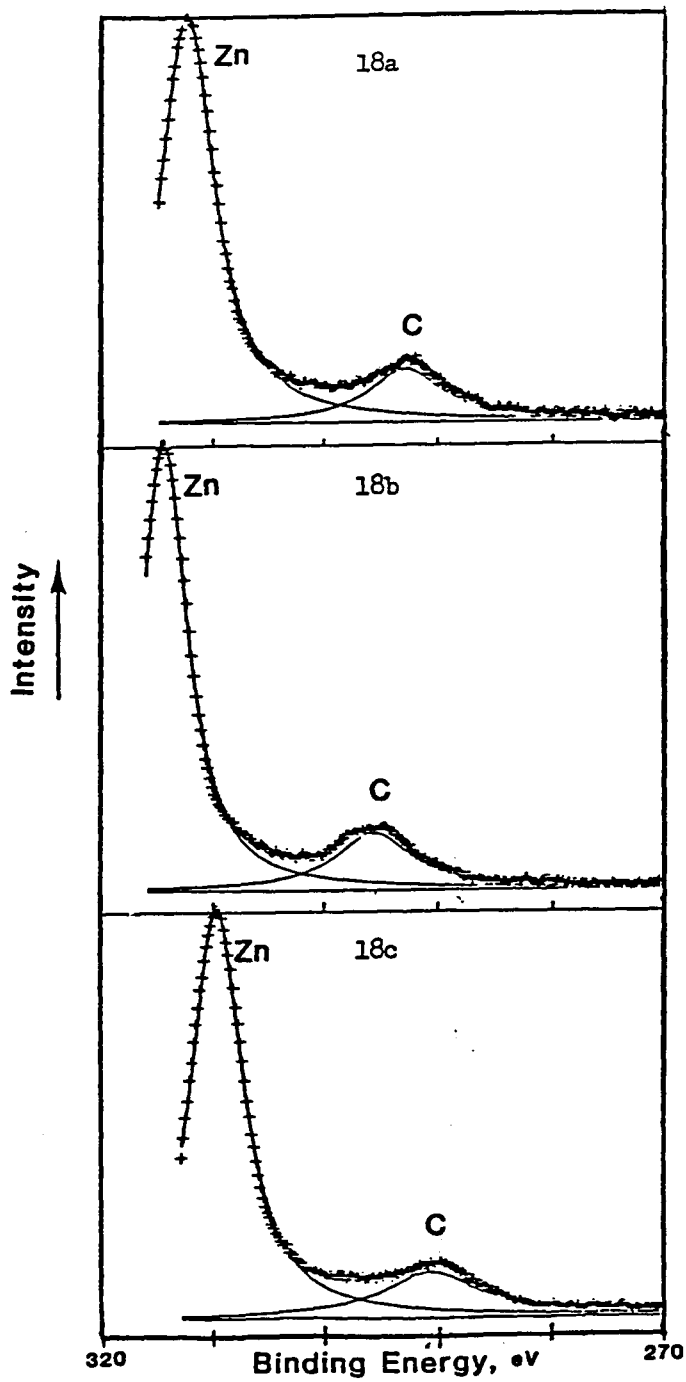

Figure 18 - Computer peak fits of carbon 1s XPS signal. Cu/ZnO (18a), 0.23% Tl/Cu/ZnO untested (18b) and tested (18c).

4.0 DISCUSSION

4.1 Catalyst Morphology

4.1.1 Untested Tl/Cu/ZnO Catalysts

A number of changes in the physical state of the Cu/ZnO catalyst occur as a result of the doping procedure.

The morphology of the reduced Cu/ZnO has been investigated previously (25). X-ray diffraction indicated that two material phases were present in the catalyst. The first phase consists of metallic copper, and the second phase is made up of zinc oxide with possible solid solution of copper in it. This solid solution was suggested to give the catalyst its characteristic color and slightly increases the zinc oxide lattice spacings. The visual observations and x-ray diffraction work done here are in agreement with the previous findings. Values for particle sizes and lattice spacings are similar to the values reported by Bulko (25). The value for the BET surface area of the reduced Cu/ZnO, 37.9 m^2/g, is similar to the values reported by others (4,25).

During the doping procedure, it was noticed that the addition of reduced Cu/ZnO to the thallium formate solution caused an evolution of a gas, and that the dry doped catalysts had a green tint. Similar results were found for the alkali-

doped catalysts of Young (13) and Vedage (28). It is apparant that the reduced catalyst had been oxidized to some extent. Evidence for this comes from the observation of the green color, which had been seen by Bulko for some slightly reoxidized Cu/ZnO catalysts, and from the x-ray diffraction scans in which the Cu (111) reflection is nearly absent for the untested samples.

The doping of the Cu/ZnO also caused a slight decrease in the surface areas of the catalysts. The attempted re-reduction of one of the Tl/Cu/ZnO catalysts showed that this slight loss of surface area was not recoverable.

If the values of the zinc oxide lattice spacings in the catalysts are indicative of the existence of dissolved copper, then the results show that the copper in zinc oxide solid solution is maintained throughout the doping procedure.

X-ray photoelectron spectroscopy results confirm that thallium is present on the surface of the doped catalysts, see Table 15. The amount of thallium detected by XPS is slightly less than one would expect assuming all the thallium introduced into the catalyst to be on the surface of the catalyst. A large systematic error is introduced by the uncertainty in the reference escape depth λ_{Zn} (16). If this value is correct, however, the attenuation of the thallium signal could be due to coverage of the thallium by the formate groups and by zinc which had gone into solution and was then redeposited upon drying (29). It is not likely that thallium had migrated into the zinc oxide or

copper lattices because of its large size.

4.1.2 Tested Tl/Cu/ZnO Catalysts

The testing procedure changed the morphology of both the undoped Cu/ZnO and the Tl/Cu/ZnO catalysts.

The first change in the physical nature of the catalysts was noticed by visual inspection of the catalyst upon its removal from the reactor. In all cases, the catalysts were a reddish-brown color, which is an indication of sintering or segregation of the copper particles in the catalyst. The fact that the catalysts were still very dark in color indicates that there was still a solid solution of copper in zinc oxide or that there was still some type of intimate contact between the zinc oxide and the copper capable of allowing this electronic interaction. Loss of this intimate contact would lead to a catalyst whose color was a mixture of the white from the zinc oxide and the red from the copper metal.

X-ray diffraction studies confirmed the size increase of the copper particles as well as the zinc oxide particles, Table 13. All of the doped catalysts seem to sinter to approximately the same extent, with more sintering occurring with prolonged testing. Likewise, testing for short periods led to only a slight increase in particle size. The 0.08% Tl/Cu/ZnO tested at 523 K and 508 K in the absence of water had a reddish-brown tint but showed essentially no increase in particle size. After

additional testing in the synthesis gas with water fed at 17 mmol/hr (per 2.45 g of catalyst), the copper particles had sintered to their final size of 14.0 nm whereas the zinc oxide particles were still relatively small, 14.9 to 18.4 nm.

The tested Tl/Cu/ZnO catalysts whowed a decrease in surface area of approximately 40%. The 0.08% Tl/Cu/ nO catalyst, tested in the water-free synthesis gas only, showed a slight decrease in the surface area. Further testing with water in the feed gas caused further decrease in surface area.

The values of the lattice spacings for both the zinc oxide and the copper changed upon catalyst testing. The decrease in the d spacings for the zinc oxide from a value slightly above that for pure zinc oxide to a value nearer to that of pure zinc oxide was observed in all catalysts, doped and undoped. Since the increase in d spacing was attributed to a solution of copper in zinc oxide, a decrease in lattice spacing would indicate removal of some copper from the zinc oxide. Copper must still be in some type of intimate contact with the zinc oxide in order to give the catalysts their dark color. While the zinc oxide lattice spacings decreased slightly, the copper lattice spacing increased slightly for most Tl/Cu/ZnO catalysts. This increase could be accounted for in terms of reduction of the zinc in the zinc oxide and formation of brass:

$$ZnO + H_2 \longrightarrow Zn + H_2O \qquad (19)$$

$$Zn + nCu \longrightarrow Cu_nZn \qquad (20)$$

In order to determine the extent of brass formation, Pearson (30) uses equation 21:

$$a = 1.92 \times 10^{-4} X_{Zn} + 0.36147 \text{ nm} \qquad a < 0.36217 \text{ nm}$$

$$a = 2.33 \times 10^{-4} X_{Zn} + 0.36132 \text{ nm} \qquad a > 0.36217 \text{ nm} \qquad (21)$$

where a is the lattice constant of copper ($a = 3^{\frac{1}{2}}d$ for Cu (111)) and X_{Zn} is the atomic fraction of zinc in copper. Values for the extent of brass formation in these samples, Table 17, indicate only slight formation of brass in samples tested only to 523 K. The formation of brass appeared slow at the low temperatures used in the testing and may also have been limited by the presence of water in the feed gas (31).

The XPS results from Section 3.5.1 show thallium to be present at near theoretical values for the catalysts prepared and tested here. The deviation of the surface thallium concentrations from the theoretical could be due to error in the experimental measurements, coverage of thallium by other species, or agglomeration of the thallium. Incorporation of thallium into the zinc oxide lattice is unlikely based upon the reduction of the zinc oxide lattice spacing upon testing. The possibility that thallium formed an alloy with the copper is dismissed since

Table 17 - Brass Formation in Tl/Cu/ZnO Catalysts

Catalyst*	Brass atom% Zn in Cu
0.02% Tl/Cu/ZnO	4.3
0.08% Tl/Cu/ZnO	2.3
0.23% Tl/Cu/ZnO	3.1

* Tested catalysts

this alloy is unknown (9), and the increase in lattice spacing of copper is readily explained in terms of the well known brass formation.

4.2 Methanol Formation Over the Tl/Cu/ZnO Catalysts

It is readily apparent from Figures 7 and 8 that there is a decreased methanol activity in the thallium-doped catalysts. The concentrations of methanol in the effluent gases from the catalysts can be used for direct comparison as an indication of the rate of methanol synthesis over these catalysts just as the methanol yield can be used. This is because the concentrations of other species in the effluent gases are essentially unchanged from one sample to the next. Whether one considers methanol concentration in the effluent gas or methanol yield, there is a decrease in the activity of the Tl/Cu/ZnO catalysts when compared with the Cu/ZnO. An attempt shall be made to develop a model explaining this thallium poisoning.

One could first consider the decreased surface area of the catalysts. A decreased surface area would expose fewer catalytically active sites which would then decrease the activity of the catalyst. While this decrease in surface area can account for some of the loss of activity, it can not account for all of it. The 0.08% Tl/Cu/ZnO catalyst tested only at 523 K for 14 hrs and at 508 K for 6 hrs had a surface area of 32 m^2/g. One would expect this 15% decrease in surface area to give a corresponding

15% decrease in formation of methanol. At the initial 523 K testing point of the 0.08% Tl/Cu/ZnO catalyst, where one would expect at most a 15% decrease in activity, a 36% decrease in activity relative to the undoped Cu/ZnO was observed. Since the surface areas of the tested samples are known, one could compare the amount of methanol in the effluent gas at the last testing point, the 508 K condition with no water in the feed gas, in which the surface area should be at its final value. All of the catalysts have shown about a 40% decrease in surface area after testing, and the amount of methanol found in the effluent gas at this last testing point (4.7, 3.6, and 2.7 mol% for the 0.02, 0.08, and 0.23% Tl/Cu/ZnO catalysts respectively) cannot match the 8.5% found for the undoped catalyst even when the surface area difference is taken into account. Therefore, the decrease in surface area can account for some but not for all of the decrease in methanol activity seen over the Tl/Cu/ZnO catalysts.

X-ray diffraction showed sintering of the copper and zinc oxide particles in the catalysts. This effect is intimately related to the surface area, since larger particles would lead to a loss of surface area. The sintering effect should then be considered essentially the same as the surface area effect in causing some but not all of the decrease in methanol activity seen over the Tl/Cu/ZnO catalysts. Other points to be considered come out of the diffraction study. First, there was some

brass formation in the Tl/Cu/ZnO catalysts. This brass formation is also seen to the same extent in the undoped Cu/ZnO and cannot therefore be the cause of the activity decrease (25). A decrease in the zinc oxide lattice spacing upon testing was observed on the Tl/Cu/ZnO catalysts but has also been reported for the undoped Cu/ZnO (25).

The lack of full explanation for the decreased catalytic activity of the Tl/Cu/ZnO catalysts by the above arguments indicates that thallium must be playing a specific chemical role in the decrease of catalyst activity. The XPS analysis determined that almost all of the thallium was present on the surface of the catalyst in the tested samples. The thallium must therefore be preventing the active sites from functioning in methanol synthesis. If the observed reaction rate is dependent upon the number of active surface sites, the rate of reaction is expressed as equation 22:

$$r = k S^n \tag{22}$$

$$r = k (S_o - S_{Tl})^n \tag{23}$$

where r is the rate, k is a rate constant, X is the number of available sites on the surface, and n is the number of sites necessary for the reaction to occur. When thallium poisons some of the sites, the number of available sites is set equal

to the number of sites on the undoped catalyst (S_o) less the number of sites poisoned by thallium (S_{Tl}), as in equation 23. Rearrangement of equation 23 gives equation 24, in which the n^{th} root of the rate is proportional to the amount of surface sites poisoned by thallium. If the thallium were uniformly

$$r^{\frac{1}{n}} = k^{\frac{1}{n}} S_o - k^{\frac{1}{n}} S_{Tl} \qquad (24)$$

distributed on the surface, located specifically on the active sites or on the surface in patches covering up the active sites and nonactive surface, one would expect a plot of $r^{\frac{1}{n}}$ versus S_{Tl} to be linear for some value of n. This was not found to be the case for these thallium-doped catalysts, under any set of conditions or for any value of n (see Figure 19 for representative plot). This lack of correlation between the rate and surface thallium concentration indicates that the thallium distribution on the surface is not uniform. The first few thallium atoms placed on the surface exert much more of a deactivation effect than the later thallium atoms places on the surface.

At this stage, it is best to present the possible models of thallium poisoning to see if they fit the data.

Herman et al (17) suggested that the active site in the Cu/ZnO is copper(I) in the zinc oxide. The amount of copper(I) dissolved in the zinc oxide as a solid solution was stated to be

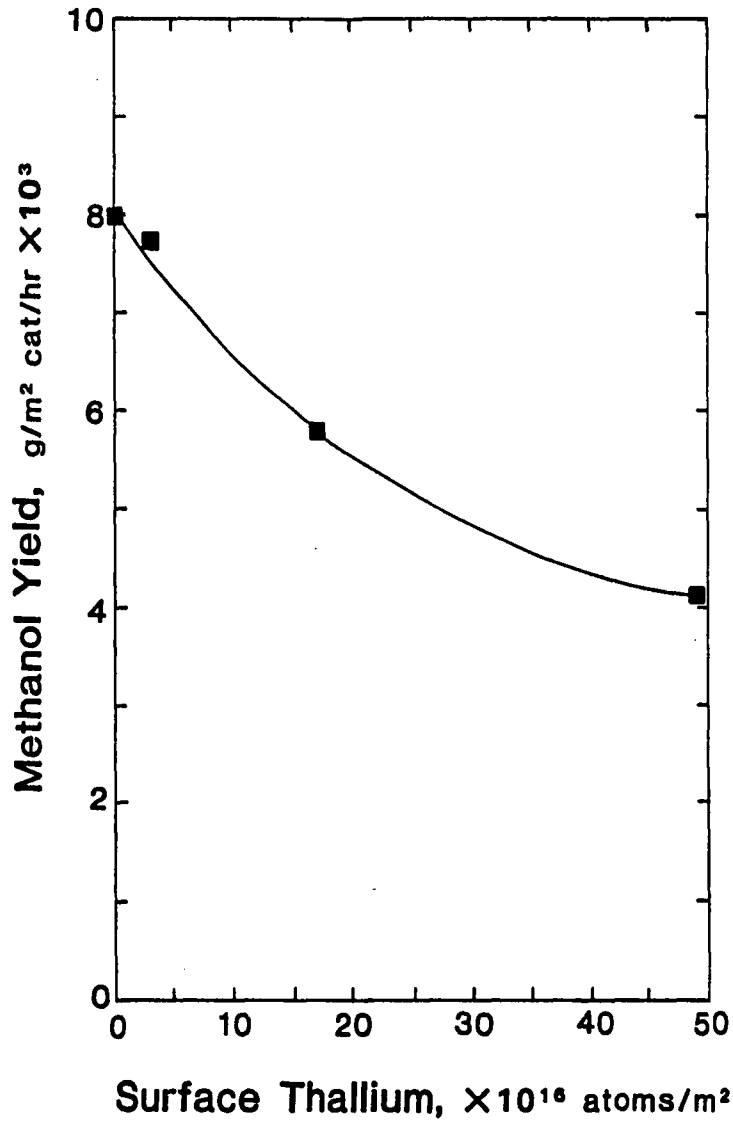

Figure 19 - Methanol yield versus surface thallium concentration (S_m). Conditions: 523 K, 7.6 MPa, 10.5 dm^3/hr H_2, 4.5 dm^3/hr CO, no H_2O. Points calculated using equation 24 with n equal to one.

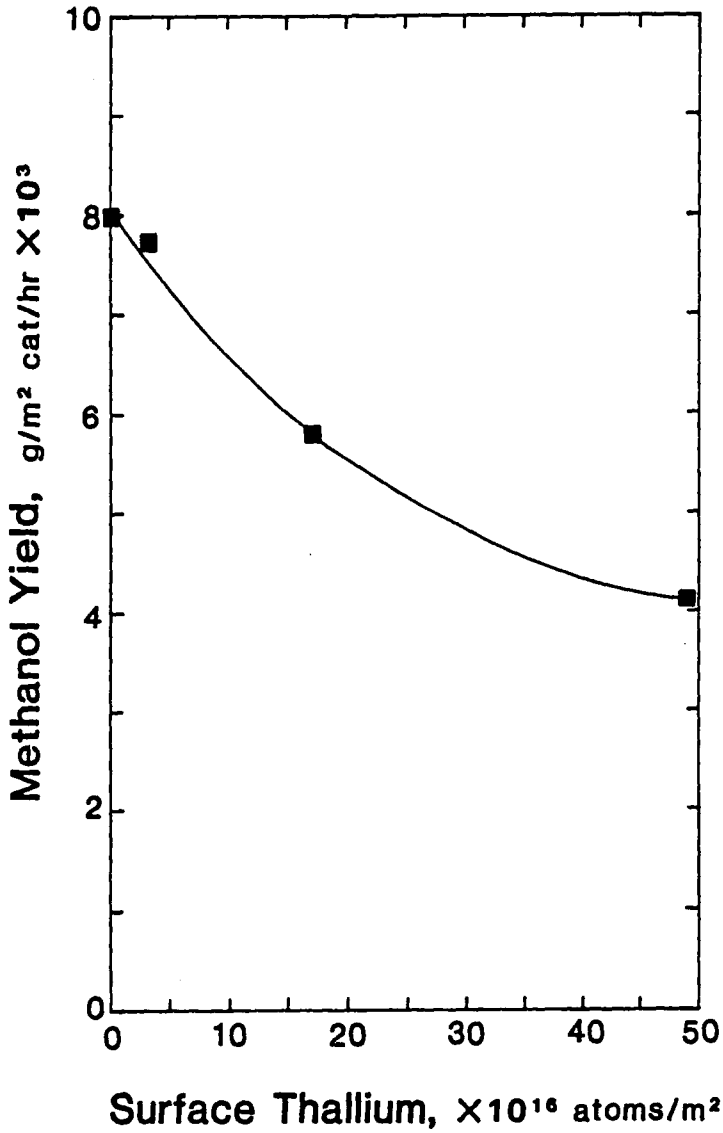

Figure 19 - Methanol yield versus surface thallium concentration (S_{Tl}). Conditions: 523 K, 7.6 MPa, 10.5 dm^3/hr H_2, 4.5 dm^3/hr CO, no H_2O. Points calculated using equation 24 with n equal to one.

up to 17 atom% for the 30/70 Cu/ZnO. The amount of copper(I) expected to be present on the surface of the zinc oxide is then assumed to be also 17 atom%. If the initial surface area of the Tl/Cu/ZnO catalysts is used and the copper to zinc oxide surface distribution of Parris (4) is used, then there is initially about 21.3 m^2/g of zinc oxide surface on the Tl/Cu/ZnO catalysts. This gives about 1.26×10^{20} zinc atoms on the catalyst surface per gram of catalyst. The 17% concentration of copper(I) in the zinc oxide then gives a surface copper(I) concentration of about 2.14×10^{19} per gram of catalyst. This copper(I) on the surface is the basis for the first model of active sites and thallium poisoning, Figure 20. The elemental analysis of the 0.02% Tl/Cu/ZnO indicates there are about 1.27×10^{18} thallium atoms per gram of catalyst, with all of the thallium assumed to be on the catalyst surface as the XPS analysis suggests. If all of the thallium atoms are locates near the specific copper(I) sites, then 1.27×10^{18} siter are blocked, leaving 2.01×10^{19} free active sites. Based upon similar calculations on the undoped catalyst, there are about 2.34×10^{19} sites per gram of Cu/ZnO. The 0.02% Tl/Cu/ZnO catalyst only has 86% of the number of active sites as the Cu/ZnO does and one would expect to see a 14% decrease in activity, with an observed activity decrease of 10%. This model was also used to calculate the number of free sites and the expected activity decrease on the other Tl/Cu/ZnO catalysts.

MODEL 1:

Active Site:

Cu^+ in ZnO

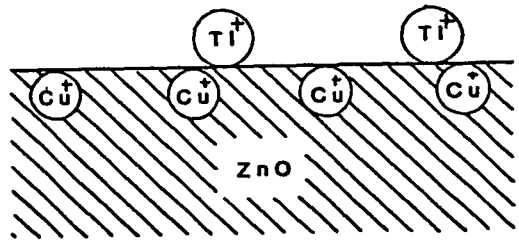

Figure 20 - Thallium poisoning Model 1. Active methanol sites: copper(I) in zinc oxide.

Table 18 - Calculated Activity Decrease Based Upon Cu(I) in ZnO Active Site.

Catalyst	Activity Decrease	
	Observed	Calculated
0.02% Tl/Cu/ZnO	10%	14%
0.08% Tl/Cu/ZnO	36%	40%
0.23% Tl/Cu/ZnO	50%	92%

The values for activity decreases are listed in Table 18. The decrease in activity is due mainly to the blockage of sites by thallium, but also has a slight contribution from the surface area decrease from 37.9 to about 36 m^2/g. From Table 18, one can see that this model can account for the observed decrease in methanol synthesis activity of these catalysts. The fact that the model accounts for more decrease in activity than is actually observed is explainable. It may be suggested that the thallium atoms have some selectivity for the copper(I) sites, and the first few thallium atoms on the surface prefer occupy these sites. As the concentration of thallium on the catalyst is increased, the thallium atoms are less selective in the sites which they occupy and become situated on nonactive sites. The thallium poisoning experiments indicate that this model of active sites is a plausible one. No assumptions about the nature of the thallium on the surface have been made in this model. The thallium may not be situated directly on top of the copper and may be associated with the copper(I) through some intermediate carbon specie or with the oxygen atoms surrounding the copper(I). The poisoning effect may be due to physical blockage of the thallium sites or chemical interaction of surface species between the copper and the thallium.

A second possible site for the methanol synthesis reaction to occur is the interface between the copper and zinc oxide. The assumption of the copper particles being hemispherical has

been used previously, and will be used here. X-ray diffraction shows copper particles to be about 8.0 nm in diameter in untested samples. Using this value, there would be about 2.08×10^{17} hemispherical particles of copper in each gram of Tl/Cu/ZnO or Cu/ZnO. In this one gram of sample, there would be 5.23×10^{18} nm of interface of the copper with the zinc oxide surface. The 0.02% Tl/Cu/ZnO contains 1.27×10^{18} atoms of thallium which can cover up 3.62×10^{17} nm of interface assuming thallium(I) with a radius of 0.24 nm (10). This interface model is depicted in Figure 21. The thallium at the interface would lead to an activity decrease of 7% on the 0.02% Tl/Cu/ZnO where a 10% decrease was observed. This is fairly good agreement, with the discrepancy due to the choice of copper particle size and thallium oxidation state. These choices were made to lead to the worst possible correlation. The calculated decrease in activity for the 0.08% Tl/Cu/ZnO is also close to the observed value, and the calculated value for the 0.23% Tl/Cu/ZnO more than accounts for the observed decrease. The calculated values are listed in Table 19. This model for thallium poisoning can also account for the observed methanol yields just as Model 1 could. In this case, the thallium only needs to selectively block the copper - zinc oxide interface, with some extra thallium on the unactive surfaces. The thallium can poison the sites just by a physical blockage effect.

The third model uses the copper surface area as the active

MODEL 2 :

Active Site

Cu/Zn Interface

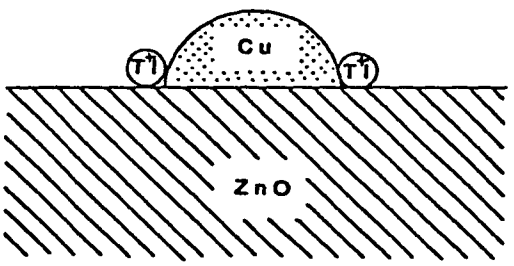

Figure 21 - Thallium poisoning Model 2. Active methanol sites: copper - zinc oxide. interface

Table 19 - Calculated Activity Decrease Based Upon Active Cu - ZnO Interface

Catalyst	Activity Decrease	
	Observed	Calculated
0.02% Tl/Cu/ZnO	10%	7%
0.08% Tl/Cu/ZnO	36%	33%
0.23% Tl/Cu/ZnO	50%	98%

methanol synthesis site. This model has also been given credibility by other workers, most recently by a group from ICI who found a correlation between methanol synthesis and copper surface area over $Cu/ZnO/Al_2O_3$ catalysts as well as copper catalysts supported by other oxides (32). The 0.02% Tl/Cu/ZnO catalyst with 34.7 m^2/g of total surface area has 14.1 m^2/g of copper surface area if one assumes the same copper and zinc oxide surface area distribution given by Parris (4). Based upon the density of metallic copper, one calculates that there are 1.93×10^{19} copper atoms on each square meter of copper surface. This gives 2.73×10^{20} surface copper atoms on each gram of the 0.02% Tl/Cu/ZnO catalyst. Some of these copper surface atoms would be blocked by the 1.27×10^{18} thallium atoms on each gram of the catalyst. The amount of sites blocked by the thallium atoms themselves is small, but the amount of surface copper available compared to the undoped Cu/ZnO, which has 2.98×10^{20} surface copper atoms per gram, is also small. The calculated activity decrease of the 0.02% Tl/Cu/ZnO is 8.7%, of which 8.4% is due to surface area differences and 0.3% due to blockage of copper sites by thallium. This 8.7% is near to the observed decrease of 10% on the 0.02% Tl/Cu/ZnO catalyst. While this first point may be acceptable in the argument for this model, the other catalysts doped with higher amounts of thallium discount it. The activity decreases observed over the thallium doped catalysts is due to two factors, a decrease in copper

MODEL 3:

Active Site:

Cu Metal

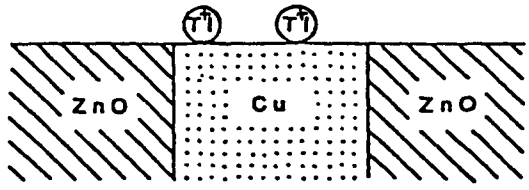

Figure 22 - Thallium poisoning Model 3. Active methanol sites: copper surface area.

Table 20 - Calculated Activity Decrease Based Upon Active Cu Surface Area

Catalyst	Activity Decrease	
	Observed	Calculated*
0.02% Tl/Cu/ZnO	10%	8.4% + 0.3%
0.08% Tl/Cu/ZnO	36%	8% + 2%
0.23% Tl/Cu/ZnO	50%	8% + 6%

*Calculated decrease comprised of decreased surface area component (first number) and thallium blockage component (second number).

sites resulting from a decreased surface area, and a decrease in copper sites due to blockage by thallium. Because the surface areas are about the same for all of the thallium-doped catalysts, the decreased activity due to the surface area change is about the same for all of the catalysts, about 8% (see Table 21). The thallium atoms on the surface then further decrease the activity of the catalysts, with this factor contributing from 0.3% to 6%. The calculated activity decreases from these two sources cannot account for the large observed activity decreases over the thallium-doped catalysts. Therefore, this model does not seem plausible based upon the results of the poisoning experiments.

There appear to be two possible models which can account for the observed thallium poisoning of methanol synthesis. The models indicate that the active sites for methanol synthesis are either copper(I) in zinc oxide or the copper - zinc oxide interface.

The deactivation toward methanol synthesis with time has not been mentioned in the analysis of the above models but it can be accounted for. In the copper(I) model, one can take into account the decrease in total surface area of the catalyst. A decrease in surface area down to 22.4 m^2/g for the 0.02% Tl/Cu/ZnO catalyst would give about 1.3×10^{19} active copper(I) sites assuming the same copper - zinc oxide surface area distribution as before. This leads to a 42% decrease in the

number of free sites if all the thallium atoms occupy active sites. The actual decrease in activity with time was 31%, and the model can account for this much deactivation. The deactivation can also be accounted for in the copper - zinc oxide interface model. Upon testing, the copper particles sinter which causes a decrease in the amount of available interface. The total amount of copper interface in the tested Tl/Cu/ZnO catalyst samples is about 1.48×10^{19} atoms based on a 12.0 nm copper particle diameter, which gives a circumference of about 2.32×10^{18} nm. The testing decreased the number of possible sites for the reaction to occur. Thallium can be assumed to block the sites as necessary to account for the deactivation.

4.3 Carbon Dioxide Formation Over Tl/Cu/ZnO Catalysts

From Figure 9, it appears that the formation of carbon dioxide over the Tl/Cu/ZnO catalysts via the Water-Gas Shift (WGS) reaction is about equal to its formation over undoped Cu/ZnO at low concentrations of water and slightly less than over Cu/ZnO at higher concentrations of water in the feed stream. The effluent gas concentrations may not be directly compared as relative rates because the concentration of methanol in the effluent gas varies from catalyst to catalyst. A determination of the rate constants for the WGS reaction is necessary in order to make comparisons.

The rate constant for the WGS reaction, k_1, can be calcu-

lated according to equation 25. The derivation of equation 25 is presented in Appendix , and the constants used are those given by Klier et al (33). This equation calculated the reaction rate near equilibrium conditions with the effect of methanol formation on the reaction rate taken into account.

$$k_1 = \frac{-\left[\Sigma F^o - (\alpha_{M,L} / 2.33)F^o_{H_2}\right]}{P\left[\langle p_{CO}\rangle - K_p^{-1}\langle p_{H_2}\rangle\right]^m} \ln\left(1 - \frac{\alpha_{M,L}}{\alpha_{L,eq}}\right) \quad (25)$$

$$\alpha_{M,L} = \frac{\Sigma F_i^o - \Sigma F_i^L}{2\, F_{CO}^o} \quad (26)$$

$$K_p = K_{eq}/K'_{eq} = \frac{K_p\, K'_\gamma}{K'_p\, K_\gamma} \quad (27)$$

$$\alpha_L = \frac{F^o_{H_2O} - F^L_{H_2O}}{F^o_{H_2O}} \quad (28)$$

$$\alpha_{L,eq} = \frac{\langle p_{CO}\rangle}{\langle p_{CO}\rangle - \frac{1}{2}\langle p_{H_2}\rangle} \quad (29)$$

In the above equations, the variables are defined as follows: F_i^o is the feed gas flow of component gas i; F_i^L is the flow of gas i in the effluent gas stream; $\alpha_{M,L}$ is the conversion to methanol as defined in equation 26; P is the total pressure of the system, 7.6 MPa; $\langle p_i\rangle$ is the average partial pressure of

component i, taken as one half of the sum of the partial pressure of i in the feed gas plus the partial pressure of i in the effluent gas; k_p is an equilibrium constant defined according to equation 27, with the values used being those of Klier (33), and k_p having a value of 8.225 MPa; m is the mass of catalyst used, 2.45 g; α_L as defined in equation 28; and $\alpha_{L,eq}$ as defined in equation 29.

Values for the rate constants of the WGS reaction are given in Table 21. The reaction rates over the thallium-doped catalystsare less than over the Cu/ZnO per unit weight of the catalyst but are equal to that of Cu/ZnO per unit surface area. The values of $\bar{k}_1$ in Table 21 are average values from the data at water concentrations of 50, 67, and 83 mmol/hr per 2.45 g of catalyst. The scatter of the values of k_1 for these three water concentrations is about 5%. The raw data in Figure 9 seemed to indicate a decrease in the rate of carbon dioxide formation over the Tl/Cu/ZnO catalysts, but this apparent decrease is caused mainly by the surface area decrease of the catalysts. This surface area decrease eliminates some of the active sites for the reaction, causing the apparent activity decrease per unit weight while maintaining the activity per unit surface area.

4.4 The Formation of Other Products Over Tl/Cu/ZnO Catalysts

Reaction products other than methanol and carbon dioxide

Table 21 - Rate of the Water Gas Shift Reaction

Catalyst	Rate Constant ($\bar{k}_1$)*	
	$\frac{mol}{kPa^2\ g\ hr}$	$\frac{mol}{kPa^2\ m^2\ hr}$
Cu/ZnO	5.85×10^{-8}	1.58×10^{-9}
0.02% Tl/Cu/ZnO	3.57×10^{-8}	1.60×10^{-9}
0.08% Tl/Cu/ZnO	3.90×10^{-8}	1.81×10^{-9}
0.23% Tl/Cu/ZnO	3.65×10^{-8}	1.69×10^{-9}

* $\bar{k}_1$ is the average rate constane, determined from water addition rates of 50, 67, and 83 mmol/hr.

observed when testing the Tl/Cu/ZnO catalysts were methyl formate, ethanol, and methane.

It was observed that the yields of methyl formate and ethanol varied in the same manner as the yield of methanol. This is to be expected since methanol or some surface C_1 species is an intermediate stage in the formation of methyl formate or ethanol. Under the conditions when methanol is formed in large quantities, there is enough C_1 species to be converted to ethanol and methyl formate by the catalyst.

Methane production seemed to follow no pattern. Methane can be formed by the hydrogenation of carbon monoxide or carbon dioxide or through the intermediacy of the Boudouart reaction. The XPS analysis for carbon showed a large amount of carbonaceous contamination on the catalyst surfaces, but most of this was due to adsorption of carbonaceous species by the catalyst surface upon exposure to air rather than by deposition of material during the catalyst testing procedure.

4.5 Mechanistic Interpretation of Thallium Poisoning

It appears that thallium poisons the formation of methanol and higher products, while perhaps not affecting the production of carbon dioxide. The active sites for methanol formation appear to be either copper(I) in the zinc oxide or the copper - zinc oxide interface. These conclusions follow from the

previous discussion.

One possible explanation for the observed results is that thallium does not interfere with the adsorption and activation of carbon monoxide on the catalyst surface, but prevents the hydrogenation of this activated carbon monoxide. This must be done without preventing the carbon dioxide from being formed from this activated carbon monoxide. This would likely have to be due to some type of chemical interaction of the thallium with the copper sites or an interaction with the surface immediately near to the active copper sites. The formate mechanism of Vedage, Pitchai, Herman, and Klier (8) is which carbon dioxide and methanol are formed from a common intermediate can still be valid if the thallium can selectively prevent the hydrogenation of the activated carbon monoxide.

Also possible is the proposed redox mechanism, in which activated carbon monoxide is the intermediate, not a formate species. In this case, the thallium may just block the alcohol half of the proposed interlocked reaction cycles. The thallium effect must be the same as above, interacting with the active site or the surface immediately next to the active site.

The model using copper surface area as being the active surface for methanol synthesis was discounted in the preceeding discussions. However, the recent work by the ICI group claims that the formation of methanol and carbon dioxide do not go through a common intermediate surface species (30). If there

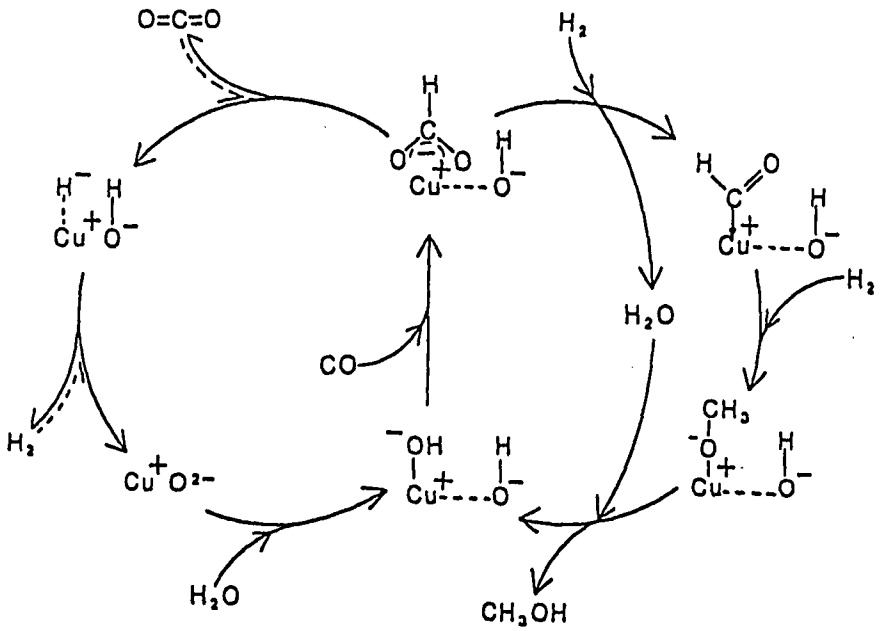

Figure 23 - Formate mechanism for methanol synthesis and the water gas shift reaction.

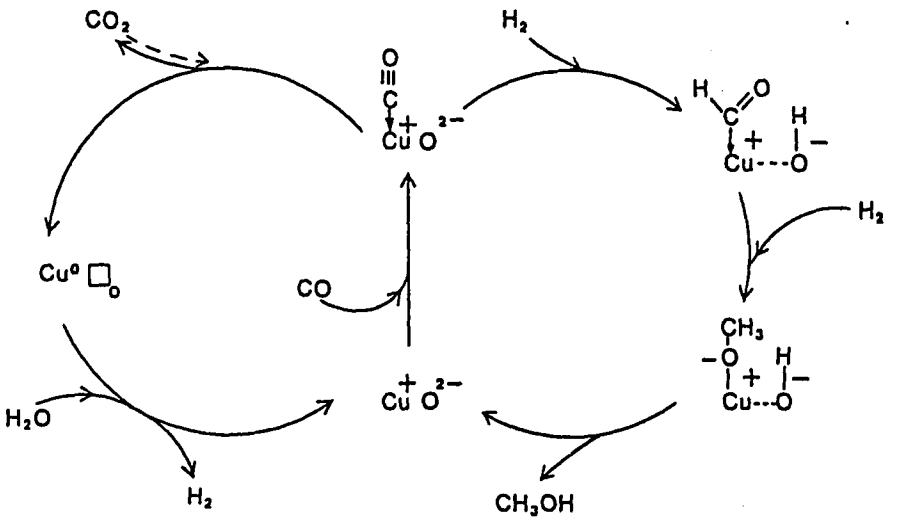

Figure 24 - Redox mechanism for methanol synthesis and the water gas shift reaction. $\square_o$ represents an oxygen vacancy.

are two separate sites for the formation of the carbon dioxide and methanol, then it is possible that thallium preferentially poisons the methanol formation sites only.

5.0 CONCLUSIONS

Doping of the Cu/ZnO methanol synthesis catalyst leads to poisoning of the methanol synthesis activity of the catalyst while not affecting the synthesis of carbon dioxide. The poisoning effect is a function of thallium concentration in the catalyst. The decrease in methanol activity is not linearly dependent upon thallium concentration, with the first added thallium having the most effect. Part of the observed decrease in methanol formation over the Tl/Cu/ZnO catalysts is due to a surface area decrease which lessens the number of active sites for the reaction to occur. The surface area decrease results from sintering of the copper and zinc oxide particles of the catalyst. The balance of the observed decreased activity of the Tl/Cu/ZnO catalysts is due to some poisoning by the thallium on the surface of the catalyst. This poisoning could result from blockage of the sites or through a chemical interaction of the thallium with some surface site.

The study of the thallium poisoning indicates that the active sites for formation of methanol are either copper(I) in zinc oxide or the copper - zinc oxide interface. There appears to be some selectivity of the thallium for these active sites, with the first thallium atoms on the surface preferentially blocking the sites. When more thallium is added to the

catalyst this selectivity is less noticeable.

A mechanism for the formation of methanol and carbon dioxide cannot be put forth but some interpretation can be made. If the two products have some common intermediate, then the thallium must be preventing the hydrogenation of the active intermediate while perhaps not preventing the formation of carbon dioxide. If there are two independent mechanisms, then the thallium is selectively blocking the sites which produce the methanol and not the carbon dioxide.

APPENDIX

An equation for the determination of the rate constant of the Water-Gas Shift reaction (WGS) was used in section 4.3, but the origin of this equation was not given. The derivation of the equation will be given here.

The WGS reaction, equation A1, runs at near equilibrium over Cu/ZnO catalysts under the conditions used for methanol synthesis. It is assumed that the rate of the reaction can be

$$CO + H_2O \underset{k_2}{\overset{k_1}{\rightleftharpoons}} CO_2 + H_2 \qquad (A1)$$

$$r = k_1 P_{CO} P_{H_2O} - k_2 P_{CO_2} P_{H_2} \qquad (A2)$$

expressed as in equation A2. The equilibrium constant for the WGS reaction can then be expressed as in equation A3.

$$K_p = \frac{k_1}{k_2} = \left(\frac{P_{CO_2} P_{H_2}}{P_{CO} P_{H_2O}} \right)_{eq} \qquad (A3)$$

Because carbon monoxide can form both methanol and carbon dioxide but water only leads to formation of carbon dioxide, the conversion to carbon dioxide, α, can be expressed as a function of the flow of water into the reactor, $F^o_{H_2O}$, and the flow out, $F^L_{H_2O}$.

$$\alpha = \frac{F^{o}_{H2O} - F^{L}_{H2O}}{F^{o}_{H2O}} \qquad (A4)$$

The pressures of carbon monoxide and hydrogen in the system are taken to be equal to the average of the partial pressures of the species entering and leaving the reactor, $p_i = (p_i^o + p_i^L)/2$. The equations for the partial pressures of carbon dioxide and water are not as simple, being related to the total pressure and the amount of all components at any given time:

$$p_{CO_2} = P\,(F_{CO_2}/\Sigma F_i) \qquad (A5)$$

$$p_{H_2O} = P\,(F_{H_2O}/\Sigma F_i) \qquad (A6)$$

where P is the total pressure, and F_i is the flow of component i. Based upon some relationships between the conversion, α, and the gas flow rates, F_i, one can derive new partial pressure equations.

$$p_{H_2O} = P\,\frac{F^{o}_{H2O}\,(1 - \alpha)}{F^{o} - (\alpha_{M,L}/2.3)F^{o}_{H_2}} \qquad (A7)$$

$$p_{CO_2} = P\,\frac{F^{o}_{H2O}\;\alpha}{F^{o} - (\alpha_{M,L}/2.3)F^{o}_{H_2}} \qquad (A8)$$

In these equations, $\alpha_{M,L}$ is the exit methanol conversion and other parameters as defined previously.

Substitution of the relations for partial pressures in terms of flows and conversions into the rate equation, equation A2, leads to equation A9.

$$r_m = k_1 P \frac{1}{F^o - (\alpha_{M,L}/2.3) F^o_{H_2}} \left[\langle p_{CO} \rangle - \alpha \left(\langle p_{CO} \rangle + \frac{\langle p_{H_2} \rangle}{K_p} \right) \right] \quad (A9)$$

The conversion to products in the integral reactor used is related to the mass of catalyst used. Integration of the reaction rate to account for catalyst mass leads to equation A10, which is solved for k_1. In the rate constant equation:

$$k_1 = \frac{- \left[F^o - (\alpha_{M,L}/2.33) F^o_{H_2} \right]}{P \left(\langle p_{CO} \rangle - K_p^{-1} \langle p_{H_2} \rangle \right) m} \ln \left(1 - \frac{\alpha_{M,L}}{\alpha_{L,eq}} \right) \quad (A10)$$

where F^o_i is the feed gas flow of component i; F^L_i is the exit flow of component gas i; $\alpha_{M,L}$ is the conversion to methanol; P is the total pressure; $\langle p_i \rangle$ is the partial pressure of i; K_p is the equilibrium constant for the reaction, which should include the fugacities (not mentioned previously); m is the mass of the catalyst; α is the conversion to carbon dioxide; and $\alpha_{L,eq}$ is the equilibrium conversion based on partial pressures of components, $\alpha_{L,eq}$ is equal to $\langle p_{CO} \rangle / (\langle p_{CO} \rangle - \frac{1}{2} \langle p_{H_2} \rangle)$.

REFERENCES

1. Chem. Eng. News, May 7, 1984.

2. Chem. Eng. News, July 16, 1984.

3. K. Klier, Advances in Catalysis, 31, 243(1982).

4. G. E. Parris, Ph.D. Dissertation, Lehigh University, Bethlehem, PA (1981).

5. C. Lormand, Ind. Eng. Chem., 17, 430(1925).

6. G. A. Vedage, Ph.D. Dissertation, Lehigh University, Bethlehem, PA (1984).

7. G. A. Vedage, R. Pitchai, R. G. Herman, K. Klier, "Proceedings of 8th International Congress on Catalysis", Vol II, 47 - 58, 1984.

8. K. Klier, R. G. Herman, G. W. Simmons, "Catalysts for Alcohols from Biomass", Report prepared for Solar Energy Research Institute, June 1984, XX-2-02173.

9. A. G. Lee, "The Chemistry of Thallium", Elsevier, Amsterdam, 1971.

10. F. A. Cotton, G. Wilkinson, "Advanced Inorganic Chemsitry", Interscience, New York, 1972.

11. A. F. Trotman, ed., "Comprehensive Inorganic Chemsitry", Vol I, Pergammon Press, Oxford, 1973.

12. A. McKillop, E. C. Taylor, Adv. Organomet. Chem., 11, 147(1973).

13. C. W. Young, K. Klier, unpublished results.

14. S. Brunauer, P. H. Emmet, E. Teller, J. Am. Chem. Soc., 60, 309(1938).

15. B. D. Cullity, "Elements of X-Ray Diffraction", Addison-Wesley, Reading MA, 1978.

16. M. J. Dreiling, Surf. Sci., 71, 231(1978).

17. R. G. Herman, K. Klier, G. W. Simmons, B. P. Finn, J. B. Bulko, J. Catal., 57, 339(1979).

18. W. A. Dietz, J. Gas Chrom., 68(1967).

19. R. G. Herman, P. Pendleton, J. B. Bulko, "Advances in Materials Characterization", ed. by D. R. Rossington, R. A. Condrate, and R. L. Snyder, Plenum Press, New York, 109(1983).

20. C. D. Wagner, W. M. Riggs, L. E. Davis, J. F. Moulder, "Handbook of X-Ray Photoelectron Spectroscopy", Perkin-Elmer Corp., Eden Prarie MN, 1979.

21. Elemental analysis by Galbraith Laboratories, Knoxville, TN. Actual analyses: wt.% Tl/Cu/ZnO - 0.04/23.15/57.88; 0.20/23.14/57.35; 0.58/22.47/56.07; 0.42/23.67/60.25.

22. Joint Committee on Powder Diffraction Standards, Swarthmore PA.

23. C. C. Chang, Surf. Sci., 48, 9(1975).

24. S. H. Scofield, J. Electron Spectroscopy, 8, 129(1976).

25. J. B. Bulko, Ph.D. Dissertation, Lehigh University, Bethlehem, PA (1980).

26. G. A. Vedage, P. Himelfarb, G. W. Simmons, K. Klier, Paper presented at Symposium on Role of Solid State Chemistry in Catalysis, ACS, Washington D. C., 1983.

27. M. P. Seah, W. A. Dench, Surface and Interface Analysis, 1, 2(1979).

28. G. A. Vedage, personnal communication.

29. G. A. Vedage, P. Himelfarb, G. W. Simmons, K. Klier, Preprints, Div. Pet. Chem. ACS, 1261(1983).

30. W. B. Pearson, "Handbook of Lattice Spacings and Structures of Metals and Alloys", Pergammon Press, New York, 1958.

31. G. Natta, Catalysis, 3, 349(1955).

32. G. C. Chinchen, P. J. Denny, D. G. Parker, G. D. Short, M. S. Spencer, K. C. Waigh, D. A. Whan, Paper to be presented Symposium on Methanol and Methyl Fuel Synthesis/Advances in Synthesis of Substitute Liquid Fuels, ACS, Phila., 1984.

33. K. Klier, V. Chatikavanij, R. G. Herman, G. W. Simmons, J. Catal., 74, 343(1982).

VITA

Paul Peter Deutsch was born in Allentown, Pennsylvania on August 8, 1959 to Paul R. and Viola K. Deutsch. Mr. Deutsch attended Lehigh University from 1977 to 1981, when he received his Bachelor of Science degree in Chemistry. From 1981 to 1983 he was employed as an assistant research chemist at Air Products and Chemicals, Inc. in Trexlertown, Pennsylvania.

Mr. Deutsch began graduate study in inorganic chemistry at Lehigh University on a full-time basis in the fall of 1983. During his career there, he worked for Professor Kamil Klier at the Center for Surface and Coatings Research.